DIFFRACTION GRATING HANDBOOK

fifth edition

Christopher Palmer

Erwin Loewen, *Editor (first edition)*

Table of Contents

The *Diffraction Grating Handbook* is supplemented by Thermo RGL's *Grating Catalog*, which lists the standard plane and concave gratings available.

If the Catalog does not offer a diffraction grating that meets your requirements, please contact us for a listing of new gratings or a quotation for a custom-designed and -fabricated grating.

Thermo RGL remains committed to maintaining its proud traditions - using the most advanced technology available to produce high-quality precision diffraction gratings, and providing competent technical assistance in the choice and use of these gratings.

THERMO RGL
Richardson Grating Laboratory
705 St. Paul Street, Rochester, New York 14605 USA
tel: 585/262-1331, fax: 585/454-1568, e-mail: information@gratinglab.com
http://www.gratinglab.com/

CONTENTS

PREFACE TO THE FIFTH EDITION

FIRST CHAPTER

TABLE OF CONTENTS

In composing the fourth edition of the *Diffraction Grating Handbook* in early 2000, I did not expect to worry about a fifth edition for several years, as Thermo RGL had 10,000 copies printed. By the beginning of 2002, however, we had distributed all but a few hundred copies, so either a reprinting of the fourth edition or of an updated version was required. The technical staff of Thermo RGL has made the latter choice, which has led to this expanded and corrected version of the *Handbook*.

Some of the corrections in the edition have been the result of errors brought to my attention by readers - I thank each one sincerely for his feedback, which has allowed this edition to be better than the last, and I ask all readers of this edition to send their comments, suggestions and corrections to me at the e-mail address below

Christopher Palmer
Thermo RGL
Rochester, New York

palmer@gratinglab.com

February 2002

PREFACE TO THE FOURTH EDITION

FIRST CHAPTER

TABLE OF CONTENTS

Thermo RGL (formerly the Richardson Grating Laboratory) is proud to build upon the heritage of technical excellence that began when Bausch & Lomb produced its first high-quality master grating over fifty years ago. A high-fidelity replication process was subsequently developed to make duplicates of the tediously generated master gratings. This process became the key to converting diffraction gratings from academic curiosities to catalog items, which in turn enabled gratings to almost completely replace prisms as the optical dispersing element of choice in modern laboratory instrumentation.

For several years, since its introduction in 1970, the *Diffraction Grating Handbook* was the primary source of information of a general nature regarding diffraction gratings. In 1982, Dr. Michael Hutley of the National Physical Laboratory published *Diffraction Gratings*, a monograph that addresses in more detail the nature and uses of gratings, as well as their manufacture. Most recently, in 1997, the original author of the Handbook, Dr. Erwin Loewen, wrote with Dr. Evgeny Popov (of the Institute of Solid State Physics, Sofia, Bulgaria) a very thorough and complete monograph entitled Diffraction Gratings and Applications. Readers of this Handbook who seek additional insight into the many aspects of diffraction grating behavior, manufacture and use are encouraged to turn to these two books.

Christopher Palmer
Rochester, New York
April 2000

1. SPECTROSCOPY AND GRATINGS

"It is difficult to point to another single device that has brought more important experimental information to every field of science than the diffraction grating. The physicist, the astronomer, the chemist, the biologist, the metallurgist, all use it as a routine tool of unsurpassed accuracy and precision, as a detector of atomic species to determine the characteristics of heavenly bodies and the presence of atmospheres in the planets, to study the structures of molecules and atoms, and to obtain a thousand and one items of information without which modern science would be greatly handicapped."

- J. Strong, *J. Opt. Soc. Am.* **50** (1148-1152), quoting G. R. Harrison

NEXT CHAPTER

TABLE OF CONTENTS

1.0. INTRODUCTION [top]

Spectroscopy is the study of electromagnetic spectra - the wavelength composition of light — due to atomic and molecular interactions. For many years, spectroscopy has been important in the study of physics, and it is now equally important in astronomical, biological, chemical, metallurgical and other analytical investigations. The first experimental tests of quantum mechanics

involved verifying predictions regarding the spectrum of hydrogen with grating spectrometers. In astrophysics, diffraction gratings provide clues to the composition of and processes in stars and planetary atmospheres, as well as offer clues to the large-scale motions of objects in the universe. In chemistry, toxicology and forensic science, grating-based instruments are used to determine the presence and concentration of chemical species in samples. In telecommunications, gratings are being used to increase the capacity of fiber-optic networks using wavelength division multiplexing (WDM).

The diffraction grating is of considerable importance in spectroscopy, due to its ability to separate (disperse) polychromatic light into its constituent monochromatic components. In recent years, the spectroscopic quality of diffraction gratings has greatly improved, and Thermo RGL has been a leader in this development.

The extremely high precision required of a modern diffraction grating dictates that the mechanical dimensions of diamond tools, ruling engines, and optical recording hardware, as well as their environmental conditions, be controlled to the very limit of that which is physically possible. Anything less results in gratings that are ornamental but have little technical or scientific value. The challenge to produce precision diffraction gratings has attracted the attention of some of the world's most capable scientists and technicians. Only a few have met with any appreciable degree of success, each limited by the technology available.

1.1. THE DIFFRACTION GRATING [top]

A *diffraction grating* is a collection of reflecting (or transmitting) elements separated by a distance comparable to the wavelength of light under study. It may be thought of as a collection of diffracting elements, such as a pattern of transparent slits (or apertures) in an opaque screen, or a collection of reflecting grooves on a substrate. A *reflection grating* consists of a grating superimposed on a reflective surface, whereas a *transmission grating* consists of a grating superimposed on a transparent surface. An electromagnetic wave incident on a grating will, upon diffraction, have its electric field amplitude, or phase, or both, modified in a predictable manner.

1.2. A BRIEF HISTORY OF GRATING DEVELOPMENT

[top]

The first diffraction grating was made by an American astronomer, David Rittenhouse, in 1785, who reported constructing a half-inch wide grating with fifty-three apertures. Apparently he developed this prototype no further, and there is no evidence that he tried to use it for serious scientific experiments.

In 1821, unaware of the earlier American report, Joseph von Fraunhofer began his work on diffraction gratings. His research was given impetus by his insight into the value that grating dispersion could have for the new science of spectroscopy. Fraunhofer's persistence resulted in gratings of sufficient quality to enable him to measure the absorption lines of the solar spectrum. He also derived the equations that govern the dispersive behavior of gratings. Fraunhofer was interested only in making gratings for his own experiments, and upon his death, his equipment disappeared.

By 1850, F.A. Nobert, a Prussian instrument maker, began to supply scientists with gratings superior to Fraunhofer's. About 1870, the scene of grating development returned to America, where L.M. Rutherfurd, a New York lawyer with an avid interest in astronomy, became interested in gratings. In just a few years, Rutherfurd learned to rule reflection gratings in speculum metal that were far superior to any that Nobert had made. Rutherfurd developed gratings that surpassed even the most powerful prisms. He made very few gratings, though, and their uses were limited.

Rutherfurd's part-time dedication, impressive as it was, could not match the tremendous strides made by H.A. Rowland, professor of physics at the Johns Hopkins University. Rowland's work established the grating as the primary optical element of spectroscopic technology.

Rowland constructed sophisticated ruling engines and invented the concave grating, a device of spectacular value to modern spectroscopists. He continued to rule gratings until his death in 1901.

After Rowland's great success, many people set out to rule diffraction gratings. The few who were successful sharpened the scientific demand for

gratings. As the advantages of gratings over prisms and interferometers for spectroscopic work became more apparent, the demand for diffraction gratings far exceeded the supply.

In 1947, Bausch & Lomb decided to make precision gratings available commercially. In 1950, through the encouragement of Prof. George R. Harrison of MIT, David Richardson and Robert Wiley of Bausch & Lomb succeeded in producing their first high quality grating. This was ruled on a rebuilt engine that had its origins in the University of Chicago laboratory of Prof. Albert A. Michelson. A high fidelity replication process was subsequently developed, which was crucial to making *replicas*, duplicates of the tediously generated master gratings. A most useful feature of modern gratings is the availability of an enormous range of sizes and groove spacings (up to 10,800 grooves per millimeter), and their enhanced quality is now almost taken for granted. In particular, the control of groove shape (or blazing) has increased spectral efficiency dramatically. In addition, interferometric and servo control systems have made it possible to break through the accuracy barrier previously set by the mechanical constraints inherent in the ruling engines.

During the subsequent decades, the Richardson Grating Laboratory (now Thermo RGL) has produced thousands of master gratings and many times that number of high quality replicas. In 1985, Milton Roy Company acquired Bausch & Lomb's gratings and spectrometer operations, and in 1995 sold these operations to Life Sciences International plc as part of Spectronic Instruments, Inc. In 1997, Spectronic Instruments was acquired by Thermo Electron Corporation, and the gratings operation is now a separate business called Thermo RGL. During these changes, Thermo RGL has continued to uphold the traditions of precision and quality established by Bausch & Lomb over fifty years ago.

1.3. THERMO RGL [top]

Thermo RGL - known throughout the world as "the Grating Lab" - is a unique facility in Rochester, New York, containing not only the Thermo RGL ruling engines and recording chambers (for making master gratings) but the replication and associated testing and inspection facilities for supplying replicated gratings in commercial quantities.

To achieve the high practical resolution characteristic of high-quality gratings, a precision of better than 1 nm (0.001 µm) in the spacing of the grooves must be maintained. Such high precision requires extraordinary control over temperature fluctuation and vibration in the ruling engine environment. This control has been established by the construction of specially-designed ruling cells that provide environments in which temperature stability is maintained at ± 0.01 °C for weeks at a time, as well as vibration isolation that suppresses ruling engine displacement to less than 0.025 µm. The installation can maintain reliable control over the important environmental factors for periods in excess of six weeks, the time required to rule large, finely-spaced gratings.

Thermo RGL contains facilities for coating and testing master and replica substrates, as well as special areas for the controlled replication itself. In order to produce the finest gratings with maximum control and efficiency, even storage, packing and shipping of finished gratings are part of the same facility.

In addition to burnishing gratings with a diamond tool, an optical interference pattern can be used to produce holographic gratings. Master holographic gratings require strict maintenance of the recording optical system to obtain the best contrast and fringe structure. Thermo RGL produces *holographic gratings* in its dedicated recording facility, in whose controlled environment thermal gradients and air currents are minimized and fine particulates are filtered from the air. These master gratings are replicated in a process identical to that for ruled master gratings.

NEXT CHAPTER

Back to top

2. THE PHYSICS OF DIFFRACTION GRATINGS

PREVIOUS CHAPTER
NEXT CHAPTER

TABLE OF CONTENTS

2.1. THE GRATING EQUATION [top]

When monochromatic light is incident on a grating surface, it is diffracted into discrete directions. We can picture each grating groove as being a very small, slit-shaped source of diffracted light. The light diffracted by each groove combines to form a diffracted wavefront. The usefulness of a grating depends on the fact that there exists a unique set of discrete angles along which, for a given spacing *d* between grooves, the diffracted light from each facet is in phase with the light diffracted from any other facet, so they combine constructively.

Diffraction by a grating can be visualized from the geometry in Figure 2-1, which shows a light ray of wavelength λ incident at an angle α and diffracted by a grating (of *groove spacing d*, also called the *pitch*) along angles β_m. These angles are measured from the grating normal, which is the dashed line perpendicular to the grating surface at its center. The sign convention for these angles depends on whether the light is diffracted on the same side or the opposite side of the grating as the incident light. In diagram (a), which shows a *reflection grating*, the angles $\alpha > 0$ and $\beta_1 > 0$ (since they are measured counter-clockwise from the grating normal) while the angles $\beta_0 < 0$ and $\beta_{-1} < 0$ (since they are measured clockwise from the grating normal). Diagram (b) shows the case for a *transmission grating*.

By convention, angles of incidence and diffraction are measured *from* the grating normal *to* the beam. This is shown by arrows in the diagrams. In both diagrams, the sign convention for angles is shown by the plus and minus symbols located on either side of the grating normal. For either reflection or transmission gratings, the algebraic signs of two angles differ if they are measured from opposite sides of the grating normal. Other sign conventions

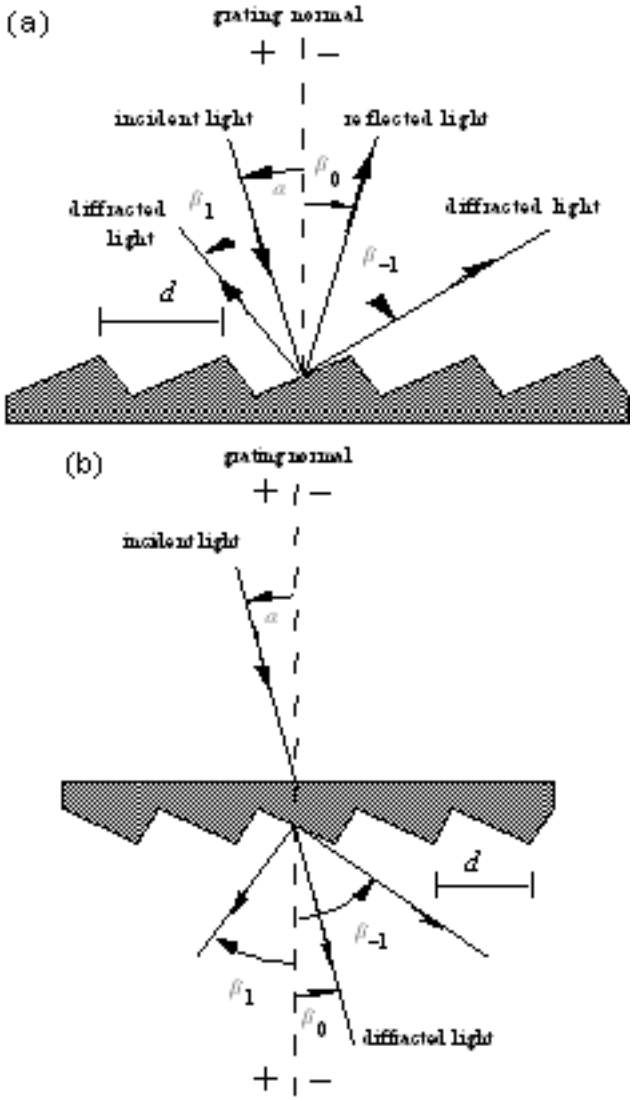

Figure 2-1. Diffraction by a plane grating. A beam of monochromatic light of wavelength λ is incident on a grating and diffracted along several discrete paths. The triangular grooves come out of the page; the rays lie in the plane of the page. The sign convention for the angles α and β is shown by the + and – signs on either side of the grating normal. (a) A *reflection grating*: the incident and diffracted rays lie on the same side of the grating. (b) A *transmission grating*: the incident and diffracted rays lies on opposite sides of the grating.

---

exist, so care must be taken in calculations to ensure that results are self-consistent. Another illustration of grating diffraction, using wavefronts (surfaces of constant phase), is shown in Figure 2-2. The geometrical path difference between light from adjacent grooves is seen to be $d \sin\alpha + d \sin\beta$. [Since $\beta < 0$, the latter term is actually negative.] The principle of interference

dictates that only when this difference equals the wavelength λ of the light, or some integral multiple thereof, will the light from adjacent grooves be in phase (leading to constructive interference). At all other angles β, there will be some measure of destructive interference between the wavelets originating from the groove facets.

These relationships are expressed by the *grating equation*

$$m\lambda = d\,(\sin\alpha + \sin\beta), \qquad (2\text{-}1)$$

which governs the angles of diffraction from a grating of groove spacing *d*. Here *m* is the *diffraction order* (or *spectral order*), which is an integer. For a particular wavelength λ, all values of *m* for which $|m\lambda/d| < 2$ correspond to physically realizable diffraction orders.

It is sometimes convenient to write the grating equation as

$$Gm\lambda = \sin\alpha + \sin\beta, \qquad (2\text{-}1')$$

where $G = 1/d$ is the *groove frequency* or *groove density*, more commonly called "grooves per millimeter".

Eq. (2-1) and its equivalent Eq. (2-1') are the common forms of the grating equation, but their validity is restricted to cases in which the incident and diffracted rays are perpendicular to the grooves (at the center of the grating). The vast majority of grating systems fall within this category, which is called *classical* (or *in-plane*) *diffraction*. If the incident light beam is not perpendicular to the grooves, though, the grating equation must be modified:

$$Gm\lambda = \cos\varepsilon\,(\sin\alpha + \sin\beta), \qquad (2\text{-}1'')$$

Here ε is the angle between the incident light path and the plane perpendicular to the grooves at the grating center (the plane of the page in Figure 2-2). If the incident light lies in this plane, $\varepsilon = 0$ and Eq. (2-1") reduces to the more familiar Eq. (2-1'). In geometries for which $\varepsilon \neq 0$, the diffracted spectra lie on a cone rather than in a plane, so such cases are termed *conical diffraction*.

For a grating of groove spacing *d*, there is a purely mathematical relationship

between the wavelength and the angles of incidence and diffraction. In a given spectral order *m*, the different wavelengths of polychromatic wavefronts incident at angle α are separated in angle:

$$\beta(\lambda) = \arcsin(m\lambda/d - \sin\alpha). \qquad (2\text{-}2)$$

When $m = 0$, the grating acts as a mirror, and the wavelengths are not separated ($\beta = -\alpha$ for all λ); this is called *specular reflection* or simply the *zero order*.

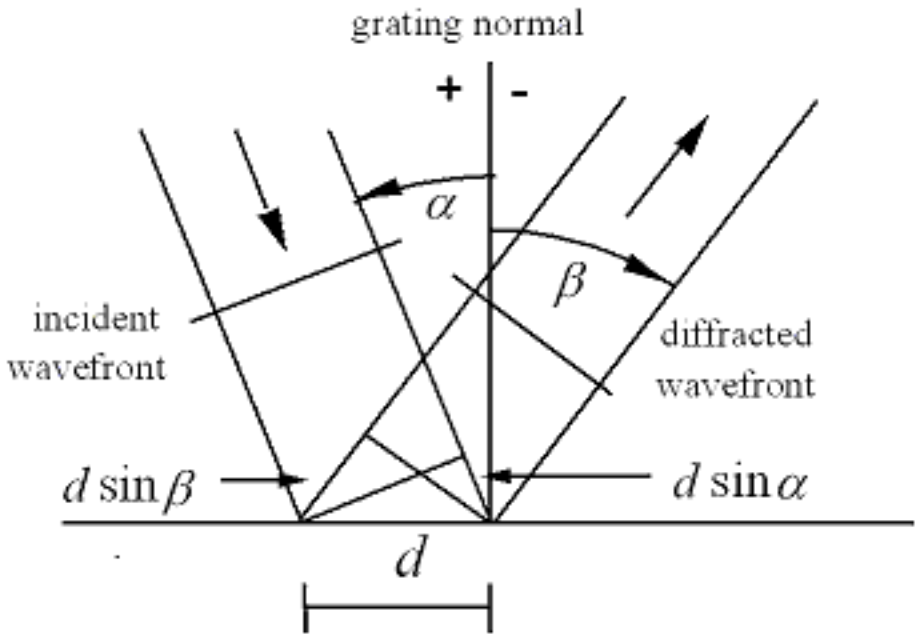

Figure 2-2. Geometry of diffraction, for planar wavefronts. The terms in the path difference, $d \sin\alpha$ and $d \sin\beta$, are shown.

A special but common case is that in which the light is diffracted back toward the direction from which it came (i.e., $\alpha = \beta$); this is called the *Littrow configuration*, for which the grating equation becomes

$$m\lambda = 2d \sin\alpha, \quad \text{in Littrow.} \qquad (2\text{-}3)$$

In many applications (such as constant-deviation monochromators), the wavelength λ is changed by rotating the grating about the axis coincident with

its central ruling, with the directions of incident and diffracted light remaining unchanged. The *deviation angle* 2*K* between the incidence and diffraction directions (also called the *angular deviation*) is

$$2K = \alpha - \beta = constant \qquad (2\text{-}4)$$

while the scan angle ϕ, which is measured from the grating normal to the bisector of the beams, is

$$2\phi = \alpha + \beta. \qquad (2\text{-}5)$$

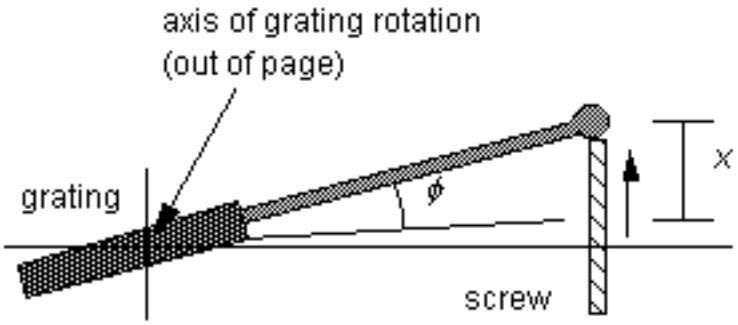

Figure 2-3. A sine bar mechanism for wavelength scanning. As the screw is extended linearly by the distance *x* shown, the grating rotates through an angle ϕ in such a way that $\sin\phi$ is proportional to *x*.

Note that ϕ changes with λ (as do α and β). In this case, the grating equation can be expressed in terms of ϕ and the *half deviation angle K* as

$$m\lambda = 2d \cos K \sin\phi. \qquad (2\text{-}6)$$

This version of the grating equation is useful for monochromator mounts (see Chapter 7). Eq. (2-6) shows that the wavelength diffracted by a grating in a monochromator mount is directly proportional to the sine of the angle ϕ through which the grating rotates, which is the basis for monochromator drives in which a sine bar rotates the grating to scan wavelengths (see Figure 2-3).

2.2. DIFFRACTION ORDERS [top]

2.2.1. Existence of Diffraction Orders.

For a particular set of values of the groove spacing *d* and the angles α and β, the grating equation (2-1) is satisfied by more than one wavelength. In fact, subject to restrictions discussed below, there may be several discrete wavelengths which, when multiplied by successive integers *m*, satisfy the condition for constructive interference. The physical significance of this is that the constructive reinforcement of wavelets diffracted by successive grooves merely requires that each ray be retarded (or advanced) in phase with every other; this phase difference must therefore correspond to a real distance (path difference) which equals an integral multiple of the wavelength. This happens, for example, when the path difference is one wavelength, in which case we speak of the positive first diffraction order ($m = 1$) or the negative first diffraction order ($m = –1$), depending on whether the rays are advanced or retarded as we move from groove to groove. Similarly, the second order ($m = 2$) and negative second order ($m = –2$) are those for which the path difference between rays diffracted from adjacent grooves equals two wavelengths.

The grating equation reveals that only those spectral orders for which $|m\lambda/d| < 2$ can exist; otherwise, $|\sin\alpha + \sin\beta| > 2$, which is physically meaningless. This restriction prevents light of wavelength λ from being diffracted in more than a finite number of orders. Specular reflection ($m = 0$) is always possible; that is, the *zero order* always exists (it simply requires $\beta = -\alpha$). In most cases, the grating equation allows light of wavelength λ to be diffracted into both negative and positive orders as well. Explicitly, spectra of all orders *m* exist for which

$$-2d < m\lambda < 2d, \quad m \text{ an integer.} \qquad (2\text{-}7)$$

For $l/d << 1$, a large number of diffracted orders will exist.

As seen from Eq. (2-1), the distinction between negative and positive spectral orders is that

$$\begin{aligned} \beta &> -\alpha \quad \text{for positive orders } (m > 0), \\ \beta &< -\alpha \quad \text{for negative orders } (m < 0), \\ \beta &= -\alpha \quad \text{for specular reflection } (m = 0), \end{aligned} \qquad (2\text{-}8)$$

This sign convention for m requires that $m > 0$ if the diffracted ray lies to the left (the counter-clockwise side) of the zero order ($m = 0$), and $m < 0$ if the diffracted ray lies to the right (the clockwise side) of the zero order. This convention is shown graphically in Figure 2-4.

2.2.2. Overlapping of Diffracted Spectra.

The most troublesome aspect of multiple order behavior is that successive spectra overlap, as shown in Figure 2-5. It is evident from the grating equation that, for any grating instrument configuration, the light of wavelength λ diffracted in the $m = 1$ order will coincide with the light of wavelength $\lambda/2$ diffracted in the $m = 2$ order, *etc*., for all m satisfying inequality (2-7). In this example, the red light (600 nm) in the first spectral order will overlap the ultraviolet light (300 nm) in the second order. A detector sensitive at both wavelengths would see both simultaneously. This superposition of wavelengths, which would lead to ambiguous spectroscopic data, is inherent in the grating equation itself and must be prevented by suitable filtering (called *order sorting*), since the detector cannot generally distinguish between light of different wavelengths incident on it (within its range of sensitivity). [See also Section 2.7 below.]

2.3. DISPERSION [top]

The primary purpose of a diffraction grating is to disperse light spatially by wavelength. A beam of white light incident on a grating will be separated into its component colors upon diffraction from the grating, with each color diffracted along a different direction. *Dispersion* is a measure of the separation (either angular or spatial) between diffracted light of different wavelengths. Angular dispersion expresses the spectral range per unit angle, and linear resolution expresses the spectral range per unit length.

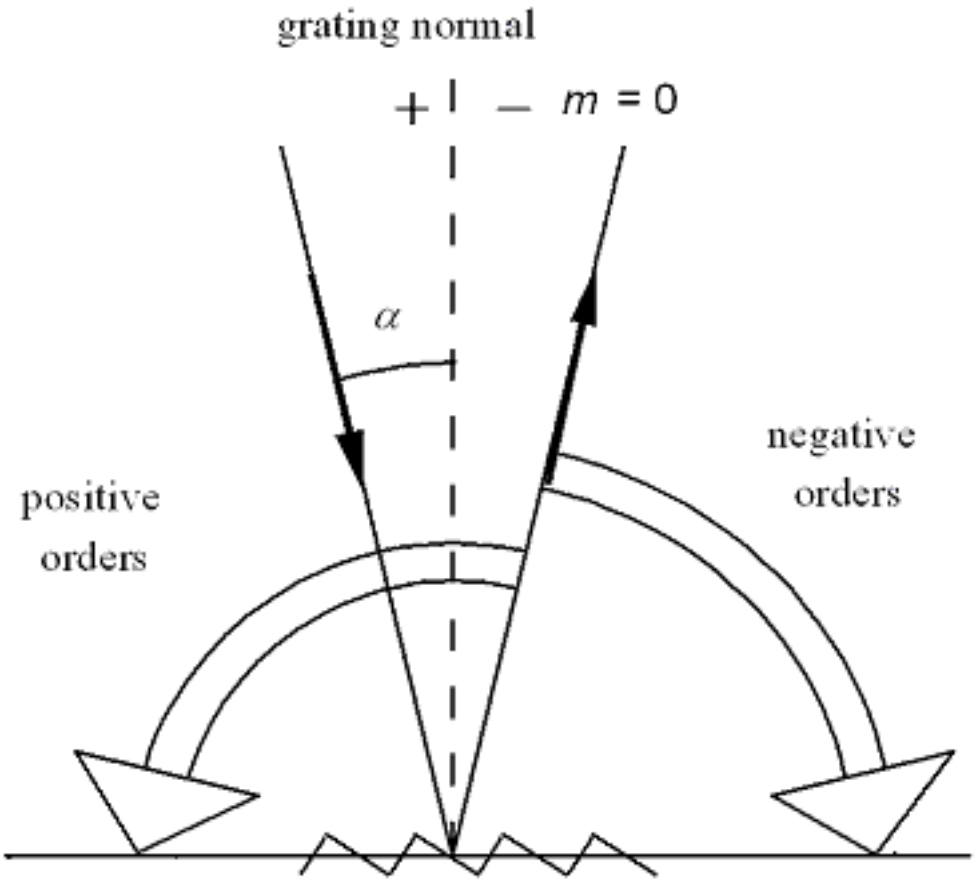

Figure 2-4. Sign convention for the spectral order m. In this example a is positive.

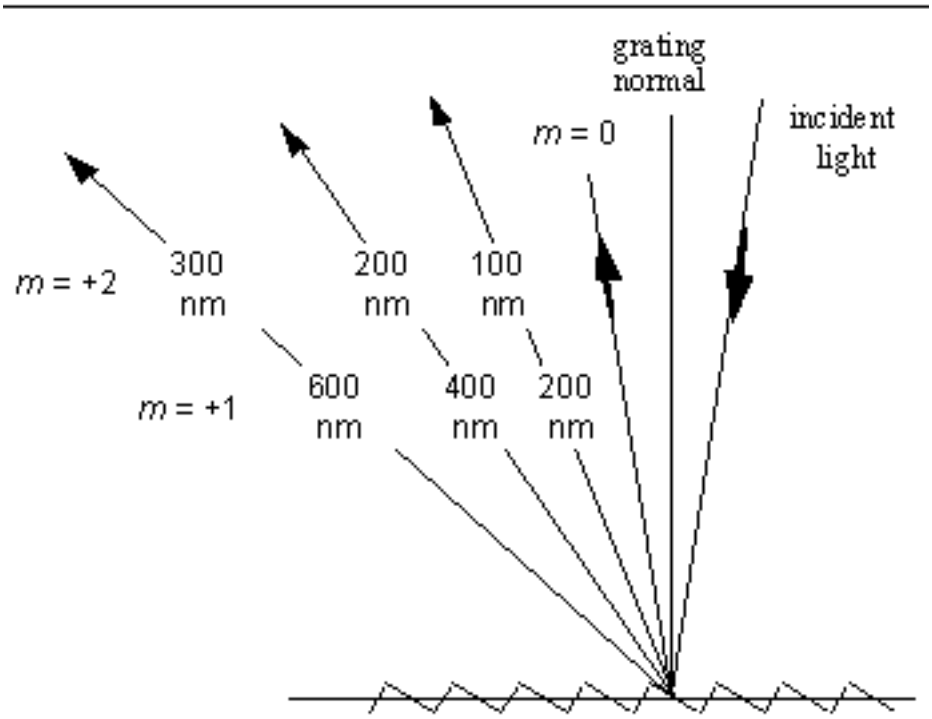

Figure 2-5. Overlapping of spectral orders. The light for wavelengths 100, 200 and 300 nm in the second order is diffracted in the same direction as the light for wavelengths 200, 400 and 600 nm in the first order. In this diagram, the light is incident from the right, so $\alpha < 0$.

2.3.1. Angular dispersion

The angular spread $d\beta$ of a spectrum of order *m* between the wavelength λ and $\lambda + d\lambda$ can be obtained by differentiating the grating equation, assuming the incidence angle α to be constant. The change *D* in diffraction angle per unit wavelength is therefore

$$D = \frac{\partial \beta}{\partial \lambda} = \frac{m}{d \cos \beta} = \frac{m}{d} \sec \beta = Gm \sec\beta \qquad (2\text{-}9)$$

where β is given by Eq. (2-2). The ratio $D = d\beta / d\lambda$ is called the *angular dispersion*. As the groove frequency $G = 1/d$ increases, the angular dispersion increases (meaning that the angular separation between wavelengths increases

for a given order *m*).

In Eq. (2-9), it is important to realize that the quantity *m*/*d* is not a ratio which may be chosen independently of other parameters; substitution of the grating equation into Eq. (2-9) yields the following general equation for the angular dispersion:

$$D = \frac{\partial \beta}{\partial \lambda} = \frac{\sin \alpha + \sin \beta}{\lambda \cos \beta} \qquad (2\text{-}10)$$

For a given wavelength, this shows that the angular dispersion may be considered to be solely a function of the angles of incidence and diffraction. This becomes even more clear when we consider the Littrow configuration ($\alpha = \beta$), in which case Eq. (2-10) reduces to

$$D = \frac{\partial \beta}{\partial \lambda} = \frac{2}{\lambda} \tan \beta , \quad \text{in Littrow.} \qquad (2\text{-}11)$$

When $|\beta|$ increases from 10° to 63° in Littrow use, the angular dispersion increases by a factor of ten, regardless of the spectral order or wavelength under consideration. Once β has been determined, the choice must be made whether a fine-pitch grating (small *d*) should be used in a low order, or a course-pitch grating (large *d*) such as an echelle grating should be used in a high order. [The fine-pitched grating, though, will provide a larger free spectral range; see Section 2.7 below.]

2.3.2. Linear dispersion

For a given diffracted wavelength λ in order *m* (which corresponds to an angle of diffraction β), the *linear dispersion* of a grating system is the product of the angular dispersion *D* and the effective focal length *r'* (β) of the system:

$$r'D = r' \frac{\partial \beta}{\partial \lambda} = \frac{mr'}{d \cos \beta} = \frac{mr'}{d} \sec \beta = Gmr' \sec\beta. \qquad (2\text{-}12)$$

The quantity $r'\,d\beta = dl$ is the change in position along the spectrum (a real distance, rather than a wavelength). We have written $r'(\beta)$ for the focal length to show explicitly that it may depend on the diffraction angle β (which, in turn, depends on λ).

The *reciprocal linear dispersion*, also called the *plate factor P*, is more often considered; it is simply the reciprocal of $r'D$, usually measured in nm/mm:

$$P = \frac{d\cos\beta}{mr'}. \qquad (2\text{-}12')$$

P is a measure of the change in wavelength (in nm) corresponding to a change in location along the spectrum (in mm). It should be noted that the terminology *plate factor* is used by some authors to represent the quantity $1/\sin\Phi$, where Φ is the angle the spectrum makes with the line perpendicular to the diffracted rays (see Figure 2-6); in order to avoid confusion, we call the quantity $1/\sin\Phi$ the *obliquity factor*. When the image plane for a particular wavelength is not perpendicular to the diffracted rays (i.e., when $\Phi \neq 90°$), *P* must be multiplied by the obliquity factor to obtain the correct reciprocal linear dispersion in the image plane.

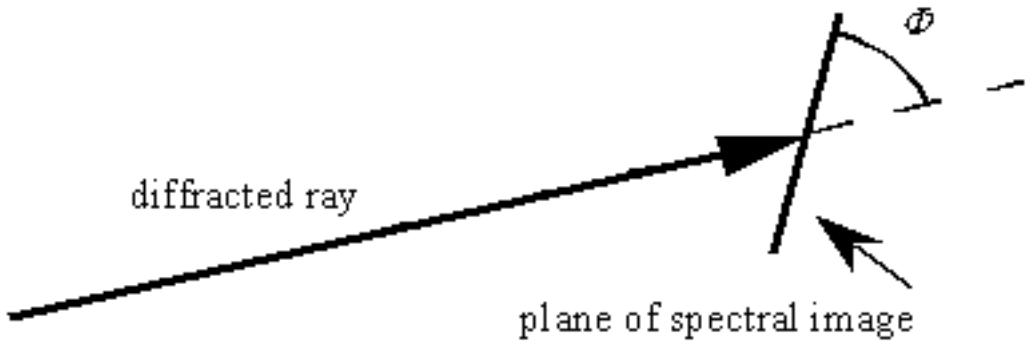

Figure 2-6. The obliquity angle Φ. The spectral image recorded need not lie in the plane perpendicular to the diffracted ray (i.e., $\Phi \neq 90°$).

2.4. RESOLVING POWER, SPECTRAL RESOLUTION, AND BANDPASS [top]

2.4.1. Resolving power

The resolving power *R* of a grating is a measure of its ability to separate adjacent spectral lines of average wavelength λ. It is usually expressed as the dimensionless quantity

$$R = \frac{\lambda}{\Delta\lambda}. \qquad (2\text{-}13)$$

Here Δλ is the *limit of resolution*, the difference in wavelength between two lines of equal intensity that can be distinguished (that is, the peaks of two wavelengths λ_1 and λ_2 for which the separation $|\lambda_1 - \lambda_2| < \Delta\lambda$ will be ambiguous). The theoretical resolving power of a planar diffraction grating is given in elementary optics textbooks as

$$R = mN. \qquad (2\text{-}14)$$

where *m* is the diffraction order and *N* is the total number of grooves illuminated on the surface of the grating. For negative orders ($m < 0$), the absolute value of *R* is considered.

A more meaningful expression for *R* is derived below. The grating equation can be used to replace *m* in Eq. (2-14):

$$R = \frac{Nd\left(\sin\alpha + \sin\beta\right)}{\lambda}. \qquad (2\text{-}15)$$

If the groove spacing *d* is uniform over the surface of the grating, and if the grating substrate is planar, the quantity *Nd* is simply the ruled width *W* of the grating, so

$$R = \frac{W(\sin\alpha + \sin\beta)}{\lambda}. \qquad (2\text{-}16)$$

As expressed by Eq. (2-16), *R* is not dependent explicitly on the spectral order or the number of grooves; these parameters are contained within the ruled width and the angles of incidence and diffraction. Since

$$|\sin\alpha + \sin\beta| < 2 \qquad (2\text{-}17)$$

the maximum attainable resolving power is

$$R_{MAX} = \frac{2W}{\lambda} \qquad (2\text{-}18)$$

regardless of the order *m* or number of grooves *N*. This maximum condition corresponds to the grazing Littrow configuration, i.e., $\alpha \approx \beta$ (Littrow), $|\alpha| \approx 90°$ (grazing).

It is useful to consider the resolving power as being determined by the maximum phase retardation of the extreme rays diffracted from the grating. Measuring the difference in optical path lengths between the rays diffracted from opposite sides of the grating provides the maximum phase retardation; dividing this quantity by the wavelength λ of the diffracted light gives the resolving power *R*.

The degree to which the theoretical resolving power is attained depends not only on the angles α and β, but also on the optical quality of the grating surface, the uniformity of the groove spacing, the quality of the associated optics, and the width of the slits and/or detector elements. Any departure of the diffracted wavefront greater than $\lambda/10$ from a plane (for a plane grating) or from a sphere (for a spherical grating) will result in a loss of resolving power due to aberrations at the image plane. The grating groove spacing must be kept constant to within about 1% of the wavelength at which theoretical performance is desired. Experimental details, such as slit width, air currents, and vibrations can seriously interfere with obtaining optimal results.

The practical resolving power is limited by the spectral half-width of the

lines emitted by the source. This explains why systems with revolving powers greater than 500,000 are usually required only in the study of spectral line shapes, Zeeman effects, and line shifts, and are not needed for separating individual spectral lines.

A convenient test of resolving power is to examine the isotopic structure of the mercury emission line at 546.1 nm. Another test for resolving power is to examine the line profile generated in a spectrograph or scanning spectrometer when a single mode laser is used as the light source. Line width at half intensity (or other fractions as well) can be used as the criterion. Unfortunately, resolving power measurements are the convoluted result of all optical elements in the system, including the locations and dimensions of the entrance and exit slits and the auxiliary lenses and mirrors, as well as the quality of these optics. Their effects are necessarily superimposed on those of the grating.

2.4.2. Spectral resolution

While resolving power can be considered a characteristic of the grating and the angles at which it is used, the ability to resolve two wavelengths λ_1 and $\lambda_2 = \lambda_1 + \Delta\lambda$ generally depends not only on the grating but on the dimensions and locations of the entrance and exit slits (or detector elements), the aberrations in the images, and the magnification of the images. The minimum wavelength difference $\Delta\lambda$ (also called the *limit of resolution*, or simply *resolution*) between two wavelengths that can be resolved unambiguously can be determined by convoluting the image of the entrance aperture (at the image plane) with the exit aperture (or detector element). This measure of the ability of a grating system to resolve nearby wavelengths is arguably more relevant than is resolving power, since it takes into account the image effects of the system. While resolving power is a dimensionless quantity, resolution has spectral units (usually nanometers).

2.4.3. Bandpass

The *bandpass B* of a spectroscopic system is the wavelength interval of the light that passes through the exit slit (or falls onto a detector element). It is

often defined as the difference in wavelengths between the points of half-maximum intensity on either side of an intensity maximum. An estimate for bandpass is the product of the exit slit width *w'* and the reciprocal linear dispersion *P*:

$$B \approx w' P. \qquad (2\text{-}19)$$

An instrument with smaller bandpass can resolve wavelengths that are closer together than an instrument with a larger bandpass. Bandpass can be reduced by decreasing the width of the exit slit (to a certain limit; see Chapter 8), but usually at the expense of decreasing light intensity as well.

Bandpass is sometimes called *spectral bandwidth*, though some authors assign distinct meanings to these terms.

2.4.4. Resolving power vs. resolution

In the literature, the terms *resolving power* and *resolution* are sometimes interchanged. While the word *power* has a very specific meaning (energy per unit time), the phrase *resolving power* does not involve *power* in this way; as suggested by Hutley, though, we may think of resolving power as 'ability to resolve'.

The comments above regarding resolving power and resolution pertain to planar classical gratings used in collimated light (plane waves). The situation is complicated for gratings on concave substrates or with groove patterns consisting of unequally spaced lines, which restrict the usefulness of the previously defined simple formulae, though they may still yield useful approximations. Even in these cases, though, the concept of maximum retardation is still a useful measure of the resolving power.

2.5. FOCAL LENGTH AND *f*/NUMBER [top]

For gratings (or grating systems) that image as well as diffract light, or

disperse light that is not collimated, a *focal length* may be defined. If the beam diffracted from a grating of a given wavelength λ and order *m* converges to a focus, then the distance between this focus and the grating center is the focal length *r′(λ)*. [If the diffracted light is collimated, and then focused by a mirror or lens, the focal length is that of the refocusing mirror or lens and not the distance to the grating.] If the diffracted light is diverging, the focal length may still be defined, although by convention we take it to be negative (indicating that there is a virtual image behind the grating). Similarly, the incident light may diverge toward the grating (so we define the incidence or entrance slit distance $r(\lambda) > 0$) or it may converge toward a focus behind the grating (for which $r(\lambda) < 0$). Usually gratings are used in configurations for which *r* does not depend on wavelength (though in such cases *r′* usually depends on λ).

In Figure 2-7, a typical concave grating configuration is shown; the monochromatic incident light (of wavelength λ) diverges from a point source at A and is diffracted toward B. Points A and B are distances *r* and *r′*, respectively, from the grating center O. In this figure, both *r* and *r′* are positive.

Calling the width (or diameter) of the grating (in the dispersion plane) *W* allows the *input* and *output f/numbers* (also called *focal ratios*) to be defined:

$$f/\mathrm{no}_{\mathrm{INPUT}} = \frac{r}{W}, \quad f/\mathrm{no}_{\mathrm{OUTPUT}} = \frac{r'(\lambda)}{W} \qquad (2\text{-}20)$$

Usually the input *f*/number is matched to the *f*/number of the light cone leaving the entrance optics (*e.g.*, an entrance slit or fiber) in order to use as much of the grating surface for diffraction as possible. This increases the amount of diffracted energy while not overfilling the grating (which would generally contribute to stray light).

For oblique incidence or diffraction, Eqs. (2-20) are often modified by replacing *W* with the projected width of the grating:

$$f/\mathrm{no}_{\mathrm{INPUT}} = \frac{r}{W\cos\alpha}, \quad f/\mathrm{no}_{\mathrm{OUTPUT}} = \frac{r'(\lambda)}{W\cos\beta} \qquad (2\text{-}21)$$

These equations account for the reduced width of the grating as seen by the entrance and exit slits; moving toward oblique angles (*i.e.*, increasing $|\alpha|$ or $|\beta$

|) decreases the projected width and therefore increases the f/number.

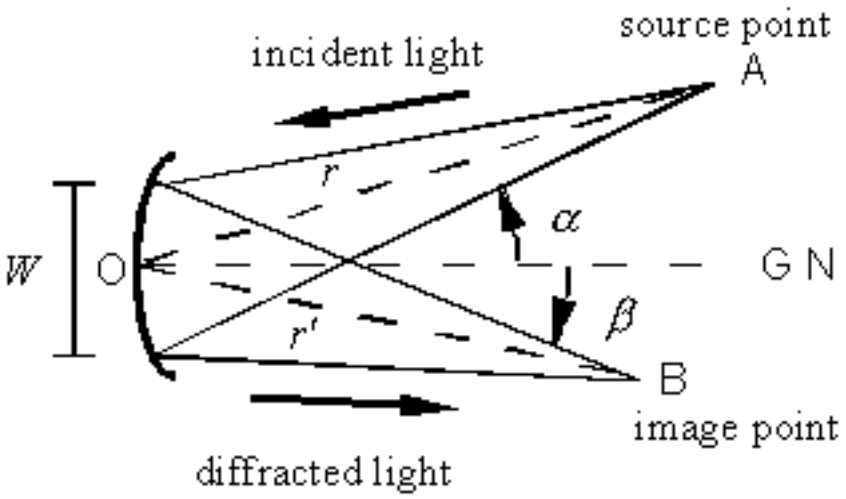

Figure 2-7. Geometry for focal distances and focal ratios (f/numbers). GN is the grating normal (perpendicular to the grating at its center, O), W is the width of the grating (its dimension perpendicular to the groove direction, which is out of the page), and A and B are the source and image points, respectively.

The focal length is an important parameter in the design and specification of grating spectrometers, since it governs the overall size of the optical system (unless folding mirrors are used). The ratio between the input and output focal lengths determines the projected width of the entrance slit that must be matched to the exit slit width or detector element size. The f/number is also important, as it is generally true that spectral aberrations decrease as f/number increases. Unfortunately, increasing the input f/number results in the grating subtending a smaller solid angle as seen from the entrance slit; this will reduce the amount of light energy the grating collects and consequently reduce the intensity of the diffracted beams. This trade-off prohibits the formulation of a simple rule for choosing the input and output f/numbers, so sophisticated design procedures have been developed to minimize aberrations while maximizing collected energy. See Chapter 7 for a discussion of the imaging properties and Chapter 8 for a description of the efficiency characteristics of grating systems.

2.6. ANAMORPHIC MAGNIFICATION [top]

For a given wavelength λ, we may consider the ratio of the width of a collimated diffracted beam to that of a collimated incident beam to be a measure of the effective magnification of the grating (see Figure 2-8). From this figure we see that this ratio is

$$\frac{b}{a} = \frac{\cos \beta}{\cos \alpha} \qquad (2\text{-}22)$$

Since α and β depend on λ through the grating equation (2-1), this magnification will vary with wavelength. The ratio *b*/*a* is called the *anamorphic magnification*; for a given wavelength λ, it depends only on the angular configuration in which the grating is used.

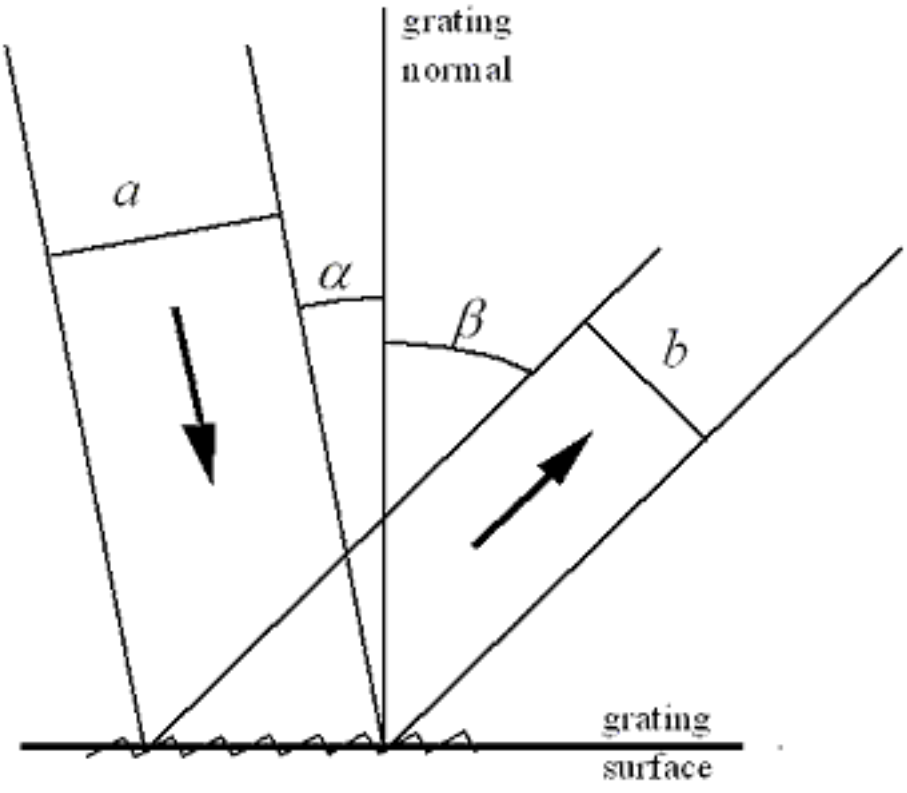

Figure 2-8. Anamorphic magnification. The ratio *b*/*a* of the beam widths equals the anamorphic magnification.

The magnification of an object not located at infinity (so that the incident rays are not collimated) is discussed in Chapter 8.

2.7. FREE SPECTRAL RANGE [top]

For a given set of incidence and diffraction angles, the grating equation is satisfied for a different wavelength for each integral diffraction order *m*. Thus light of several wavelengths (each in a different order) will be diffracted along the same direction: light of wavelength λ in order *m* is diffracted along the same direction as light of wavelength λ/2 in order 2*m*, *etc*.

The range of wavelengths in a given spectral order for which superposition of light from adjacent orders does not occur is called the *free spectral range Fλ*. It can be calculated directly from its definition: in order *m*, the wavelength of light that diffracts along the direction of λ_1 in order *m*+1 is $\lambda_1 + \Delta\lambda$, where

$$\lambda_1 + \Delta\lambda = \frac{m+1}{m}\lambda_1 \qquad (2\text{-}23)$$

from which

$$F_\lambda = \Delta\lambda = \frac{\lambda_1}{m}\,. \qquad (2\text{-}24)$$

The concept of free spectral range applies to all gratings capable of operation in more than one diffraction order, but it is particularly important in the case of echelles, because they operate in high orders with correspondingly short free spectral ranges.

Free spectral range and order sorting are intimately related, since grating systems with greater free spectral ranges may have less need for filters (or cross-dispersers) that absorb or diffract light from overlapping spectral orders. This is one reason why first-order applications are widely popular.

2.8. ENERGY DISTRIBUTION (GRATING EFFICIENCY) [top]

The distribution of incident field power of a given wavelength diffracted by a grating into the various spectral order depends on many parameters, including the power and polarization of the incident light, the angles of incidence and diffraction, the (complex) index of refraction of the metal (or glass or dielectric) of the grating, and the groove spacing. A complete treatment of grating efficiency requires the vector formalism of electromagnetic theory (*i.e.*, Maxwell's equations), which has been studied in detail over the past few decades. While the theory does not yield conclusions easily, certain rules of thumb can be useful in making approximate predictions. The topic of grating efficiency is addressed more fully in Chapter 9.

Recently, computer codes have become commercially available that accurately predict grating efficiency for a wide variety of groove profiles over wide spectral ranges.

2.9. SCATTERED AND STRAY LIGHT [top]

All light that reaches the image plane from anywhere other than the grating, by any means other than diffraction as governed by Eq. (2-1), is called *stray light*. All components in an optical system contribute stray light, as will any baffles, apertures, and partially reflecting surfaces. Unwanted light originating from the grating itself is often called *scattered light*.

2.9.1. Scattered light

Of the radiation incident on the surface of a diffraction grating, some will be diffracted according to Eq. (2-1) and some will be absorbed by the grating itself. The remainder is unwanted energy called *scattered light*. Scattered light may arise from several factors, including imperfections in the

shape and spacing of the grooves and roughness on the surface of the grating.

Diffuse scattered light is scattered into the hemisphere in front of the grating surface. It is due mainly to grating surface microroughness. It is the primary cause of scattered light in interference gratings. For monochromatic light incident on a grating, the intensity of diffuse scattered light is higher near the diffraction orders for that wavelength than between the diffracted orders. M.C. Hutley (National Physical Laboratory) found this intensity to be proportional to slit area, and probably proportional to $1/\lambda^4$.

In-plane scatter is unwanted energy in the dispersion plane. Due primarily to random variations in the groove spacing or groove depth, its intensity is directly proportional to slit area and probably inversely proportional to the square of the wavelength.

Ghosts are caused by periodic errors in the groove spacing. Characteristic of ruled gratings, interference gratings are free from ghosts when properly made.

2.9.2. Instrumental stray light

Stray light for which the grating cannot be blamed is called *instrumental stray light*. Most important is the ever-present light reflected into the zero order, which must be trapped so that it does not contribute to stray light. Light diffracted into other orders may also find its way to the detector and therefore constitute stray light. Diffraction from sharp edges and apertures causes light to propagate along directions other than those predicted by the grating equation. Reflection from instrument chamber walls and mounting hardware also contributes to the redirection of unwanted energy toward the image plane; generally, a smaller instrument chamber presents more significant stray light problems. Light incident on detector elements may be reflected back toward the grating and rediffracted; since the angle of incidence may now be different, light rediffracted along a given direction will generally be of a different wavelength than the light that originally diffracted along the same direction. Baffles, which trap diffracted energy outside the spectrum of interest, are intended to reduce the amount of light in other orders and in other wavelengths, but they may themselves diffract and reflect this light so that it ultimately

reaches the image plane.

2.10. SIGNAL-TO-NOISE RATIO (SNR) [top]

The *signal-to-noise ratio* (SNR) is the ratio of diffracted energy to unwanted light energy. While we might be tempted to think that increasing diffraction efficiency will increase SNR, stray light usually plays the limiting role in the achievable SNR for a grating system.

Replicated gratings from ruled master gratings generally have quite high SNRs, though holographic gratings sometimes have even higher SNRs, since they have no ghosts due to periodic errors in groove location and lower interorder stray light.

As SNR is an instrument function, not a property of the grating only, there exist no clear rules of thumb regarding what type of grating will provide higher SNR.

PREVIOUS CHAPTER NEXT CHAPTER

Back to top

3. RULED GRATINGS

PREVIOUS CHAPTER
NEXT CHAPTER

TABLE OF CONTENTS

3.0. INTRODUCTION [top]

The first diffraction gratings made for commercial use were mechanically ruled, manufactured by burnishing grooves individually with a diamond tool against a thin coating of evaporated metal applied to a plane or concave surface. Such *ruled gratings* comprise the majority of diffraction gratings used in spectroscopic instrumentation.

3.1. RULING ENGINES [top]

The most vital component in the production of ruled diffraction gratings is the apparatus, called a *ruling engine*, on which master gratings are ruled. At present, Thermo RGL has three ruling engines in full-time operation, each producing substantial numbers of high-quality master gratings every year. Each of these systems produce gratings with very low Rowland ghosts and high

resolving power.

Selected diamonds, whose crystal axis is oriented for optimum behavior, are used to shape the grating grooves. The ruling diamonds are carefully shaped by skilled diamond tool makers to produce the exact groove profile required for each grating. The carriage that carries the diamond back and forth during ruling must maintain its position to better than a few nanometers for ruling periods that may last for one day or as long as six weeks.

The mechanisms for advancing the grating carriages on all Thermo RGL engines are designed to make it possible to rule gratings with a wide choice of groove spacings. The current *Diffraction Grating Catalog* shows the range of groove spacings available.

3.1.1. The Michelson engine

In 1947 Bausch & Lomb acquired its first ruling engine from the University of Chicago; this engine was originally designed by Albert Michelson in the 1910s and rebuilt by B. Gale. It underwent further refinement, which greatly improved its performance, and has produced a continuous supply of high quality gratings of up to 200 x 250 mm ruled area.

The Michelson engine originally used an interferometer system to plot, every few years, the error curve of the screw, from which an appropriate mechanical correction cam was derived. In 1990, this system was superseded by the addition of a digital computer servo control system based on a laser interferometer. The Michelson engine is unusual in that it covers the widest range of groove spacings of any ruling engine: it can rule gratings as coarse as 20 grooves per millimeter (g/mm) and as fine as 10,800 g/mm.

3.1.2. The Mann engine

The second engine, installed at the Laboratory has been producing gratings since 1953, was originally built by David W. Mann of Lincoln, Massachusetts. Bausch & Lomb equipped it with an interferometric control system following the technique of Prof. George Harrison of MIT. The Mann

engine can rule areas up to 110 x 110 mm, with virtually no ghosts and nearly theoretical resolving power.

While the lead screws of the ruling engines are lapped to the highest precision attainable, there are always residual errors in both threads and bearings that must be compensated to produce the highest quality gratings. The Mann engine is equipped with an automatic interferometer servo system that continually adjusts the grating carriage to the correct position as each groove is ruled. In effect, the servo system simulates a perfect screw.

3.1.3. The MIT 'B' engine

The third engine was built by Harrison and moved to Rochester in 1968. It has the capacity to rule plane gratings to the greatest precision ever achieved; these gratings may be up to 400 mm wide, with grooves (between 20 and 1500 per millimeter) up to 300 mm long. It uses a double interferometer control system, based on a frequency-stabilized laser, to monitor not only table position but to correct residual yaw errors as well. This engine produces gratings with nearly theoretical resolving powers, virtually eliminating Rowland ghosts and minimizing stray light. It has also ruled almost perfect echelle gratings, the most demanding application of a ruling engine.

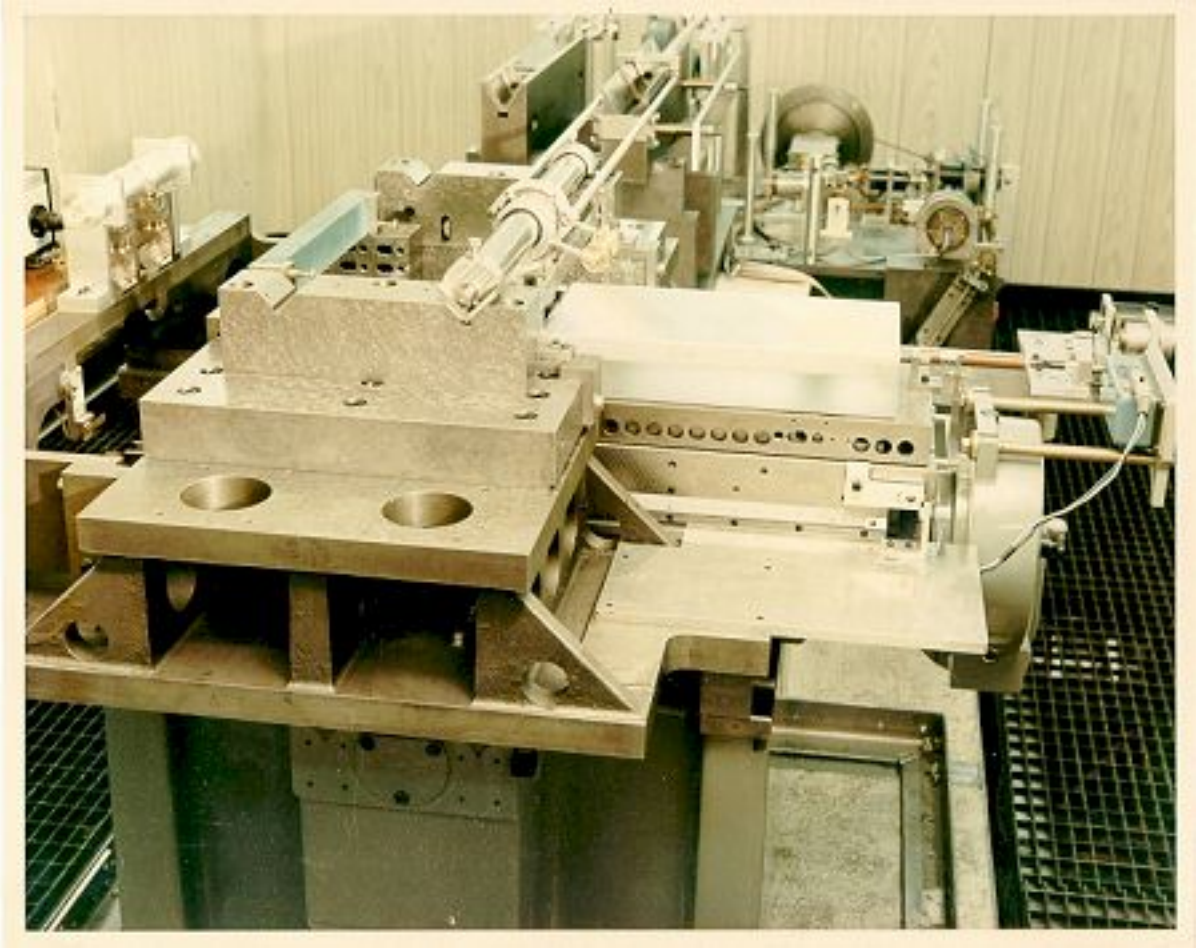

Figure 3-1. MIT 'B' Engine. This ruling engine, now in operation at Thermo RGL, is shown with its cover removed.

3.2. THE RULING PROCESS [top]

Master gratings are ruled on carefully selected well-annealed substrates of several different materials. The choice is generally between BK-7 optical glass, special grades of fused silica, or a special grade of ZeroDur®. The optical surfaces of these substrates are polished to closer than λ/10 for green light (about 50 nm), then coated with a reflective film (usually aluminum or gold).

Compensating for changes in temperature and atmospheric pressure is especially important in the environment around a ruling engine. Room

temperature must be held constant to within 0.01 °C for small ruling engines (and to within 0.005 °C for larger engines). Since the interferometric control of the ruling process uses monochromatic light, whose wavelength is sensitive to the changes of the refractive index of air with pressure fluctuations, atmospheric pressure must be compensated for by the system. A change in pressure of 2.5 mm Hg results in a corresponding change in wavelength of one part per million. This change is negligible if the optical path of the interferometer is near zero, but becomes significant as the optical path increases during the ruling. If this effect is not compensated, the carriage control system of the ruling engine will react to this change in wavelength, causing a variation in groove spacing.

The ruling engine must also be isolated from vibrations, which are easily transmitted to the diamond; this may be done by suspending the engine mount from springs that isolate vibrations between frequencies from 2 or 3 Hz (which are of no concern) to about 60 Hz, above which vibration amplitudes are usually too small to have a noticeable effect.

The actual ruling of a master grating is a long, slow and painstaking process. The set-up of the engine, prior to the start of the ruling, requires great skill and patience. This critical alignment is impossible without the use of a high-power interference microscope, or an electron microscope for more finely spaced grooves.

After each microscopic examination, the diamond is readjusted until the operator is completely satisfied that the groove shape is the best possible for the particular grating being ruled. This painstaking adjustment, although time consuming, results in very "bright" gratings with nearly all the diffracted light energy concentrated in a specific angular range of the spectrum. This ability to concentrate the light selectively at a certain part of the spectrum is what distinguishes blazed diffraction gratings from all others.

Finished master gratings are carefully tested to be certain that they have met specifications completely. The wide variety of tests run to evaluate all the important properties include resolution, efficiency, Rowland ghost intensity, and surface accuracy. Wavefront interferometry is used when appropriate. If a grating meets all specifications, it is then used as a master for the production of our replica gratings.

3.3. VARIED LINE-SPACE (VLS) GRATINGS [top]

For the last century great effort has been expended in keeping the spacing between successive grooves uniform as a master grating is ruled. As early as 1875, A. Cornu realized that variations in the groove spacing modified the curvature of the diffracted wavefronts. While periodic and random variations were understood to produce stray light, a uniform variation in groove spacing across the grating surface was recognized by Cornu to change the location of the focus of the spectrum, which need not be considered a defect if properly taken into account. He determined that a planar classical grating, which by itself would have no focusing properties if used in collimated incident light, would focus the diffracted light if ruled with a systematic 'error' in its groove spacing. He was able to verify this by ruling three gratings whose groove positions were specified to vary as each groove was ruled. Such gratings, in which the pattern of straight parallel grooves has a variable yet well-defined (though not periodic) spacing between successive grooves, are now called *varied line-space (VLS) gratings*.

The Michelson engine, which has digital computer control, can readily rule VLS gratings. Any groove spacing *d(y)* that varies reasonably as a function of position *y* along the grating surface (and no more than about ±100 nm from the nominal groove spacing) can be programmed into the computer. The relationship between groove spacing (and curvature) and imaging is discussed in Chapter 7.

PREVIOUS CHAPTER NEXT CHAPTER

Back to top

4. HOLOGRAPHIC GRATINGS

PREVIOUS CHAPTER
NEXT CHAPTER

TABLE OF CONTENTS

4.0. INTRODUCTION
4.1. PRINCIPLE OF MANUFACTURE
4.1.1. Formation of an interference pattern
4.1.2. Formation of the grooves
4.2. CLASSIFICATION OF HOLOGRAPHIC GRATINGS
4.2.1. Single-beam interference
4.2.2. Double-beam interference
4.3. THE RECORDING PROCESS
4.4. DIFFERENCES BETWEEN RULED AND HOLOGRAPHIC GRATINGS
4.4.1. Differences in grating efficiency
4.4.2. Differences in scattered light
4.4.3. Differences and limitations in the groove profile
4.4.4. Limitations in obtainable groove frequencies
4.4.5. Differences in the groove patterns
4.4.6. Differences in the substrate shapes
4.4.7. Differences in generation time for master gratings

4.0. INTRODUCTION [top]

Since the late 1960s, a method distinct from mechanical ruling has also been used to manufacture diffraction gratings. This method involves the photographic recording of a stationary interference fringe field. Such

interference gratings, more commonly (though inaccurately) known as *holographic gratings*, have several characteristics that distinguish them from ruled gratings.

In 1901 Aimé Cotton produced experimental interference gratings, fifty years before the concepts of holography were developed by Gabor. A few decades later, Michelson considered the interferometric generation of diffraction gratings obvious, but recognized that an intense monochromatic light source and a photosensitive material of sufficiently fine granularity did not then exist. In the mid 1960s, ion lasers and photoresists (grainless photosensitive materials) became available; the former provided a strong monochromatic line, and the latter was photoactive at the molecular level, rather than at the crystalline level (unlike, for example, photographic film). In 1967 D. Rudolph and G. Schmahl at the University of Göttingen and A. Labeyrie and J. Flamand in France independently produced the first holographic diffraction gratings of spectroscopic quality.

4.1. PRINCIPLE OF MANUFACTURE [top]

4.1.1. Formation of an interference pattern

When two sets of coherent equally polarized monochromatic optical plane waves of equal intensity intersect each other, a standing wave pattern will be formed in the region of intersection if both sets of waves are of the same wavelength λ (see Figure 4-1). The combined intensity distribution forms a set of straight equally-spaced fringes (bright and dark lines). Thus a photographic plate would record a fringe pattern, since the regions of zero field intensity would leave the film unexposed while the regions of maximum intensity would leave the film maximally exposed. Regions between these extremes, for which the combined intensity is neither maximal nor zero, would leave the film partially exposed. The combined intensity varies sinusoidally with position as the interference pattern is scanned along a line. If the beams are not of equal intensity, the minimum intensity will no longer be zero, thereby decreasing the contrast between the fringe. As a consequence, all portions of the photographic plate will be exposed to some degree.

The centers of adjacent fringes (that is, adjacent lines of maximum

intensity) are separated by a distance *d*, where

$$d = \frac{\lambda}{2 \sin \theta} \qquad (4\text{-}1)$$

and θ is the half the angle between the beams. A small angle between the beams will produce a widely spaced fringe pattern (large *d*), whereas a larger angle will produce a fine fringe pattern. The lower limit for *d* is λ/2, so for visible recording light, thousands of fringes per millimeter may be formed.

4.1.2. Formation of the grooves

Master holographic diffraction gratings are recorded in photoresist, a material whose intermolecular bonds are either strengthened or weakened by exposure to light. Commercially available photoresists are more sensitive to some wavelengths than others; the recording laser line must be matched to the type of photoresist used. The proper combination of an intense laser line and a photoresist that is highly sensitive to this wavelength will reduce exposure time.

Photoresist gratings are chemically developed after exposure to reveal the fringe pattern. A photoresist may be *positive* or *negative*, though the latter is rarely used. During chemical development, the portions of a substrate covered in positive photoresist that have been exposed to light are dissolved, while for negative photoresist the unexposed portions are dissolved. Upon immersion in the chemical developer, a surface relief pattern is formed: for positive photoresist, valleys are formed where the bright fringes were, and ridges where the dark fringes were. At this stage a master holographic grating has been produced; its grooves are sinusoidal ridges. This grating may be coated and replicated like master ruled gratings.

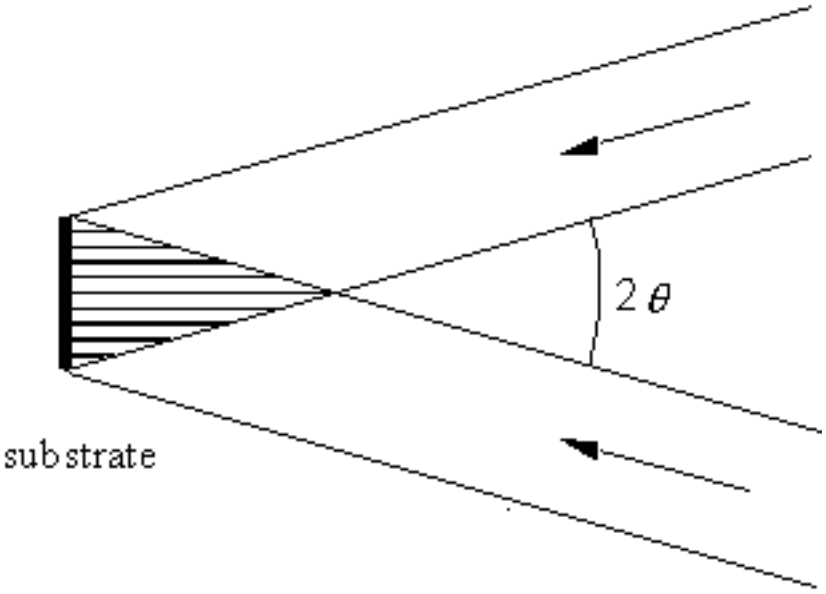

Figure 4-1. Formation of interference fringes. Two collimated beams of wavelength λ form an interference pattern composed of straight equally spaced planes of intensity maxima (shown as the horizontal lines). A sinusoidally varying interference pattern is found at the surface of a substrate placed perpendicular to these planes.

4.2. CLASSIFICATION OF HOLOGRAPHIC GRATINGS

[top]

4.2.1. Single-beam interference

An interference pattern can be generated from a single collimated monochromatic coherent light beam if it is made to reflect back upon itself. A standing wave pattern will be formed, with intensity maxima forming planes parallel to the wavefronts. The intersection of this interference pattern with a photoresist-covered substrate will yield on its surface a pattern of grooves, whose spacing *d* depends on the angle θ between the substrate surface and the planes of maximum intensity (see Figure 4-2); the relation between *d* and θ is identical to Eq. (4-1), though it must be emphasized that the recording geometry behind the single-beam holographic grating (or *Sheridon grating*) is different from that of the double-beam geometry for which Eq. (4-1) was

derived.

The groove depth *h* for a Sheridon grating is dictated by the separation between successive planes of maximum intensity (nodal planes); explicitly,

$$h = \frac{\lambda}{2n} \qquad (4\text{-}2)$$

where λ is the wavelength of the recording light and *n* the refractive index of the photoresist. This severely limits the range of available blaze wavelengths, typically to those between 200 and 250 nm.

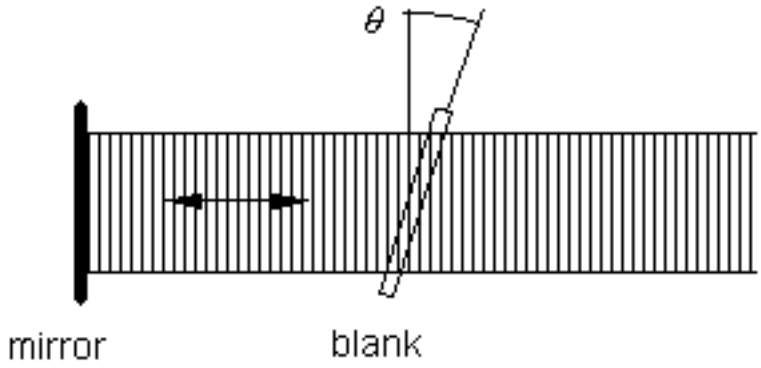

Figure 4-2. Sheridon recording method. A collimated beam of light, incident from the right, is retroreflected by a plane mirror, which forms a standing wave pattern whose intensity maxima are shown. A transparent blank (substrate), inclined at an angle θ to the fringes, will have its surfaces exposed to a sinusoidally varying intensity pattern.

4.2.2. Double-beam interference

The double-beam interference pattern shown in Figure 4-1 is a series of straight parallel fringe planes, whose intensity maxima (or minima) are equally spaced throughout the region of interference. Placing a substrate covered in photoresist in this region will form a groove pattern defined by the intersection

of the surface of the substrate with the fringe planes. If the substrate is planar, the grooves will be straight, parallel and equally spaced, though their spacing will depend on the angle between the substrate surface and the fringe planes. If the substrate is concave, the grooves will be curved and unequally spaced, forming a series of circles of different radii and spacings. Regardless of the shape of the substrate, the intensity maxima are equally spaced planes, so the grating recorded will be a *classical equivalent holographic grating* (more often called simply a *classical grating*). This name recognizes that the groove pattern (on a planar surface) is identical to that of a planar classical ruled grating. Thus all holographic gratings formed by the intersection of two sets of plane waves are called classical equivalents, even if their substrates are not planar (and therefore groove patterns are not straight equally spaced parallel lines).

If two sets of spherical wavefronts are used instead, as in Figure 4-3, a *first generation holographic grating* is recorded. The surfaces of maximum intensity are now confocal hyperboloids (if both sets of wavefronts are converging, or if both are diverging) or ellipsoids (if one set is converging and the other diverging). This interference pattern can be obtained by focusing the recording laser light through pinholes (to simulate point sources). Even on a planar substrate, the fringe pattern will be a collection of unequally spaced curves. Such a groove pattern will alter the curvature of the diffracted wavefronts, regardless of the substrate shape, thereby providing focusing. Modification of the curvature and spacing of the grooves can be used to reduce aberrations in the spectral images (see Chapter 6).

The addition of auxiliary concave mirrors or lenses into the recording beams can render the recording wavefronts toroidal (that is, their curvature in two perpendicular directions will generally differ). The grating thus recorded is a *second generation holographic grating*. The additional degrees of freedom in the recording geometry (*e.g.*, the location, orientation and radii of the auxiliary mirrors) provide for further aberration reduction above that of first generation holographic gratings.

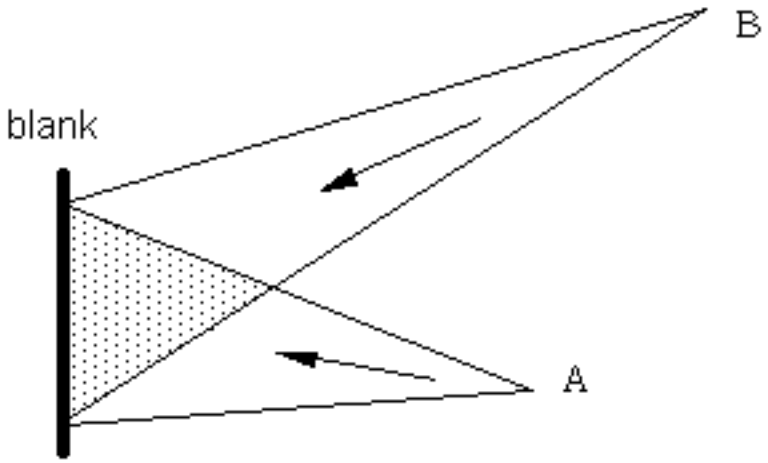

Figure 4-3. First-generation recording method.. Laser light focused through pinholes at A and B diverges toward the grating blank (substrate). The standing wave region is shaded; the intensity maxima are confocal hyperboloids.

4.3. THE RECORDING PROCESS [top]

Holographic gratings are recorded by placing a light-sensitive surface in an interferometer. The generation of an holographic grating of spectroscopic quality requires a stable optical bench and laser as well as precision optical components (mirrors, collimating optics, *etc.*). Ambient light must be eliminated so that fringe contrast is maximal. Thermal gradients and air currents, which change the local index of refraction in the beams of the interferometer, must be avoided. Thermo RGL records master holographic gratings in its specially-designed facility.

During the recording process, the components of the optical system must be of nearly diffraction-limited quality, and mirrors, pinholes and spatial filters must be adjusted as carefully as possible. Any object in the optical system receiving laser illumination may scatter this light toward the grating, which will contribute to stray light. Proper masking and baffling during recording are essential to the successful generation of a holographic grating, as is single-mode operation of the laser throughout the duration of the exposure.

The substrate on which the master holographic grating is to be produced

must be coated with a highly uniform, virtually defect-free coating of photoresist. Compared with photographic film, photoresists are somewhat insensitive to light during exposure, due to the molecular nature of their interaction with light. As a result, typical exposures may take from minutes to hours, during which time an extremely stable fringe pattern (and, therefore, optical system) is required. After exposure, the substrate is immersed in a developing agent, which forms a surface relief fringe pattern; coating the substrate with metal then produces a master holographic diffraction grating.

4.4. DIFFERENCES BETWEEN RULED AND HOLOGRAPHIC GRATINGS [top]

Due to the distinctions between the fabrication processes for ruled and holographic gratings, each type of grating has advantages and disadvantages relative to the other, some of which are described below.

4.4.1. Differences in grating efficiency

The efficiency curves of ruled and holographic gratings generally differ considerably, though this is a direct result of the differences in groove profiles and not strictly due to method of making the master grating. For example, holographic gratings made using the Sheridon method described in Section 4.2.1 above have nearly triangular groove profiles, and therefore have efficiency curves that look more like those of ruled gratings than those of sinusoidal-groove holographic gratings.

There exist no clear "rules of thumb" for describing the differences in efficiency curves between ruled and holographic gratings; the best way to gain insight into these differences is to look at representative curves of each grating type. Chapter 9 in this *Handbook* contains a number of curves; the paper[1] on which this chapter is based contains even more curves, and the book *Diffraction Gratings and Applications*[2] by Loewen and Popov has an extensive collection of efficiency curves and commentary regarding the efficiency behavior of plane reflection gratings, transmission gratings, echelle gratings

and concave gratings.

4.4.2. Differences in scattered light

Since holographic gratings do not involve burnishing grooves into a thin layer of metal, the surface irregularities on its grooves differ from those of mechanically ruled gratings. Moreover, errors of ruling, which are a manifestation of the fact that ruled gratings have one groove formed after another, are nonexistent in interferometric gratings, for which all grooves are formed simultaneously. If properly made, then, holographic gratings can be entirely free of both small periodic and random groove placement errors found on even the best mechanically ruled gratings. Holographic gratings may offer advantages to spectroscopic systems in which light scattered from the grating surface is performance-limiting, such as in the study of the Raman spectra of solid samples, though proper instrumental design is essential to ensure that the performance of the system is not limited by other sources of stray light.

4.4.3. Differences and limitations in the groove profile

The groove profile has a significant effect on the light intensity diffracted from the grating (see Chapter 8). While ruled gratings may have triangular or trapezoidal groove profiles, holographic gratings usually have sinusoidal (or nearly sinusoidal) groove profiles (see Figure 4-4). A ruled grating and an holographic grating, identical in every way except in groove profile, will have demonstrably different efficiencies (diffraction intensities) for a given wavelength and spectral order. Moreover, ruled gratings are more easily blazed (by choosing the proper shape of the burnishing diamond) than are holographic gratings, which are usually blazed by ion bombardment (ion etching). Differences in the intensity diffracted into the order in which the grating is to be used implies differences in the intensities in all other orders as well; excessive energy in other orders usually makes the suppression of stray light more difficult.

The distribution of groove profile characteristics across the surface of a grating may also differ between ruled and holographic gratings. For a ruled concave grating, the facet angles are not aligned identically and the effective

blaze wavelength varies from one side of the grating to the other. An holographic grating, on the other hand, usually demonstrates much less variation in efficiency characteristics across its surface. Gratings have been ruled by changing the facet angle at different places on the substrate during ruling. These so-called "multipartite" gratings, in which the ruling is interrupted and the diamond reoriented at different places across the width of the grating, demonstrate enhanced efficiency but do not provide the resolving power expected from an uninterrupted ruling (since each section of grooves may be out of phase with the others)[3].

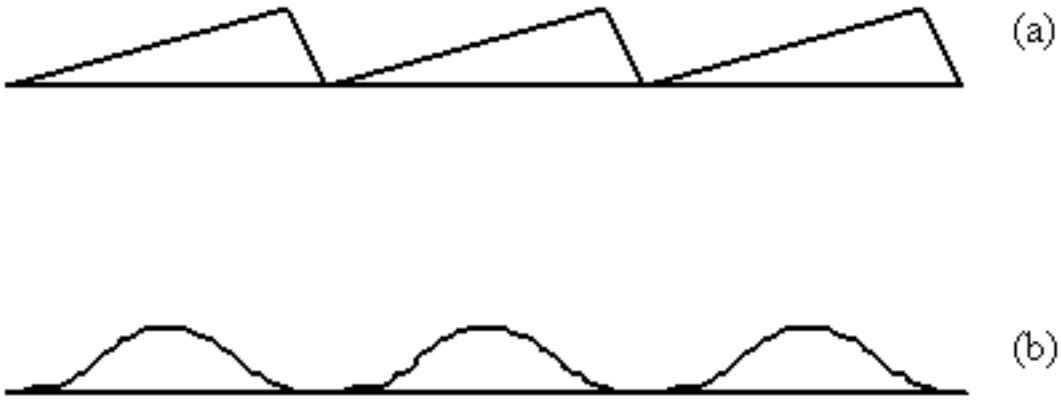

Figure 4-4. Groove profiles for ruled and holographic gratings.. (a) Triangular groove profile of a mechanically ruled grating. (b) Sinusoidal groove profile of an holographic grating.

4.4.4. Differences and limitations in the groove profile

Limits on the number of grooves per millimeter differ between ruled and holographic gratings: ruled gratings offer a much wider range of groove spacings. Below a few hundred grooves per millimeter the recording optical system necessary to generate holographic gratings becomes cumbersome, while ruled gratings can have as few as thirty grooves per millimeter. As upper limits, holographic gratings recorded with visible light are usually limited to a few thousand grooves per millimeter, whereas ruled gratings have been produced with over 10,000 grooves per millimeter.

4.4.5. Differences in the groove patterns

Classical ruled plane gratings, which constitute the vast majority of ruled gratings, have straight equally-spaced grooves. Classical ruled concave gratings have unequally spaced grooves that form circular arcs on the grating surface, but this groove pattern, when projected onto the plane tangent to the grating at its center, is still a set of straight equally spaced lines. [It is the projected groove pattern that governs imaging] Even ruled varied line-space (VLS) gratings (see Chapter 3) do not contain curved grooves, except on curved substrates. The aberration reduction possible with ruled gratings is therefore limited to that possible with straight grooves, though this limitation is due to the mechanical motions possible with present-day ruling engines rather than with the burnishing process itself.

Holographic gratings, on the other hand, need not have straight grooves. Groove curvature can be modified to reduce aberrations in the spectrum, thereby improving the throughput and resolution of imaging spectrometers. A common spectrometer mount is the *flat-field spectrograph*, in which the spectrum is imaged onto a flat detector array and several wavelengths are monitored simultaneously. Holographic gratings can significantly improve the imaging of such a grating system, whereas classical ruled gratings are not suitable for forming well-focused planar spectra without auxiliary optics.

4.4.6. Differences in the substrate shapes

The interference pattern used to record holographic gratings is not dependent on the substrate shape or dimension, so gratings can be recorded interferometrically on substrates of low f/number more easily than they can be mechanically ruled on these substrates. Consequently, holographic concave gratings lend themselves more naturally to systems with short focal lengths. Holographic gratings of unusual curvature can be recorded easily; of course, there may still remain technical problems associated with the replication of such gratings.

The substrate shape affects both the grating efficiency characteristics its imaging performance.

- Grating efficiency depends on the groove profile as well as the angle at which the light is incident and diffracted; for a concave grating, the both the groove profile and the local angles vary with position on the grating surface. This leads to the efficiency curve being the sum of the various efficiency curves for small regions of the grating, each with its own groove profile and incidence and diffraction angles.
- Grating imaging depends on the directions of the diffracted rays over the surface of the grating, which in turn are governed by the local groove spacing and curvature (*i.e.*, the *groove pattern*) as well as the local incidence angle. For a conventional plane grating used in collimated light, the groove pattern is the same everywhere on the grating surface, as is the incidence angle, so all diffracted ray are parallel. For a grating on a concave substrate, though, the groove pattern is generally position-dependent, as is the local incidence angle, so the set of diffracted rays are not parallel - thus the grating has focal (imaging) properties as well as dispersive properties.

4.4.7. Differences in generation time for master gratings

A ruled master grating is formed by burnishing each groove individually; to do so, the ruling diamond may travel a very large distance to rule one grating. For example, a square grating of dimensions 100 x 100 mm with 1000 grooves per millimeter will require the diamond to move 10 km (over six miles), which may take several weeks to rule.

In the fabrication of a master holographic grating, on the other hand, the grooves are created simultaneously. Exposure times vary from a few minutes to tens of minutes, depending on the intensity of the laser light used and the spectral response (sensitivity) of the photoresist at this wavelength. Even counting preparation and development time, holographic master gratings are produced much more quickly than ruled master gratings. Of course, an extremely stable and clean optical recording environment is necessary to record precision holographic gratings. For plane gratings, high-grade collimating optics are required, which can be a limitation for larger gratings.

Master holographic gratings as large as 180 mm in diameter are made routinely at Thermo RGL.

PREVIOUS CHAPTER NEXT CHAPTER

Back to top

5. REPLICATED GRATINGS

PREVIOUS CHAPTER
NEXT CHAPTER

TABLE OF CONTENTS

5.0. INTRODUCTION
5.1. THE REPLICATION PROCESS
5.2. REPLICA GRATINGS VS. MASTER GRATINGS
5.3. STABILITY OF REPLICATED GRATINGS

5.0. INTRODUCTION [top]

Decades of research and development at Thermo RGL have contributed to the process for manufacturing replicated diffraction gratings (*replicas*). This process is capable of producing thousands of duplicates of master gratings which equal the quality and performance of the master gratings. The replication process has reduced the price of a typical diffraction grating by a factor of 100 or more, compared with the cost of acquiring a master grating.

5.1. THE REPLICATION PROCESS [top]

The process for making replica gratings results in a grating whose grooves are formed in a very thin layer of resin that adheres strongly to the surface of the substrate material. The optical surface of a reflection replica is usually coated with aluminum, but gold or platinum is recommended for greater diffracted energy in certain spectral regions. Transmission gratings have no reflective coating.

The production of a replicated diffraction grating is a sequential process.

- *Submaster selection.* The replication process starts with the selection of a suitable *submaster* grating that has the desired specifications (groove frequency, blaze angle, size, …). [A submaster grating is a grating replicated from a master, or from another submaster, but is itself used not as an final optical product but as a mold for the replication of product gratings.]
- *Application of parting agent.* A parting agent is applied to the surface of the master grating. The parting agent serves no optical purpose and has no optical effects but aids in the separation of the delicate submaster and product grating surfaces.
- *Application of transfer coating.* After the parting agent is applied, a reflective coating (usually aluminum) is applied as well. This coating will form the optical surface of the product grating upon separation. To obtain an optical quality coating, this step is performed in a vacuum deposition chamber. [Since this coating is applied to the submaster, but transfers to the product grating upon separation, it is called a *transfer coating*.] Typical transfer coating thicknesses are about one micron.
- *Cementing.* A substrate is then cemented with a layer of resin to the grooved surface of the master grating; this layer can vary in thickness, but it is usually tens of microns thick. It is the resin that holds the groove profile and replicates it from the submaster to the product; the transfer coating is much too thin for this purpose. The "sandwich" formed by the substrate and submaster cemented together is shown in Figure 5-1.

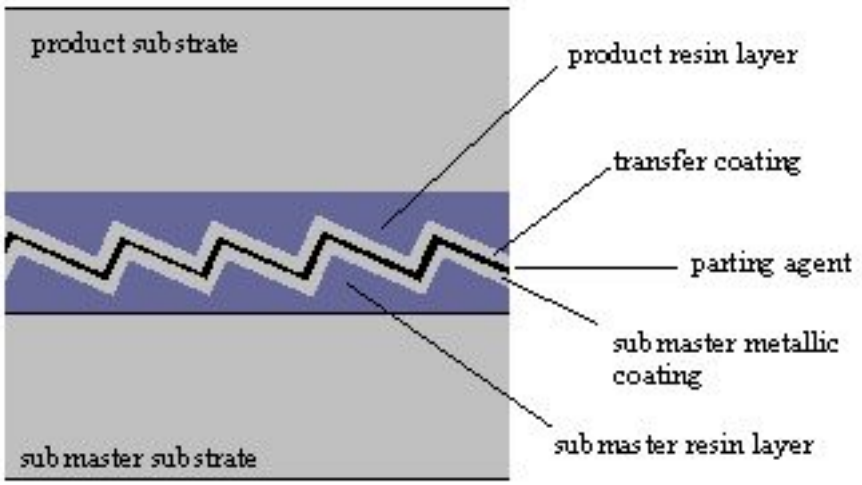

Figure 5-1. The replication "sandwich", showing the substrates, the resin

layers, the metallic coatings, and the parting agent.

Since the resin is in the liquid state when it is applied to the submaster, it must harden sufficiently to ensure that it can maintain the groove profile faithfully when the product grating is separated from the submaster. This hardening, or curing, is usually accomplished by a room-temperature cure period (lasting from hours to days) or by heating the resin to accelerate the curing.

- *Separation.* After the resin is fully cured, the groove profile is faithfully replicated in the resin when the submaster and product are separated. The parting agent serves as the weak interface and allows the separation to take place between the submaster coating and the transfer metallic coating. The groove profile on the product is the inverse of the groove profile on the submaster; if this profile is not symmetric with respect to this inversion, the efficiency characteristics of the two gratings will generally differ. In such cases, an additional replication must be done to invert the inverted profile, resulting in a profile identical to that of the original submaster. However, for certain types of gratings, inversion of the groove increases efficiency significantly.

  At this stage, if a transmission grating is desired, the transfer coating is removed from the product, leaving the groove structure intact in the transparent resin.

- *Inspection.* After separation, both the submaster and the product gratings are inspected for surface or substrate damage. The product grating may also be tested for key performance characteristics (*e.g.*, efficiency, wavefront flatness (or curvature), scattered light, alignment of the grooves to a substrate edge) depending on requirements.

The product grating formed by this replication process may be used as a grating, or it may serve as a mold (replication tool) by being considered a submaster. In this way, a single master grating can make several submasters, each of which can make several more submasters, *etc.*, to form a replication tree (see Figure 5-2).

The replication tree shown in Figure 5-2 illustrates two important features of replication: extension horizontally (within a generation) and vertically (to subsequent generations). Replication within a generation is accomplished by the successive replication of a single grating (much as a parent can have many children). Replication to additional generations is accomplished by forming a replica (child), which itself forms a replica (grandchild), *etc.* Thus replication can extend both within generations (X-1, X-2, X-3, X-4, …) and to subsequent generations (X-1, X-1-3, X-1-3-1, X-1-3-1-4, …) to create a large number of replicas from a single master grating.

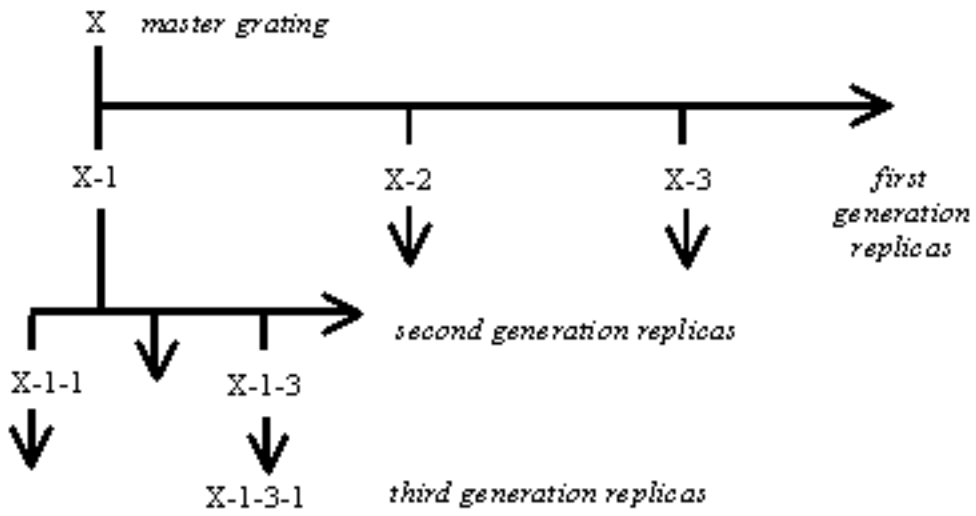

Figure 5-2. A replication tree. Master X is replicated to create several first-generation replicas (X-1, X-2, …), which themselves are replicated to form second-generation replicas (X-1-1, …), &c.

As an example, consider a master grating X from which five first-generation replicas are made (X-1 through X-5). Each of these is used as a submaster to form five replicas: X-1 forms X-1-1 through X-1-5, X-2 forms X-2-1 through X-2-5, and so on. This forms twenty-five second generation replicas. If each of these replicas is itself replicated five times, we arrive at 125 third-generation products (X-1-1-1, X-1-1-2, …, through X-5-5-5). This example illustrates that a large number of replicas can be made from a single master grating, assuming a conservative number of replicas and a reasonable number of generations.

The number N of replicas of a particular generation that can be made from a single master can be estimated using the following formula,

$$N = R^g \qquad (5\text{-}1)$$

where R is the number of replications per generation and g is the number of generations. Reasonable values of R are 5 to 10 (though values well above 20 are not unheard of), and g generally ranges from 3 to 9. Conservatively, then, for $R = 5$ and $g = 3$, we have $N = 125$ third-generation replicas; at the other end of the ranges we have $R = 10$ and $g = 9$ so that $N = 1{,}000{,}000{,}000$ ninth-generation replicas. Of course, one billion replicas of a single grating has never been required, but even if it were, Eq. (5-1) assumes that each replica in every generation (except the last) is replicated R times, whereas in practice most gratings cannot be replicated too many times before being damaged or otherwise rendered unusable. That is, some branches of the replication tree are truncated prematurely. Consequently, Eq. (5-1) must be taken as an upper limit, which becomes unrealistically high as either R or g increase. In practice, N can be in the thousands, and can be even higher if care is taken to ensure that the submasters in the replication tree are not damaged.

5.2. REPLICA GRATINGS VS. MASTER GRATINGS [top]

There are two fundamental differences between master gratings and replica gratings: how they are made and what they are made of.

- *Manufacturing process.* Replica gratings are made by the replication process outlined in Section 5.1 above - they are resin castings of master gratings. The master gratings themselves, though, are not castings: their grooves are created either by burnishing (in the case of ruled gratings) or by optical exposure and chemical development (in the case of holographic gratings).
- *Composition.* Replica gratings are composed of a metallic coating on a resin layer, which itself rests on a substrate (usually glass). Master gratings also usually have glass substrates, but have no resin (the grooves of a ruled master are contained entirely within a metallic layer on the substrate, and those of a holographic master are contained entirely

within a layer of photoresist or similar photosensitive material).

The differences in manufacturing processes naturally provide an advantage in both production time and unit cost to replica gratings, thereby explaining their popularity, but the replication process itself must be designed and carried out to ensure that the performance characteristics of the replicated grating match those of the master grating. Exhaustive experimentation has shown how to eliminate loss of resolution between master and replica - this is done by ensuring that the surface figure of the replica matches that of the master, and that the grooves are not displaced as a result of replication. The efficiency of a replica matches that of its master when the groove profile is reproduced faithfully. Other characteristics, such as scattered light, are generally matched as well, provided care is taken during the transfer coating step to ensure a dense metallic layer. [Even if the layer were not dense enough, so that its surface roughness caused increased scattered light from the replica when compared with the master, this would be diffuse scatter; scatter in the dispersion plane, due to irregularities in the groove spacing, would be faithfully replicated by the resin and does not depend significantly on the quality of the coating.] Circumstances in which a master grating is shown to be superior to a replicated grating are quire rare, and can often be attributed to flaws or errors in the particular replication process used, not to the fact that the grating was replicated.

In one respect, replicated gratings can provide an advantage over master gratings: those cases where the ideal groove profile is not obtainable in a master grating, but the inverse profile is obtainable. Echelle gratings, for example, are ruled so that their grooves exhibit a sharp trough but a relatively less sharp peak. By replicating, the groove profile is inverted, leaving a first-generation replica with a sharp peak. The efficiency of the replica will be considerably higher than the efficiency of the master grating. In such cases, only odd-generation replicas are used as products, since the even-generation replicas have the same groove profile (and therefore the same efficiency characteristics) as the master itself.

The most prominent hazard to a grating during the replication process, either master or replica, is scratching, since the grating surface consists of a thin metal coating on a resin layer. Scratches involve damage to the groove profile, which generally leads to increased stray light, though in some applications this may be tolerable. Scratches faithfully replicate from master to submaster to product, and cannot be repaired, since the grating surface is not a

polished surface, and an overcoating will not repair the damaged grooves.

Another hazard during replication is surface contamination from fingerprints; should this happen, a grating can sometimes (but not always) be cleaned or recoated to restore it to its original condition. [In use, accidentally evaporated contaminants, typical of vacuum spectrometry pumping systems, can be especially harmful when baked on the surface of the grating with ultraviolet radiation.]

5.3. STABILITY OF REPLICATED GRATINGS [top]

Temperature. There is no evidence of deterioration or change in standard replica gratings with age or when exposed to thermal variations from the boiling point of nitrogen (77 K = –196 °C) to 50 °C. Gratings that must withstand higher temperatures can be made with a special resin whose glass transition temperature is high enough to prevent the resin from flowing at high temperatures (thereby distorting the grooves). In addition to choosing the appropriate resin, the cure cycle can be modified to result in a grating whose grooves will not distort under high temperature.

Gratings replicated onto substrates made of low thermal expansion materials behave as the substrate dictates: the resin and aluminum, which have much higher thermal expansion coefficients, are present in very thin layers compared with the substrate thickness and therefore do not expand and contract with temperature changes since they are fixed rigidly to the substrate.

Relative Humidity. Standard replicas generally do not show signs of degradation in normal use in high relative humidity environments, but some applications (*e.g.*, fiber-optic telecommunications) require extended exposure to very high humidity environments. Coatings and epoxies that resist the effects of water vapor are necessary for these applications.

Instead of a special resin, the metallic coating on a reflection grating made with standard resin is often sufficient to protect the underlying resin from the effects of water vapor.

Temperature and Relative Humidity. Recent developments in fiber optic

telecommunications require diffraction gratings that meet harsh environmental standards, particularly those in the Telcordia (formerly Bellcore) document GR-1221, "Generic Reliability Assurance Requirements for Passive Optical Components". Special resin materials, along with specially-designed replication techniques, can be used so that replicated gratings can meet demanding requirement with no degradation in performance.

High Vacuum. Even the highest vacuum, such as that of outer space, has no effect on replica gratings. Concerns regarding outgassing from the resin are addressed by recognizing that the resin is fully cured.

Energy Density of the Beam. For applications in which the energy density at the surface of the grating is very high (*e.g.*, some pulsed laser applications), it may be necessary to make the transfer coat thicker than normal, or to apply a second metallic layer (an overcoat) to increase the opacity of the metal film(s) sufficiently to protect the underlying resin from exposure to the light and to permit the thermal energy absorbed from the pulse to be dissipated without damaging the groove profile. Using a metal rather than glass substrate is also helpful in that it permits the thermal energy to be dissipated; in some cases, a water-cooled metal substrate is used for additional benefit.

Pulsed lasers often require optical components with high damage thresholds, due to the short pulse duration and high energy of the pulsed beam. For gratings used in the infrared, gold is used as the reflective coating, and a standard gold-coated replica grating can tolerate an energy density at 10 microns of about 10 J/cm^2; for a 10 nsec pulse this corresponds to a power density of 1 GW/cm^2. The damage threshold for a subnanosecond 1 micron is about 400 mJ/cm^2. Doubling the thickness of the reflective layer can greatly increase the damage threshold of a replicated grating used in pulsed beams.

Experimental damage thresholds for continuous wave (cw) beams, reported by Loewen and Popov[4], are given in Table 5-1.

Grating Type	*Damage Threshhold (energy density)*

Standard replica grating on glass substrate	40 to 80 W/cm^2
Standard replica grating on copper substrate	c. 100 W/cm^2
Standard replica grating on water-cooled copper substrate	150 to 250 W/cm^2

Table 5-1. Damage thresholds for continuous wave (cw) beams.

PREVIOUS CHAPTER NEXT CHAPTER

Back to top

6. PLANE GRATINGS AND THEIR MOUNTS

PREVIOUS CHAPTER
NEXT CHAPTER

TABLE OF CONTENTS

6.1. GRATING MOUNT TERMINOLOGY
6.2. PLANE GRATING MONOCHROMATOR MOUNTS
6.2.1. The Czerny-Turner Monochromator
6.2.2. The Ebert-Fastie Monochromator
6.2.3. The Monk-Gillieson Monochromator
6.2.4. The Littrow Mount
6.2.5. Double & Triple Monochromators

6.1. GRATING MOUNT TERMINOLOGY [top]

The auxiliary collimating and focusing optics that modify the wavefronts incident on and diffracted by a grating, as well as the angular configuration in which it is used, is called its *mount*. Grating mounts are a class of *spectrometer*, a term which usually refers to any spectroscopic instrument, regardless of whether it scans wavelengths individually or entire spectra simultaneously, or whether it employs a prism or grating. For this discussion we consider grating spectrometers only.

A *monochromator* is a spectrometer that images a single wavelength or wavelength band at a time onto an exit slit; the spectrum is scanned by the relative motion of the entrance (and/or exit) optics (usually slits) with respect to the grating. A *spectrograph* is a spectrometer that images a range of wavelengths simultaneously, either onto photographic film or a series of detector elements, or through several exit slits (sometimes called a

polychromator). The defining characteristic of a spectrograph is that an entire section of the spectrum is recorded at once.

6.2. PLANE GRATING MONOCHROMATOR MOUNTS

[top]

A *plane grating* is one whose surface is flat. Plane gratings are normally used in collimated incident light, which is dispersed by wavelength but do not focused. These mounts require auxiliary optics, such as lenses or mirrors, to collect and focus the energy. Some simplified plane grating mounts illuminate the grating with converging light, though the focal properties of the system will then depend on wavelength. For simplicity, only plane reflection grating mounts are discussed below, though each mount may have a transmission grating analogue.

6.2.1. The Czerny-Turner Monochromator

This design involves a classical plane grating illuminated by collimated light. The incident light is usually diverging from a source or slit, and collimated by a concave mirror (the *collimator*), and the diffracted light is focused by a second concave mirror (the *camera*); see Figure 6-1. Ideally, since the grating is planar and classical, and used in collimated incident light, no aberrations should be introduced into the diffracted wavefronts. In practice, aberrations are contributed by the off-axis use of the concave spherical mirrors.

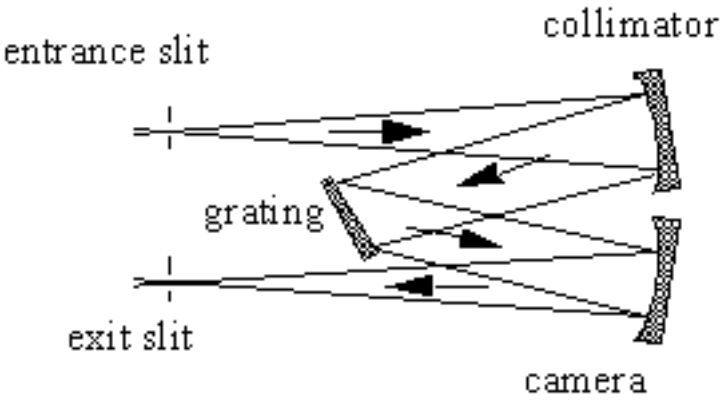

Figure 6-1. The Czerny-Turner mount. The plane grating provides dispersion and the concave mirrors provide focusing.

Like all monochromator mounts, the wavelengths are imaged individually. The spectrum is scanned by rotating the grating; this moves the grating normal relative to the incident and diffracted beams, which (by Eq. (2-1)) changes the wavelength diffracted toward the camera. For a Czerny-Turner monochromator, light incident and diffracted by the grating is collimated, so the spectrum remains at focus at the exit slit for each wavelength, since only the grating can introduce wavelength-dependent focusing properties.

Aberrations caused by the auxiliary mirrors include astigmatism and spherical aberration (each of which is contributed additively by the mirrors); as with all concave mirror geometries, astigmatism increases as the angle of reflection increases. Coma, though generally present, can be eliminated at one wavelength through proper choice of the angles of reflection at the mirrors; due to the anamorphic (wavelength-dependent) tangential magnification of the grating, the images of the other wavelengths experience subsidiary coma (which becomes troublesome only in special systems).

6.2.2. The Ebert-Fastie Monochromator

This design is a special case of a Czerny-Turner mount in which a single relatively large concave mirror serves as both the collimator and the camera (Fig. 6-2). Its use is limited, since stray light and aberrations are difficult to control.

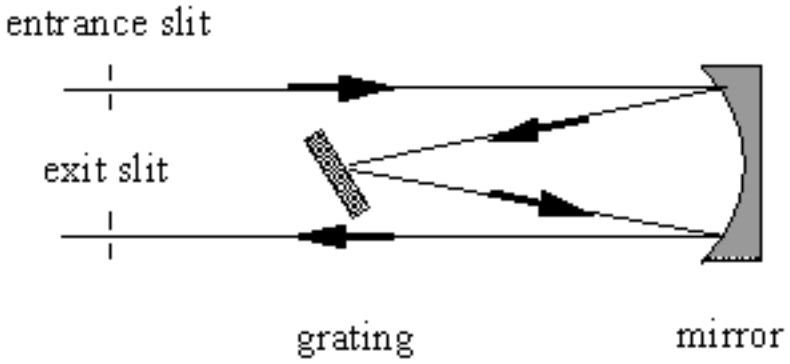

Figure 6-2. The Ebert-Fastie mount. A single concave mirror replaces the two concave mirrors found in Czerny-Turner mounts.

6.2.3. The Monk-Gillieson Monochromator

In this mount (see Figure 6-3), a plane grating is illuminated by converging light ($r < 0$). Usually light diverging from an entrance slit (or fiber) is rendered converging by off-axis reflection from a concave mirror (which introduces aberrations, so the light incident on the grating is not composed of perfectly spherical converging wavefronts). The grating diffracts the light, which converges toward the exit slit; the spectrum is scanned by rotating the grating to bring different wavelengths into focus at or near the exit slit. Often the angles of reflection (from the primary mirror), incidence and diffraction are small (measured from the appropriate surface normals), which keeps aberrations (especially off-axis astigmatism) to a minimum.

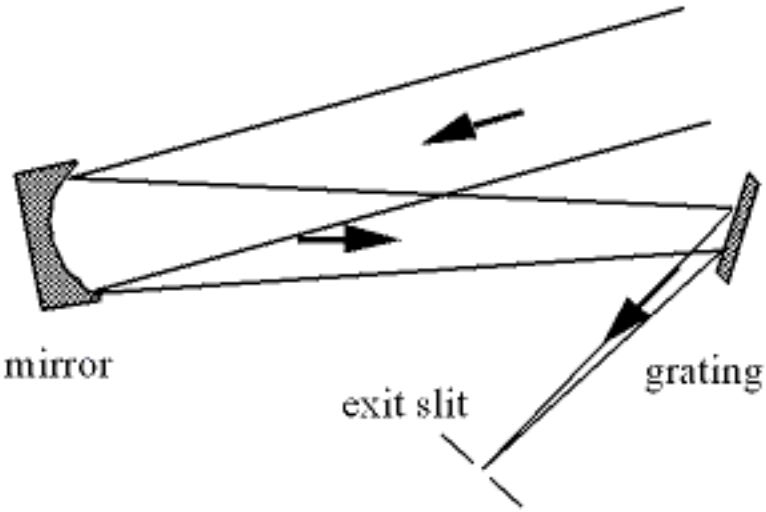

Figure 6-3. The Monk-Gillieson mount. A plane grating is used in converging light.

Since the incident light is not collimated, the grating introduces wavelength-dependent aberrations into the diffracted wavefronts (see Chapter 7). Consequently the spectrum cannot remain in focus at a fixed exit slit when the grating is rotated (unless this rotation is about an axis displaced from the central groove of the grating, as pointed out by Schroeder[5]). For low-resolution applications, the Monk-Gillieson mount enjoys a certain amount of popularity, since it represents the simplest and least expensive spectrometric system imaginable.

6.2.4. The Littrow Mount

A grating used in the Littrow or autocollimating configuration diffracts light of wavelength λ back along the incident light direction (Fig. 6-4). In a *Littrow monochromator*, the spectrum is scanned by rotating the grating; this reorients the grating normal, so the angles of incidence α and diffraction β change (even though $\alpha = \beta$ for all λ). The same auxiliary optics can be used as both

---

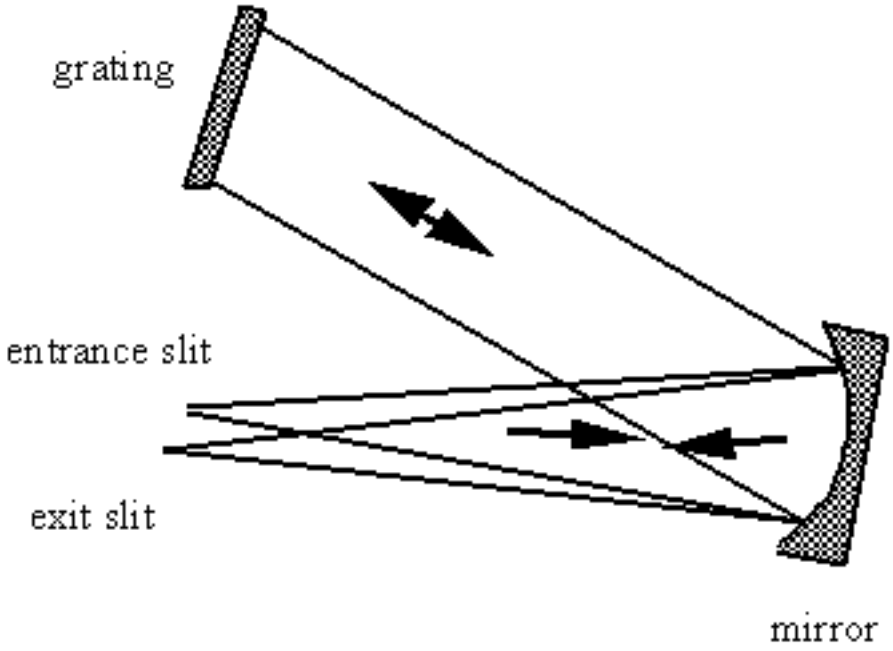

Figure 6-4. The Littrow monochromator mount. The entrance and exit slits are slightly above and below the dispersion plane, respectively; they are shown separated for clarity.

---

collimator and camera, since the diffracted rays retrace the incident rays. Usually the entrance slit and exit slit (or image plane) will be offset slightly along the direction parallel to the grooves so that they do not coincide; of course, this will generally introduce out-of-plane aberrations. As a result, true Littrow monochromators are quite popular in laser tuning applications (see Chapter 12).

6.2.5. Double & Triple Monochromators

Two monochromator mounts used in series form a *double monochromator*. The exit slit of the first monochromator usually serves as the entrance slit for the second monochromator (see Figure 6-5). Stray light in a double

---

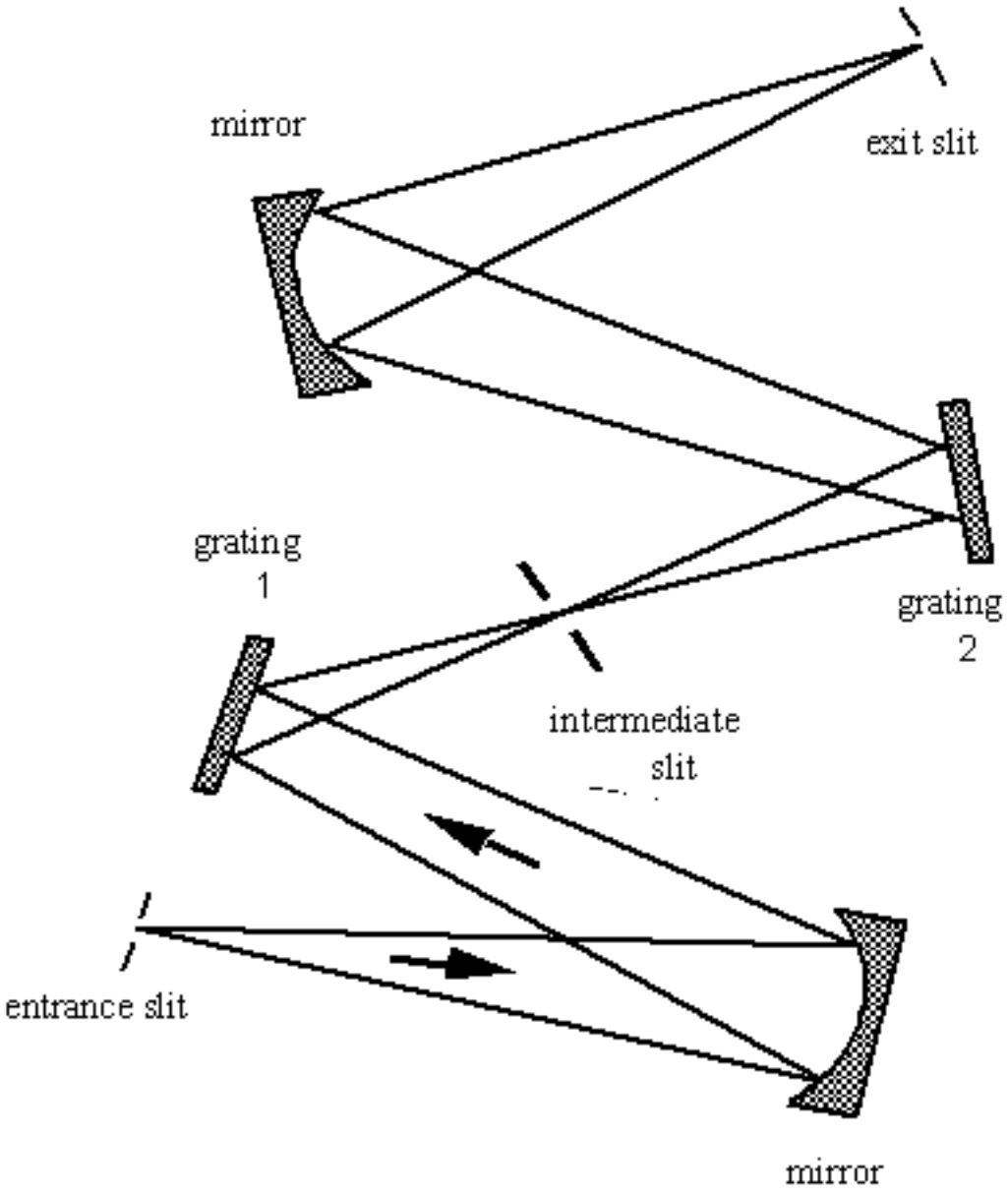

Figure 6-5. A double monochromator mount.

---

monochromator is much lower than in a single monochromator: it is the product of ratios of stray light intensity to parent line intensity for each system. Also, the reciprocal linear dispersion of the entire system is the sum of the reciprocal linear dispersions of each monochromator.

A *triple monochromator* mount consists of three monochromators in series. These mounts are used only when the demands to reduce stray light are extraordinarily severe (*e.g.*, Raman spectroscopy).

PREVIOUS CHAPTER NEXT CHAPTER

Back to top

7. CONCAVE GRATINGS AND THEIR MOUNTS

PREVIOUS CHAPTER
NEXT CHAPTER

TABLE OF CONTENTS

7.0. INTRODUCTION [top]

A concave reflection grating can be modeled as a concave mirror that disperses; it can be thought to reflect and focus light by virtue of its concavity, and to disperse light by virtue of its groove pattern.

Since their invention by Henry Rowland in 1883, concave diffraction gratings have played an important role in spectrometry. Compared with plane gratings, they offer one important advantage: they provide the focusing

(imaging) properties to the grating that otherwise must be supplied by separate optical elements. For spectroscopy below 110 nm, for which the reflectivity of available mirror coatings is low, concave gratings allow for systems free from focusing mirrors that would reduce throughput two or more orders of magnitude.

Many configurations for concave spectrometers have been proposed. Some are variations of the Rowland circle, while some place the spectrum on a flat field, which is more suitable for charge-coupled device (CCD) array instruments. The Seya-Namioka concave grating monochromator is especially suited for scanning the spectrum by rotating the grating around its own axis.

7.1. CLASSIFICATION OF GRATING TYPES [top]

The imaging characteristics of a concave grating system are governed by the size, location and orientation of the entrance and exit optics (the *mount*), the aberrations due to the grating, and the aberrations due to any auxiliary optics in the system. [In this chapter we address only simple systems, in which the concave grating is the single optical element; auxiliary mirrors and lenses are not considered.] The imaging properties of the grating itself are determined completely by the shape of its substrate (blank) (its *curvature* or *figure*) and the spacing and curvature of the grooves (its *groove pattern*).

Gratings are classified both by their groove patterns and by their substrate curvatures. In Chapter 6, we restricted our attention to plane classical gratings and their mounts. In this chapter, more general gratings and grating systems are considered.

7.1.1. Groove patterns

A *classical grating* is one whose grooves, when projected onto the tangent plane, form a set of straight equally-spaced lines. Until the last few decades, the vast majority of gratings were classical, in that any departure from uniform spacing, groove parallelism or groove straightness was considered a flaw. Classical gratings are made routinely both by mechanical ruling and interferometric recording.

A *first generation interference grating* has its grooves formed by the intersection of a family of confocal hyperboloids (or ellipsoids) with the grating substrate. When projected onto the tangent plane, these grooves have both unequal spacing and curvature. First generation interference gratings are formed by recording the master grating in a field generated by two sets of spherical wavefronts, which may emanate from a point source or be focused toward a virtual point.

A *second generation interference grating* has the light from its point sources reflected by concave mirrors so that the recording wavefronts are toroidal.

A *varied line-space (VLS) grating* is one whose grooves, when projected onto the tangent plane, form a set of straight parallel lines whose spacing varies from groove to groove. Varying the groove spacing across the surface of the grating moves the tangential focal curve, while keeping the groove straight and parallel keeps the sagittal focal curve fixed.

7.1.2. Substrate (blank) shapes

A *concave grating* is one whose surface is concave, regardless of its groove pattern or profile, or the mount in which it is used. Examples are spherical substrates (whose surfaces are portions of a sphere, which are definable with one radius) and toroidal substrates (definable by two radii). Spherical substrates are by far the most common type of concave substrates, since they are easily manufactured and toleranced, and can be replicated in a straightforward manner. Toroidal substrates are much more difficult to align, tolerance and replicate. More general substrate shapes are also possible, such as ellipsoidal or paraboloidal substrates, but tolerancing and replication complications relegate these grating surfaces out of the mainstream.

The shape of a concave grating can be characterized either by its radii or its curvatures. The radii of the slice of the substrate in the principal (dispersion) plane is called the *tangential radius R*, while that in the plane parallel to the grooves at the grating center is called the *sagittal radius* ρ. Equivalently, we can define tangential and sagittal curvatures $1/R$ and $1/\rho$, respectively.

A *plane grating* is one whose surface is planar. While plane gratings can be thought of as a special case of concave gratings (for which the radii of curvature of the substrate become infinite), we treat them separately here (see the previous chapter).

7.2. CLASSICAL CONCAVE GRATING IMAGING [top]

In Figure 7-1, a classical grating is shown; the Cartesian axes are defined as follows: the *x*-axis is the outward *grating normal* to the grating surface at its center (point O), the *y*-axis is tangent to the grating surface at O and perpendicular to the grooves there, and the *z*-axis completes the right-handed triad of axes (and is therefore parallel to the grooves at O). Light from point source A(ξ , η, 0) is incident on a grating at point O; light of wavelength λ in order *m* is diffracted toward point B(ξ', η', 0). Since point A was assumed, for simplicity, to lie in the *xy* plane, to which the grooves are perpendicular at point O, the image point B will lie in this plane as well; this plane is called the *principal plane* (also called the *tangential plane* or the *dispersion plane* (see Figure 7-2). Ideally, any point P(*x*, *y*, *z*) located on the grating surface will also diffract light from A to B.

The plane through points O and B perpendicular to the principal plane is called the *sagittal plane*, which is unique for this wavelength. The *grating tangent plane* is the plane tangent to the grating surface at its center point O (*i.e.*, the *yz* plane). The imaging effects of the groove spacing and curvature can be completely separated from those due to the curvature of the substrate if the groove pattern is projected onto this plane.

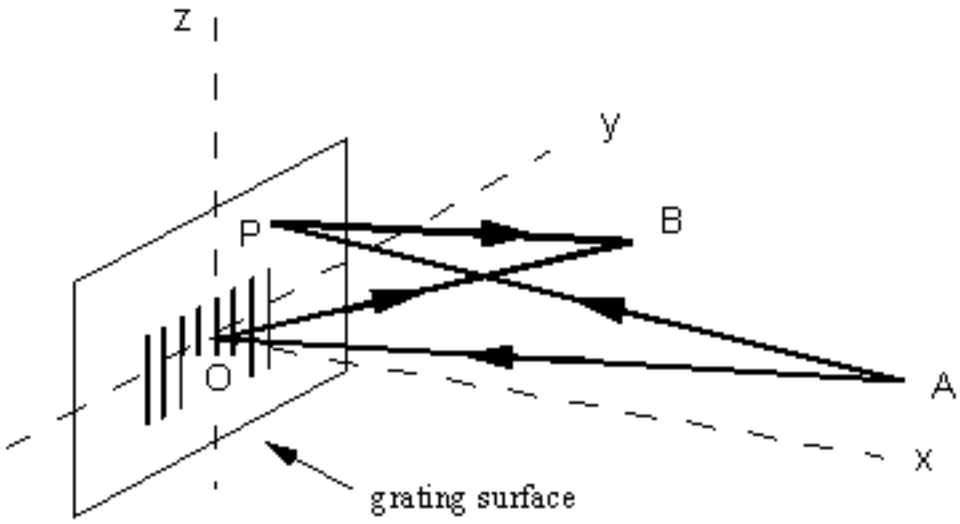

Figure 7-1. Use geometry. The grating surface centered at O diffracts light from point A to point B. P is a general point on the grating surface. The *x*-axis points out of the grating from its center, the *z*-axis points along the central groove, and the *y*-axis completes the traid.

The imaging of this optical system can be investigated by considering the optical path difference *OPD* between the *pole ray* AOB (where O is the center of the grating) and the *general ray* APB (where P is an arbitrary point on the grating surface). Application of Fermat's principle to this path difference, and the subsequent expansion of the results in power series of the coordinates of the tangent plane (*y* and *z*), yields expressions for the aberrations of the system.

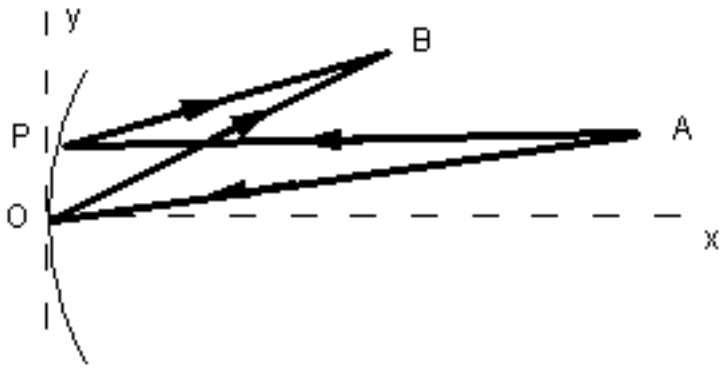

Figure 7-2. Use geometry – the principal plane. Points A, B and O lie in the *xy* (principal) plane; the general point P on the grating surface may lie outside this plane. The *z*-axis comes out of the page at O.

The optical path difference is

$$OPD = \langle APB \rangle - \langle AOB \rangle + Nm\lambda, \qquad (7\text{-}1)$$

where <APB> and <AOB> are the geometric lengths of the general and pole rays, respectively (both multiplied by the index of refraction), m is the diffraction order, and N is the number of grooves on the grating surface between points O and P. The last term in Eq. (7-1) accounts for the fact that the distances and need not be exactly equal for the light along both rays to be in phase at B: due to the wave nature of light, the light is in phase at B even if there are an integral number of wavelengths between these two distances. If points O and P are one groove apart ($N = 1$), the number of wavelengths in the difference - determines the order of diffraction m.

From geometric considerations, we find

$$\begin{aligned} \langle APB \rangle &= \langle AP \rangle + \langle PB \rangle \\ &= \sqrt{(\xi - x)^2 + (\eta - y)^2 + z^2} + \sqrt{(\xi' - x)^2 + (\eta' - y)^2 + z^2} \end{aligned} \qquad (7\text{-}1)$$

and similarly for <AOB>, if the medium of propagation is air ($n \approx 1$). The optical path difference can be expressed more simply if the coordinates of points A and B are plane polar rather than Cartesian: letting

$$\langle AO \rangle = r, \quad \langle OB \rangle = r', \qquad (7\text{-}3)$$

we may write

$$\begin{aligned} \xi &= r\cos\alpha, \quad \eta = r\sin\alpha; \\ \xi' &= r'\cos\beta, \quad \eta' = r'\sin\beta; \end{aligned} \qquad (7\text{-}4)$$

where the angles of incidence and diffraction (α and β) follow the sign convention described in Chapter 2.

The power series for *OPD* can be written in terms of the grating surface point coordinates *y* and *z*:

$$OPD = \sum_{i=0}^{\infty} \sum_{j=0}^{\infty} F_{ij} y^i z^j \ , \qquad (7\text{-}5)$$

where F_{ij}, the expansion coefficient of the (*i*,*j*) term, describes how the rays (or wavefronts) diffracted from point P toward the ideal image point B differ (in direction, or curvature, *etc.*) in proportion to $y^i z^j$ from those from point O. The *x*-dependence of *OPD* has been suppressed by writing

$$x = x(y,z) = \sum_{i=0}^{\infty} \sum_{j=0}^{\infty} a_{ij} y^i z^j \ , \qquad (7\text{-}6)$$

This equation makes use of the fact that the grating surface is usually a regular function of position, so *x* is not independent of *y* and *z* (*i.e.*, if it is a spherical surface of radius *R*, then $(x - R)^2 + y^2 + z^2 = R^2$)

By analogy with the terminology of lens and mirror optics, we call each term in series (7-5) an *aberration*, and F_{ij} its *aberration coefficient.* An aberration is absent from the image of a given wavelength (in a given diffraction order) if its associated coefficient F_{ij} is zero.

Since we have imposed a plane of symmetry on the system (the principal (*xy*) plane), all terms F_{ij} for which *j* is odd vanish. Moreover, $F_{00} = 0$, since the expansion (7-5) is about the origin O. The lowest- (first-) order term F_{10} in the expansion, when set equal to zero, yields the grating equation:

$$m\lambda = d\,(\sin\alpha + \sin\beta). \qquad (2\text{-}1)$$

By Fermat's principle, we may take this equation to be satisfied for all images, which leaves the second-order aberration terms as those of lowest order that

need not vanish. The generally accepted terminology is that a *stigmatic image* has vanishing second-order coefficients even if higher-order aberrations are still present.

$$F_{20} = \cos\alpha\left(\frac{\cos\alpha}{2r} - a_{20}\right) + \cos\beta\left(\frac{\cos\beta}{2r'} - a_{20}\right) = T(r, \alpha) + T(r', \beta), \qquad (7\text{-}7)$$

$$F_{02} = \left(\frac{1}{2r} - a_{02}\cos\alpha\right) + \left(\frac{1}{2r'} - a_{02}\cos\beta\right) = S(r, \alpha) + S(r', \beta), \qquad (7\text{-}8)$$

F_{20} governs the tangential (or spectral) focusing of the grating system, while F_{02} governs the sagittal focusing. The associated aberrations are called *defocus* and *astigmatism*, respectively. The two aberrations describe the extent of a monochromatic image: defocus pertains to the blurring of the image - its extent of the image along the dispersion direction (*i.e.*, in the tangential plane). Astigmatism pertains to the extent of the image in the direction perpendicular to the dispersion direction. In more common (but sometimes misleading) terminology, defocus applies to the "width" of the image in the spectral (dispersion) direction, and astigmatism applies to the "height" of the spectral image; these terms imply that the *xy (tangential)* plane be considered as "horizontal" and the *yz* (*sagittal*) plane as "vertical".

Actually *astigmatism* more correctly defines the condition in which the tangential and sagittal foci are not coincident, which implies a line image at the tangential focus. It is a general result of the off-axis use of a concave mirror (and, by extension, a concave reflection grating as well). A complete three-dimensional treatment of *OPD* shows that the image is actually an arc; image points away from the center of the ideal image are diffracted toward the longer wavelengths. This effect, which technically is not an aberration, is called *(spectral) line curvature*, and is most noticeable in the spectra of Paschen-Runge mounts (see later in this chapter). Figure 7-3 shows astigmatism in the image of a wavelength diffracted off-axis from a concave grating, ignoring line curvature.

Since grating images are generally astigmatic, the focal distances r' in Eqs. (7-7) and (7-8) should be distinguished. Calling r'_T and r'_S the *tangential*

and *sagittal focal distances*, respectively, we may set these equations equal to zero and solve for the focal curves $r'_T(\lambda)$ and $r'_S(\lambda)$:

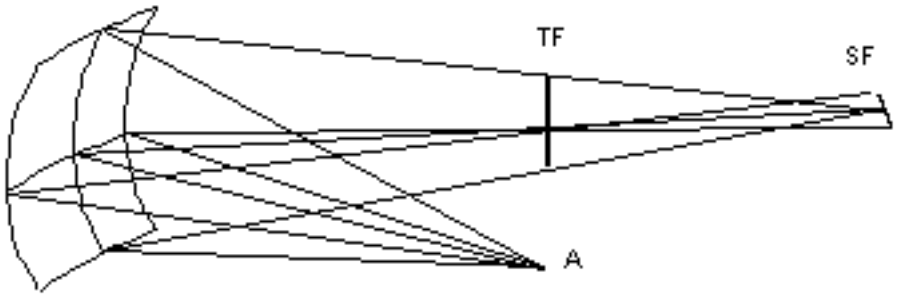

Figure 7-3. Astigmatic focusing of a concave grating. Light from point A is focused into a line parallel to the grooves at TF (the tangential focus) and perpendicular to the grooves at SF (the sagittal focus). Spectral resolution is maximized at TF.

$$r'_T(\lambda) = \frac{\cos^2\beta}{A + B\cos\beta}, \qquad (7\text{-}9)$$

$$r'_S(\lambda) = \frac{1}{D + E\cos\beta}, \qquad (7\text{-}10)$$

Here we have defined

$$A = B\cos\alpha - \frac{\cos^2\alpha}{r}, \quad B = 2a_{20},$$
$$D = E\cos\alpha - \frac{1}{r}, \quad E = 2a_{02}, \qquad (7\text{-}11)$$

where a_{20} and a_{02} are the coefficients in Eq. (7-6) (*e.g.*, $a_{20} = a_{02} = 1/(2R)$ for a spherical grating of radius R). These expressions are completely general for classical grating systems; that is, they apply to any type of grating mount or configuration.

Of the two primary (second-order) focal curves, that corresponding to defocus (F_{20}) is of greater importance in spectroscopy, since it is spectral resolution that is most crucial to grating systems. For this reason we do not concern ourselves with locating the image plane at the "circle of least confusion"; rather, we try to place the image plane at or near the tangential focus (where $F_{20} = 0$). For concave gratings ($a_{20} \neq 0$), there are two well-known solutions to the defocus equation $F_{20} = 0$.

The *Rowland circle* is a circle whose diameter is equal to the tangential radius of the grating substrate, and which passes through the grating center (point O in Figure 7-5). If the point source A is placed on this circle, the tangential focal curve also lies on this circle. This solution is the basis for the Rowland circle and Paschen-Runge mounts. For the Rowland circle mount,

$$r = \frac{\cos\alpha}{2a_{20}} = R\cos\alpha, \qquad r'_T = \frac{\cos\beta}{2a_{20}} = R\cos\beta. \tag{7-12}$$

The sagittal focal curve is

$$r'_S = \left(\frac{\cos\alpha + \cos\beta}{\rho} - \frac{1}{R\cos\alpha}\right)^{-1} \tag{7-13}$$

(where ρ is the sagittal radius of the grating), which is always greater than r'_T (even for a spherical substrate, for which $\rho = R$) unless $\alpha = \beta = 0$. Consequently this mount suffers from astigmatism, which in some cases is considerable.

The *Wadsworth mount* is one in which the source light is collimated ($r \rightarrow \infty$), so that the tangential focal curve is given by

$$r'_T = \frac{\cos^2\beta}{2a_{20}(\cos\alpha + \cos\beta)} = \frac{R\cos^2\beta}{\cos\alpha + \cos\beta} \tag{7-14}$$

The sagittal focal curve is

$$r'_S = \frac{1}{2a_{02}(\cos\alpha + \cos\beta)} = \frac{\rho}{\cos\alpha + \cos\beta} \qquad (7\text{-}15)$$

In this mount, the imaging from a classical spherical grating ($\rho = R$) is such that the astigmatism of the image is zero only for $\beta = 0$, though this is true for any incidence angle α.

While higher-order aberrations are usually of less importance than defocus and astigmatism, they can be significant. The third-order aberrations, *primary* or *tangential coma* F_{30} and *secondary* or *sagittal coma* F_{12}, are given by

$$F_{30} = \frac{\sin\alpha}{r} T(r, \alpha) = \frac{\sin\beta}{r'} T(r', \beta) - a_{30}(\cos\alpha + \cos\beta) \qquad (7\text{-}16)$$

$$F_{12} = \frac{\sin\alpha}{r} S(r, \alpha) = \frac{\sin\beta}{r'} T(r', \beta) - a_{12}(\cos\alpha + \cos\beta) \qquad (7\text{-}17)$$

where T and S are defined in Eqs. (7-7) and (7-8). Often one or both of these third-order aberrations is significant in a spectral image, and must be minimized with the second-order aberrations.

7.3. NONCLASSICAL CONCAVE GRATING IMAGING [top]

For nonclassical groove patterns, the aberration coefficients F_{ij} must be generalized to account for the image modifying effects of the variations in curvature and spacing of the grooves, as well as for the focusing effects of the concave substrate:

$$F_{ij} = M_{ij} + \frac{m\lambda}{\lambda_0} H_{ij} \equiv M_{ij} + H'_{ij} \qquad (7\text{-}18)$$

The terms M_{ij} are simply the F_{ij} coefficients for classical concave grating mounts, discussed above. The *H'ij* coefficients describe the groove pattern. For classical gratings, $H'ij = 0$ for all terms of order two or higher ($i + j \geq 2$). The tangential and sagittal focal distances (Eqs. (7-9) and (7-10)) must now be generalized:

$$r'_T(\lambda) = \frac{\cos^2 \beta}{A + B \cos \beta + C \sin \beta}, \qquad (7\text{-}19)$$

$$r'_S(\lambda) = \frac{1}{D + E \cos \beta + F \sin \beta}, \qquad (7\text{-}20)$$

where in addition to Eqs. (7-11) we have

$$C = -H'_{20}, \quad F = -H'_{02}. \qquad (7\text{-}21)$$

Here H'_{20} and H'_{02} are the terms that govern the effect of the groove pattern on the tangential and sagittal focusing. For a first generation interference grating, for example, the H_{ij} coefficients may be written in terms of the parameters of the recording geometry (see Figure 7-4):

$$H'_{20} = -T(r_C, \gamma) + T(r_D, \delta) \qquad (7\text{-}22)$$

$$H'_{02} = -S(r_C, \gamma) + S(r_D, \delta) \qquad (7\text{-}23)$$

where $C(r_C, \gamma)$ and $D(r_D, \delta)$ are the plane polar coordinates of the recording points. These equations are quite similar to Eqs. (7-7) and (7-8), due to the similarity in Figures 7-4 and 7-2.

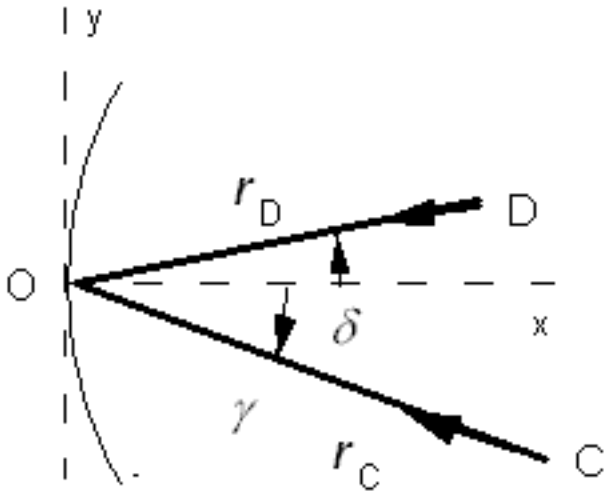

Figure 7-4. Recording parameters. Spherical waves emanate from point sources C and D; the interference pattern forms fringes on the concave substrate centered at O.

For VLS gratings (see Chapter 4), the terms H_{ij} are written in terms of the groove spacing coefficients rather than in terms of recording coordinates.[6]

More details on the imaging properties of gratings systems can be found in Namioka[7] and Noda et al.[8]

7.4. REDUCTION OF ABERRATIONS [top]

In the design of grating systems, there exists several degrees of freedom whose values may be chosen to optimize image quality. For monochromators, the locations of the entrance slit A and exit slit B relative to the grating center O provide three degrees of freedom (or five, if no plane of symmetry is imposed); the missing degree of freedom is restricted by the grating equation, which sets the angular relationship between the lines AO and BO. For spectrographs, the location of the entrance slit A as well as the location, orientation and curvature of the image field provide degrees of freedom

(though the grating equation must be satisfied). In addition, the curvature of the grating substrate provides freedom, and the aberration coefficients H'_{ij} for an interference grating (or the equivalent terms for a VLS grating) can be chosen to improve imaging. Even in systems for which the grating use geometry has been specified, there exist several degrees of freedom due to the aberration reduction possibilities of the grating itself.

Algebraic techniques can find sets of design parameters that minimize image size at one or two wavelengths, but to optimize the imaging of an entire spectral range is usually so complicated that computer implementation of a design procedure is essential. Thermo RGL has developed a set of proprietary computer programs that are used to design and analyze grating systems. These programs allow selected sets of parameters governing the use and recording geometries to vary within prescribed limits. Optimal imaging is found by comparing the imaging properties for systems with different sets of parameters values.

7.5. CONCAVE GRATING MOUNTS [top]

7.5.1. The Rowland Circle Spectrograph

The first concave gratings of spectroscopic quality were ruled by Rowland, who invented them in 1881, also designing their first mounting. Placing the ideal source point on the Rowland circle forms spectra on that circle free from defocus and primary coma at all wavelengths (*i.e.*, $F_{20} = F_{30} = 0$ for all λ); while spherical aberration is residual and small, astigmatism is usually severe. Originally a Rowland circle spectrograph employed a photographic plate bent along a circular arc on the Rowland circle to record the spectrum in its entirety.

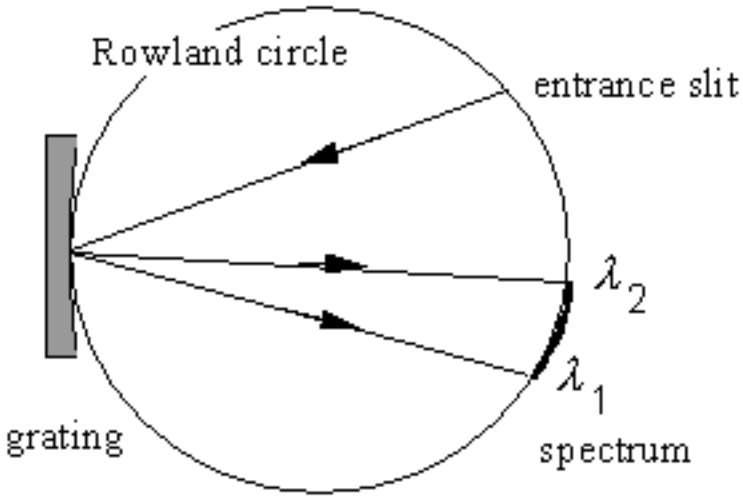

Figure 7-5. The Rowland Circle spectrograph. Both the entrance slit and the diffracted spectrum lie on the Rowland circle, whose diameter equals the tangential radius of curvature R of the grating and that passes through the grating center. Light of two wavelengths is shown focused at different points on the Rowland circle.

Today it is more common for a series of exit slits to be cut into a circular mask to allow the recording of several discrete wavelengths photoelectrically; this system is called the *Paschen-Runge mount*. Other configurations based on the imaging properties of the Rowland circle are the *Eagle mount* and the *Abney mount*, both of which are described by Hutley and by Meltzer (see the Bibliography).

Unless the exit slits (or photographic plates) are considerably taller than the entrance slit, the astigmatism of Rowland circle mounts usually prevents more than a small fraction of the diffracted light from being recorded, which greatly decreases the efficiency of the instrument. Increasing the exit slit heights helps collect more light, but since the images are curved, the exits slits would have to be curved as well to maintain optimal resolution. To complicate matters further, this curvature depends on the diffracted wavelength, so each exit slit would require a unique curvature. Few instruments have gone to such trouble, so most Rowland circle grating mounts collect only a small portion of the light incident on the grating. For this reason these mounts are adequate for strong sources (such as the observation of the solar spectrum) but not for less intense sources (such as stellar spectra).

The imaging properties of instruments based on the Rowland circle spectrograph, such as direct readers and atomic absorption instruments, can be improved by the use of nonclassical gratings. Replacing the usual concave classical gratings with concave aberration-reduced gratings, astigmatism can be improved substantially. Rowland circle mounts modified in this manner direct more diffracted light through the exit slits without degrading resolution.

7.5.2. The Wadsworth Spectrograph

When a classical concave grating is illuminated with collimated light (rather than from a point source on the Rowland circle), spectral astigmatism on and near the grating normal is greatly reduced. Such a grating system is called the *Wadsworth mount* (see Figure 7-6). The wavelength-dependent aberrations of the grating are compounded by the aberration of the collimating optics, though use of a paraboloidal mirror illuminated on-axis will eliminate off-axis aberrations and spherical aberrations. The Wadsworth mount suggests itself in situations in which the light incident on the grating is naturally collimated (from, for example, synchrotron radiation sources). In other cases, an off-axis parabolic mirror would serve well as the collimating element.

Figure 7-6. The Wadsworth spectrograph. Collimated light is incident on a concave grating; light of two wavelengths is shown focused at different points. GN is the grating normal.

7.5.3. Flat Field Spectrographs

One of the advantages of changing the groove pattern (as on a first- or second- generation interference grating or a VLS grating) is that the focal curves can be modified, yielding grating mounts that differ from the classical ones. A logical improvement of this kind on the Rowland circle spectrograph is the *flat-field spectrograph*, in which the tangential focal curve is removed from the Rowland circle and rendered nearly linear over the spectrum of interest (see Figure 7-7). While a grating cannot be made that images a spectrum perfectly on a line, one that forms a spectrum on a sufficiently flat surface is ideal for use in linear detector array instruments of moderate resolution. This development has had a significant effect on spectrograph design.

The relative displacement between the tangential and sagittal focal curves can also be reduced via VLS or interferometric modification of the groove pattern. In this way, the resolution of a flat-field spectrometer can be maintained (or improved) while its astigmatism is decreased; the latter effect allows more light to be transmitted through the exit slit (or onto the detector elements). An example of the process of aberration reduction is shown in Figure 7-8.

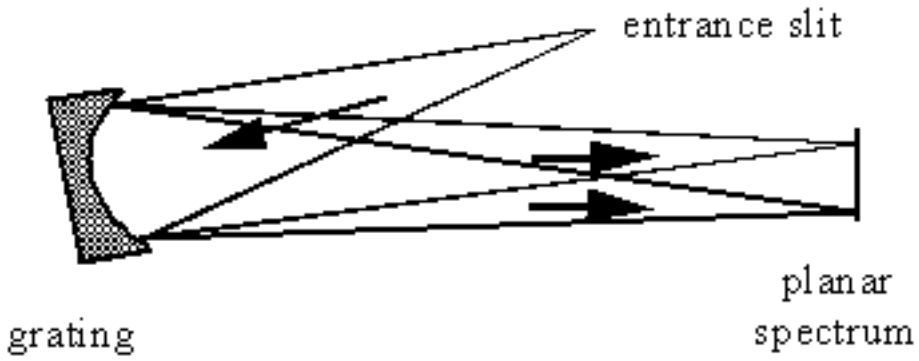

Figure 7-7. A flat-field spectrograph.

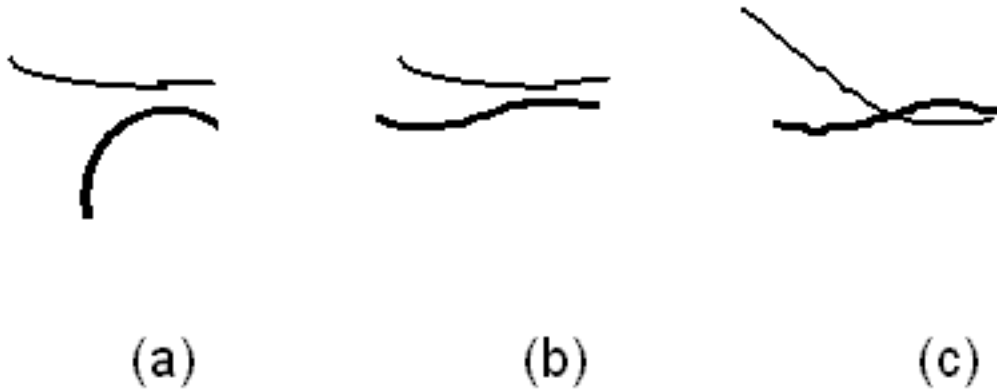

Figure 7-8. Modification of focal curves. The primary tangential focal curve ($F_{20} = 0$) is thick; the primary sagittal focal curve ($F_{02} = 0$) is thin. (a) Focal curves for a classical ($H_{20} = H_{02} = 0$) concave grating, illuminated off the normal ($\alpha \neq 0$) - the dark curve is an arc of the Rowland circle. (b) Choosing a suitable nonzero H_{20} value moves the tangential focal arc so that part of it is nearly linear, suitable for a flat-field spectrograph detector. (c) Choosing a suitable nonzero value of H_{02} moves the sagittal focal curve so that it crosses the tangential focal curve, providing a stigmatic image.

7.5.4. Constant-Deviation Monochromators

In a constant-deviation monochromator, the angle 2*K* between the entrance and exit arms is held constant as the grating is rotated (thus scanning the spectrum; see Figure 7-9). This angle is called the *deviation angle* or *angular deviation*. While plane or concave gratings can be used in constant-deviation mounts, only in the latter case can imaging be made acceptable over an entire spectrum without auxiliary focusing optics.

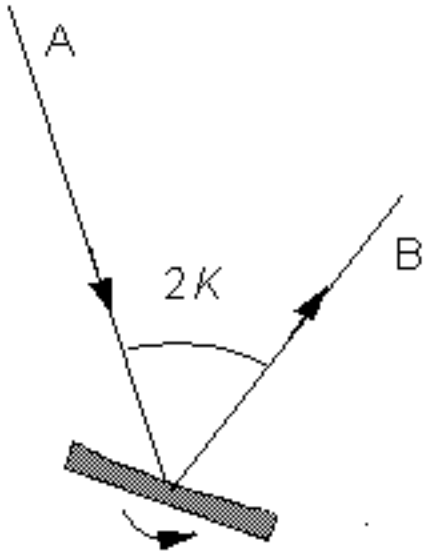

Figure 7-9. Constant-deviation monochromator geometry. To scan wavelengths, the entrance slit A and exit slit B remain fixed as the grating rotates. The deviation angle 2*K* is measured from the exit arm to the entrance arm.

The *Seya-Namioka monochromator* is a very special case of constant-deviation mount using a classical spherical grating, in which the deviation angle 2*K* between the beams and the entrance and exit slit distances (*r* and *r'*) are given by

$$2K = 70°30', \quad r = r' = R\cos(70°30'/2), \qquad (7\text{-}24)$$

where *R* is the radius of the spherical grating substrate. The only moving part in this system is the grating, through whose rotation the spectrum is scanned. Resolution may be quite good in part of the spectrum, though it degrades farther from the optimal wavelength; astigmatism is high, but at an optimum. Replacing the grating with a classical toroidal grating can reduce the astigmatism, if the minor radius of the toroid is chosen judiciously. The reduction of astigmatism by suitably designed interference gratings is also helpful, though the best way to optimize the imaging of a constant-deviation monochromator is to relax the restrictions (7-24) on the use geometry.

PREVIOUS CHAPTER NEXT CHAPTER

Back to top

8. IMAGING PROPERTIES OF GRATING SYSTEMS

PREVIOUS CHAPTER
NEXT CHAPTER

TABLE OF CONTENTS

8.1. CHARACTERIZATION OF IMAGING QUALITY
8.1.1. Geometric Raytracing & Spot Diagrams
8.1.2. Linespread Calculations
8.2. INSTRUMENTAL IMAGING
8.2.1. Magnification of the entrance aperture
8.2.2. Effects of the entrance aperture dimensions
8.2.3. Effects of the exit aperture dimensions

8.1. CHARACTERIZATION OF IMAGING QUALITY [top]

In Chapter 7, we formulated the optical imaging properties of a grating system in terms of wavefront aberrations. After arriving at a design, though, this approach is not ideal for observing the imaging properties of the system. Two tools of image analysis - spot diagrams and linespread functions - are discussed below.

8.1.1. Geometric Raytracing & Spot Diagrams

Raytracing (using the laws of geometrical optics) is superior to wavefront aberration analysis in the determination of image quality. Aberration analysis is an approximation to image analysis, since it involves expanding quantities in infinite power series and considering only a few terms.

Raytracing, on the other hand, does not involve approximations, but shows (in the absence of the diffractive effects of physical optics) where each ray of light incident on the grating will diffract. It would be more exact to design grating systems with a raytracing procedure as well, though to do so would be computationally demanding.

The set of intersections of the diffracted rays and the image plane forms a set of points, called a *spot diagram*. In Figure 8-1, several simple spot diagrams are shown; their horizontal axes are in the plane of dispersion (the tangential plane), and their vertical axes are in the sagittal plane. In (a) an uncorrected (out-of-focus) image is shown; (b) shows good tangential focusing, and (c) shows virtually point-like imaging. All three of these images are simplistic in that higher-order aberrations (such as coma and spherical aberration) render typical spot diagrams asymmetric, as in (d).

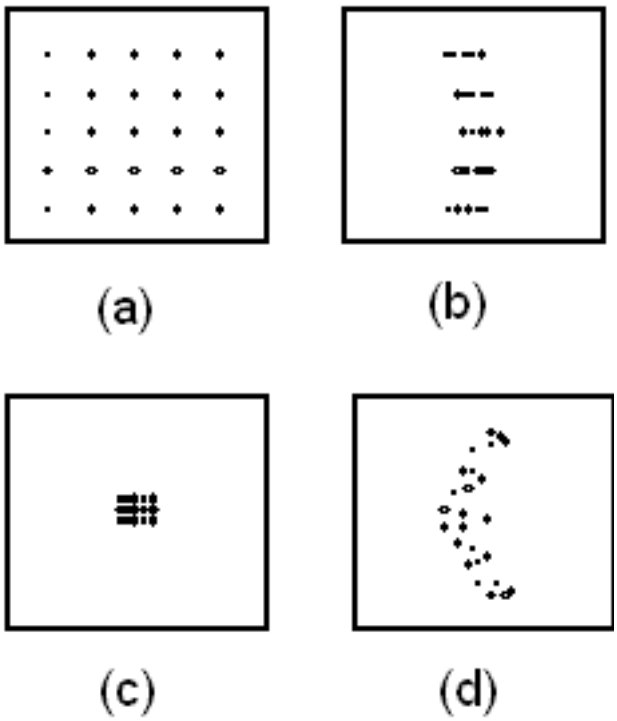

Figure 8-1. Spot diagrams. In (a) the image is out of focus. In (b), the image is well focused in the tangential plane only; the line curvature inherent to grating-diffracted images is shown. In (c) the image is well focused in both directions - the individual spots are not discernible. In (d) a more realistic image is shown.

A straightforward method of evaluating the imaging properties of a spectrometer at a given wavelength is to measure the tangential and sagittal extent of an image (often called the width *w'* and height *h'* of the image, respectively).

Geometric raytracing provides spot diagrams in good agreement with observed spectrometer images, except for well-focused images, in which the wave nature of light dictates a minimum size for the image. Even if the image of a point object is completely without aberrations, it is not a point image, due to the diffraction effects of the pupil (which is usually the perimeter of the grating). The minimal image size, called the *diffraction limit*, can be easily estimated for a given wavelength as the diameter *a* of the Airy disk for a mirror in the same geometry:

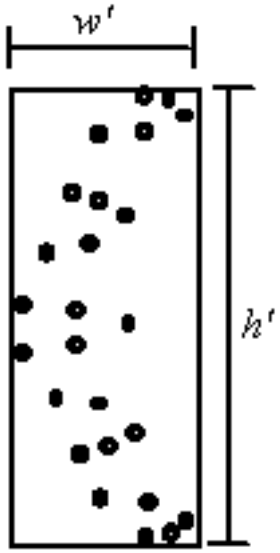

Figure 8-2. Image dimensions. The width *w'* and height *h'* of the image in the image plane are the dimensions of the smallest rectangle that contains the spots.

$$a = 2.44\lambda\, f/\mathrm{no}_{\mathrm{OUTPUT}} = 2.44\lambda\, \frac{r'(\lambda)}{W \cos\beta} \qquad (8\text{-}1)$$

Here $f/\mathrm{no}_{\mathrm{OUTPUT}}$ is the output focal ratio, $r'(\lambda)$ is the focal distance for this wavelength, and W is the width of the grating (see Eq. (2-20), Chapter 2).

Results from raytrace analyses that use the laws of geometrical optics only should not be considered valid if the dimensions of the image are found to be near or below the diffraction limit calculated from Eq. (8-1).

8.1.2. Linespread Calculations

A fundamental problem with geometric raytracing procedures (other than that they ignore the variations in energy density throughout a cross-section of the diffracted beam and the diffraction efficiency of the grating) is its ignorance of the effect that the size and shape of the exit aperture has on the measured resolution of the instrument.

An alternative to merely measuring the extent of a spectral image is to compute its *linespread function*, which is the convolution of the (monochromatic) image of the entrance slit with the exit aperture (the exit slit in a monochromator, or a detector element in a spectrograph). A close physical equivalent is scanning the monochromatic image by moving the exit aperture past it in the image plane, and recording the light intensity passing through the slit as a function of position in this plane.

The linespread calculation thus described accounts for the effect that the entrance and exit slit dimensions have on the resolution of the grating system.

8.2. INSTRUMENTAL IMAGING [top]

With regard to the imaging of actual optical instruments, it is not sufficient to state that ideal performance (in which geometrical aberrations are completely eliminated and the diffraction limit is ignored) is to focus a point object to a point image. All real sources are extended sources - that is, they have finite widths and heights. The ideal imaging of a square light source is not even a square image, since the magnification of the image (in both directions) is a natural and unavoidable consequence of diffraction from a grating.

8.2.1. Magnification of the entrance aperture

The image of the entrance slit, ignoring aberrations and the diffraction limit, will not have the same dimensions as the entrance slit itself. Calling *w* and *h* the width and height of the entrance slit, and *w'* and *h'* the width and height of the image, the *tangential* and *sagittal magnifications* χ_T and χ_S are

$$\chi_T \equiv \frac{w'}{w} = \frac{r' \cos\alpha}{r \cos\beta}, \quad \chi_S \equiv \frac{h'}{h} = \frac{r'}{r}. \qquad (8\text{-}2)$$

These relations, which indicate that the size of the image of the entrance slit will usually differ from that of the entrance slit itself, are derived below.

Figure 8-3 shows the plane of dispersion. The grating center is at O; the *x*-axis is the grating normal and the *y*-axis is the line through the grating center perpendicular to the grooves at O. Monochromatic light of wavelength λ leaves the entrance slit (of width *w*) located at the polar coordinates (*r*, α) from the grating center O and is diffracted along angle β. When seen from O, the entrance slit subtends an angle $\Delta\alpha = w/r$ in the dispersion (*xy*) plane. Rays from one edge of the entrance slit have incidence angle α, and are diffracted along β; rays from the other edge have incidence angle $\alpha + \Delta\alpha$, and are diffracted along $\beta - \Delta\beta$. The image (located a distance *r'* from O), therefore subtends an angle $\Delta\beta$ when seen from O, has width $w' = r' \Delta\beta$. The ratio $\chi_T = w'/w$ is the tangential magnification.

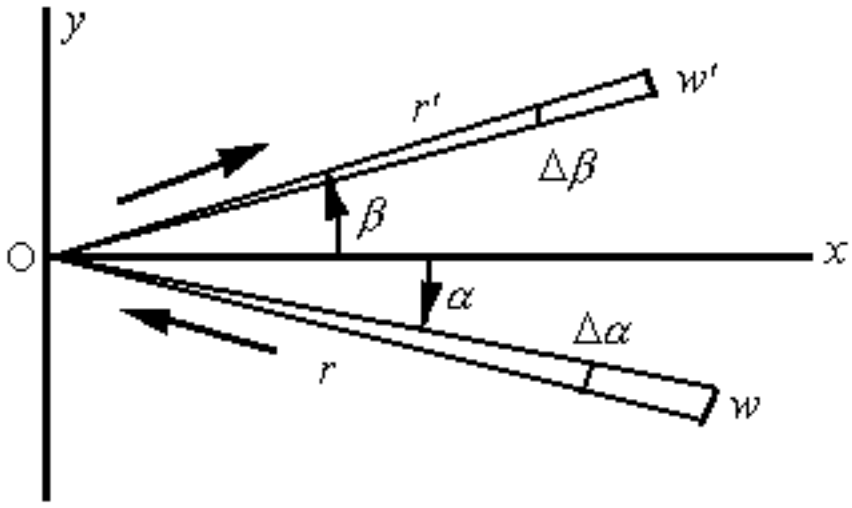

Figure 8-3. Geometry showing tangential magnification. Monochromatic light

from the entrance slit, of width *w*, is projected by the grating to form an image of width *w'*.

We may apply the grating equation to the rays on either side of the entrance slit:

$$Gm\lambda = \sin\alpha + \sin\beta \qquad (8\text{-}3)$$

$$Gm\lambda = \sin(\alpha + \Delta\alpha) + \sin(\beta - \Delta\beta) \qquad (8\text{-}4)$$

Here G (= 1/d) is the groove frequency along the y-axis at O, and m is the diffraction order. Expanding $\sin(\alpha + \Delta\alpha)$ in Eq. (8-4) in a Taylor series about $\Delta\alpha = 0$, we obtain

$$\sin(\alpha + \Delta\alpha) = \sin\alpha + (\cos\alpha)\Delta\alpha + ..., \qquad (8\text{-}5)$$

where terms of order two or higher in $\Delta\alpha$ have been truncated. Using Eq. (8-5) (and its analogue for $\sin(\beta - \Delta\beta)$) in Eq. (8-4), and subtracting it from Eq. (8-3), we obtain

$$\cos\alpha\,\Delta\alpha = \cos\beta\,\Delta\beta, \qquad (8\text{-}6)$$

and therefore

$$\frac{\Delta\beta}{\Delta\alpha} = \frac{\cos\alpha}{\cos\beta}, \qquad (8\text{-}7)$$

from which the first of Eqs. (8-2) follows.

Figure 8-4 shows the same situation in the sagittal plane, which is perpendicular to the principal plane and contains the pole diffracted ray. The entrance slit is located below the principal plane; consequently, its image is above this plane. A ray from the top of the center of the entrance slit is shown. Since the grooves are parallel to the sagittal plane at O, the grating acts as a mirror in this plane, so the angles ϕ and ϕ' are equal in magnitude. Ignoring

signs, their tangents are equal as well:

$$\tan\phi = \tan\phi' \rightarrow \frac{z}{r} = \frac{z'}{r'}, \qquad (8\text{-}8)$$

where z and z' are the distances from the entrance and exit slit points to the principal plane. A ray from an entrance slit point a distance $|z + h|$ from this plane will image toward a point $|z' + h'|$ from this plane, where h' now defines the height of the image. As this ray is governed by reflection as well,

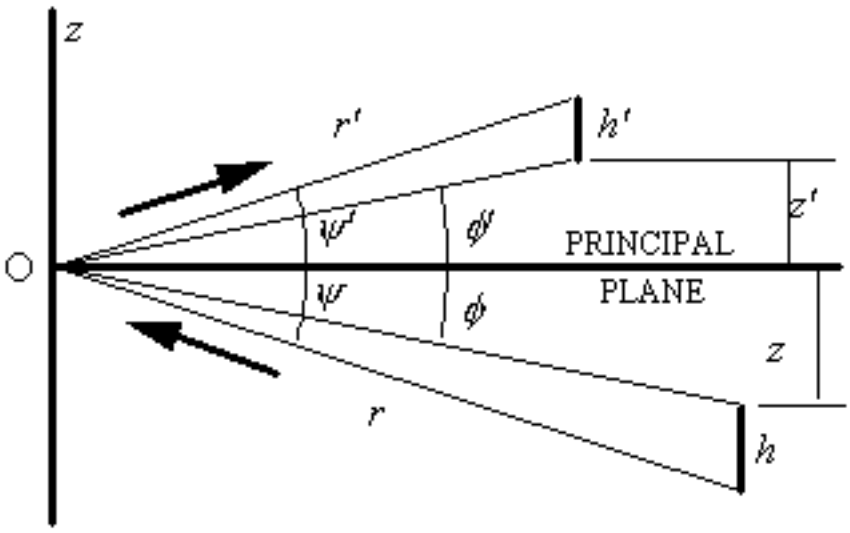

Figure 8-4. Geometry showing sagittal magnification. Monochromatic light from the entrance slit, of height h, is projected by the grating to form an image of height h'.

$$\tan\psi = \tan\psi' \rightarrow \frac{z + h}{r} = \frac{z' + h'}{r'}. \qquad (8\text{-}9)$$

Simplifying this using Eq. (8-8) yields the latter of Eqs. (8-2).

8.2.2. Effects of the entrance aperture dimensions

In most instances, good approximations to the width w' and height h' of the image of an entrance slit of width w and height h are given by

$$w' = \chi_T\, w + \delta w', \qquad h' = \chi_S\, h + \delta h', \tag{8-10}$$

where $\delta w'$ and $\delta h'$ are the width and height of the image of a point source. This equation allows the imaging properties of a grating system with an entrance slit of finite area to be estimated quite well from the imaging properties of the system in which an infinitesimally small object point is considered. In effect, rays need only be traced from one point in the entrance slit (which determines $\delta w'$ and $\delta h'$), from which the image dimensions for an extended entrance slit can be calculated using Eqs. (8-10). These approximations ignore subtle out-of-plane imaging effects that occur when the object point A lies outside of the principal plane, though such effects are usually negligible if the center of the entrance slit lies in this plane and if the entrance slit dimensions are small compared with the distance r between the entrance slit and the grating center.

8.2.3. Effects of the exit aperture dimensions

The linespread function for a spectral image, as defined above, depends on the width of the exit aperture as well as on the width of the diffracted image itself. In determining the optimal width of the exit slit (or single detector element), a rule of thumb is that the width w'' of the exit aperture should roughly match the width w' of the image of the entrance aperture, as explained below.

Typical linespread curves for the same diffracted image scanned by three different exit slit widths are shown in Figure 8-5. For simplicity, we have assumed $\chi_T = 1$ for these examples. The horizontal axis is position along the image plane, in the plane of dispersion. This axis can also be thought of as a wavelength axis (that is, in spectral units); the two axes are related via the dispersion. The vertical axis is relative light intensity at the image plane; its bottom and top represent no intensity and total intensity (or no rays entering the slit and all rays entering the slit), respectively. Changing the horizontal coordinate represents scanning the monochromatic image by moving the exit

slit across it, in the plane of dispersion. This is approximately equivalent to changing the wavelength while keeping the exit slit fixed in space.

An exit slit less wide than the image ($w'' < w'$) will result in a linespread graph such as that seen in Figure 8-5(a). In no position of the exit slit (or, for no diffracted wavelength) does the totality of diffracted rays fall within the slit, as it is not wide enough; the relative intensity does not reach its maximum value of unity. In (b), the exit slit width matches the width of the image: $w'' = w'$. At exactly one point during the scan, all of the diffracted light is contained within the exit slit; this point is the peak (at a relative intensity of unity) of the curve. In (c) the exit slit is wider than the image ($w'' > w'$). The exit slit contains the entire image for many positions of the exit slit.

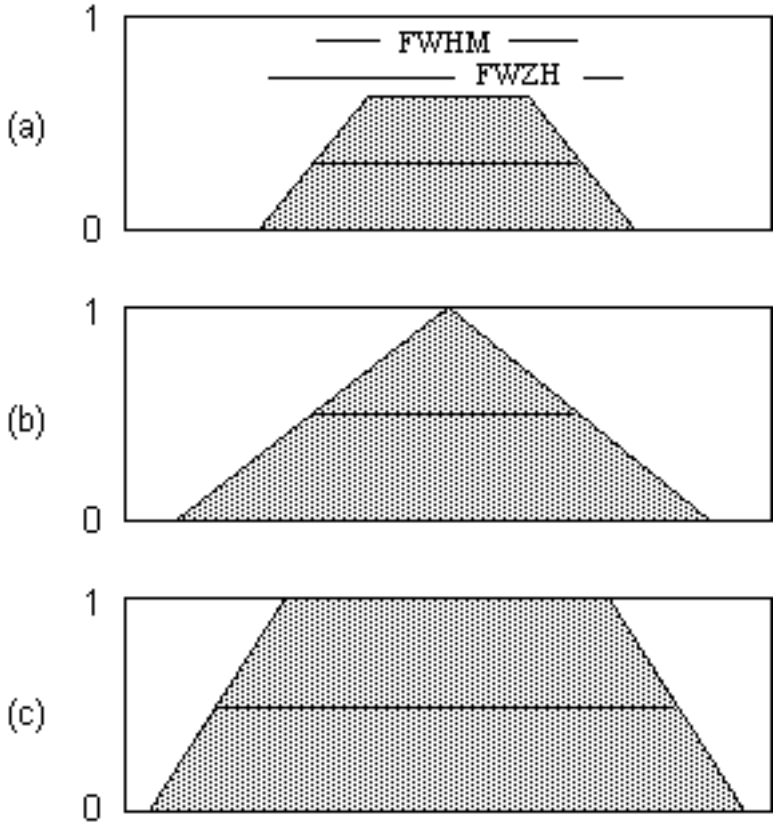

Figure 8-5. Linespread curves for different exit slit widths. The vertical axis is relative intensity at the exit aperture, and the horizontal axis is position along the image plane (in the plane of dispersion). For a given curve, the dark horizontal line shows the FWHM (the width of that portion of the curve in which its amplitude exceeds its half maximum); the FWZH is the width of the entire curve. (a) $w'' < w'$; (b) $w'' = w'$; (c) $w'' > w'$. In (a) the peak is below unity.

In (a) and (b), the FWHM are approximately equal. Severely aberrated images will yield linespread curves that differ from those above (in that they will be asymmetric), although their overall shape will be similar.

In these figures the quantities FWZH and FWHM are shown. These are abbreviations for *full width at zero height* and *full width at half maximum*. The FWZH is simply the total extent of the linespread function, usually expressed in spectral units. The FWHM is the spectral extent between the two extreme points on the linespread graph that are at half the maximum value. The FWHM is often used as a quantitative measure of image quality in grating systems; it is often called the *effective spectral bandwidth*. The FWZH is sometimes called the *full spectral bandwidth*. It should be noted that the terminology is not universal among authors and sometimes quite confusing.

As the exit slit width w' is decreased, the effective bandwidth will generally decrease. If w' is roughly equal to the image width w, though, further reduction of the exit slit width will not reduce the bandwidth appreciably. This can be seen in Figure 8-5, in which reducing w' from case (c) to case (b) results in a decrease in the FWHM, but further reduction of w' to case (a) does not reduce the FWHM.

The situation in $w'' < w'$ is undesirable in that diffracted energy is lost (the peak relative intensity is low) since the exit slit is too narrow to collect all of the diffracted light at once. The situation $w'' > w'$ is also undesirable, since the FWHM is excessively large (or, similarly, an excessively wide band of wavelengths is accepted by the wide slit). The situation $w'' = w'$ seems optimal: when the exit slit width matches the width of the spectral image, the relative intensity is maximized while the FWHM is minimized. An interesting curve is shown in Figure 8-6, in which the ratio FWHM/FWZH is shown *vs.* the ratio w''/w' for a typical grating system. This ratio reaches its single minimum near $w'' = w'$.

The height of the exit aperture has a more subtle effect on the imaging properties of the spectrometer, since by 'height' we mean extent in the direction perpendicular to the plane of dispersion. If the exit slit height is less than the height (sagittal extent) of the image, some diffracted light will be lost, as it will not pass through the aperture. Since diffracted images generally display curvature, truncating the sagittal extent of the image by choosing a short exit

slit also reduces the width of the image (see Figure 8-7). This latter effect is especially noticeable in Paschen-Runge mounts.

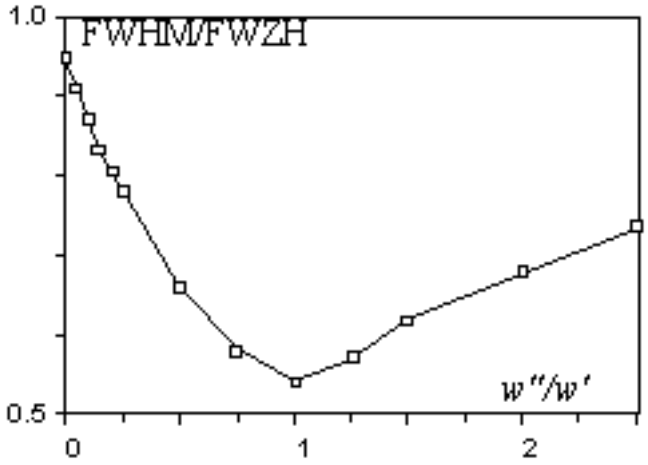

Figure 8-6. FWHM/FWZH vs. w''/w' for a typical system.

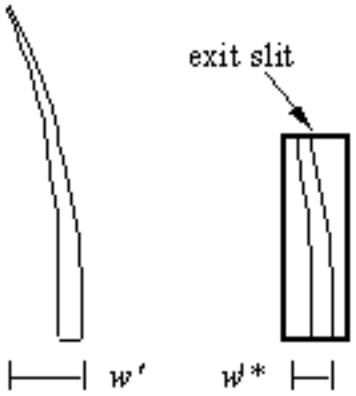

Figure 8-7. Effect of exit slit height on image width. Both the width and the height of the image are reduced by the exit slit chosen. Even if the width of the exit slit is greater than the width of the image, truncating the height of the image yields $w'^* < w'$. [Only the top half of each image is shown.]

In this discussion we have ignored the diffraction effects of the grating aperture: the comments above consider only the effects of geometrical optics

on instrumental imaging. For cases in which the entrance and exit slits are equal in width, and this width is two or three times the diffraction limit, the linespread function is approximately Gaussian in shape rather than the triangle shown in Figure 8-5(b).

PREVIOUS CHAPTER NEXT CHAPTER

Back to top

9. EFFICIENCY CHARACTERISTICS OF DIFFRACTION GRATINGS

PREVIOUS CHAPTER
NEXT CHAPTER

TABLE OF CONTENTS

9.0. INTRODUCTION
9.1. GRATING EFFICIENCY AND GROOVE SHAPE
9.2. EFFICIENCY CHARACTERISTICS FOR TRIANGULAR-GROOVE GRATINGS
9.3. EFFICIENCY CHARACTERISTICS FOR SINUSOIDAL-GROOVE GRATINGS
9.4. THE EFFECTS OF FINITE CONDUCTIVITY
9.5. DISTRIBUTION OF ENERGY BY DIFFRACTION ORDER
9.6. USEFUL WAVELENGTH RANGE
9.7. BLAZING OF RULED TRANSMISSION GRATINGS
9.8. BLAZING OF HOLOGRAPHIC REFLECTION GRATINGS
9.9. OVERCOATING OF REFLECTION GRATINGS

9.0. INTRODUCTION [top]

Efficiency and its variation with wavelength and spectral order are important characteristics of a diffraction grating. For a reflection grating, efficiency is defined as the energy flow (power) of monochromatic light diffracted into the order being measured, relative either to the energy flow of the incident light (*absolute efficiency*) or to the energy flow of specular reflection from a polished mirror substrate coated with the same material (*relative efficiency*). Efficiency is defined similarly for transmission gratings, except that an uncoated substrate is used in the measurement of relative efficiency.

High-efficiency gratings are desirable for several reasons. A grating with high efficiency is more useful than one with lower efficiency in measuring weak transition lines in optical spectra. A grating with high efficiency may allow the reflectivity and transmissivity specifications for the other components in the spectrometer to be relaxed. Moreover, higher diffracted energy may imply lower instrumental stray light due to other diffracted orders, as the total energy flow for a given

wavelength leaving the grating is conserved (being equal to the energy flow incident on it minus any scattering and absorption).

Control over the magnitude and variation of diffracted energy with wavelength is called *blazing*, and it involves the manipulation of the micro-geometry of the grating grooves. In the 1888 edition of *Encyclopædia Brittanica*, Lord Rayleigh recognized that the energy flow distribution (by wavelength) of a diffraction grating could be altered by modifying the shape of the grating grooves. A few decades later, R.W. Wood showed this to be true when he ruled a grating on which he had controlled the groove shape, thereby producing the first deliberately blazed diffraction grating.

The choice of an optimal efficiency curve for a grating depends on the specific application. Often the desired instrumental efficiency is linear; that is, the intensity of light transformed into signal at the image plane must be constant across the spectrum. To approach this as closely as possible, the spectral emissivity of the light source and the spectral response of the detector should be considered, from which the desired grating efficiency curve can be derived. Usually this requires peak grating efficiency in the region of the spectrum where the detectors are least sensitive; for example, a visible-light spectrometer using a silicon detector would be much less sensitive in the blue than in the red, suggesting that the grating itself be blazed to yield a peak efficiency in the blue.

A typical *efficiency curve* (a plot of absolute or relative diffracted efficiency *vs.* diffracted wavelength λ) is shown in Figure 9-1. Usually such a curve shows

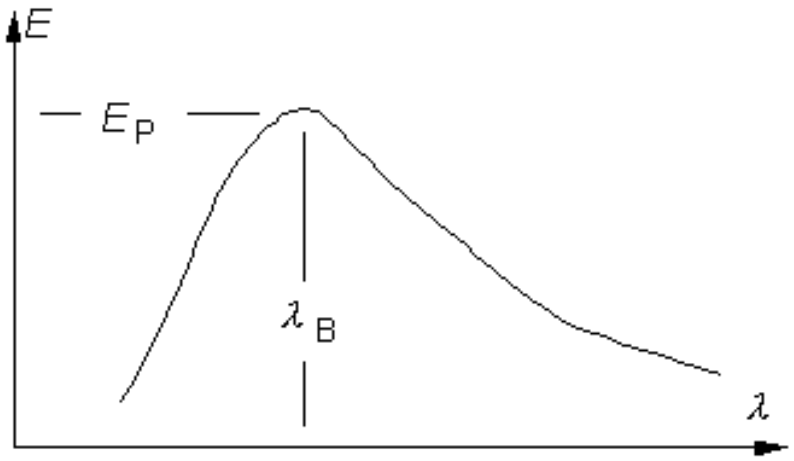

Figure 9-1. A typical (simplified) efficiency curve. This curve shows the efficiency E of a grating in a given spectral order m, measured *vs.* the diffracted wavelength λ. The peak efficiency E_P occurs at the blaze wavelength λ_B.

a single maximum, at the *peak wavelength* (or *blaze wavelength*) λ_B. This curve corresponds to a

given diffraction order *m*; the peak of the curve decreases in magnitude and shifts toward shorter wavelengths as |*m*| increases. The efficiency curve also depends on the angles of use (*i.e.*, the angles of incidence and diffraction). Moreover, the curve depends on the groove spacing *d* (more appropriately, on the dimensionless parameter λ/d) and the material with which the grating is coated (for reflection gratings) or made (for transmission gratings).

In many instances the diffracted power depends on the polarization of the incident light. *P-plane* or *TE polarized light* is polarized parallel to the grating grooves, while *S-plane* or *TM polarized light* is polarized perpendicular to the grating grooves (see Figure 9-2). For completely unpolarized incident light, the efficiency curve will be exactly halfway between the P and S efficiency curves.

Usually light from a single spectral order *m* is used in a spectroscopic instrument, so a grating with ideal efficiency characteristics would diffract all of the power incident on it into this order (for the wavelength range considered). In practice, this is never true: the distribution of the power by the grating depends in a complicated way on the groove spacing and profile, the spectral order, the wavelength, and the grating material.

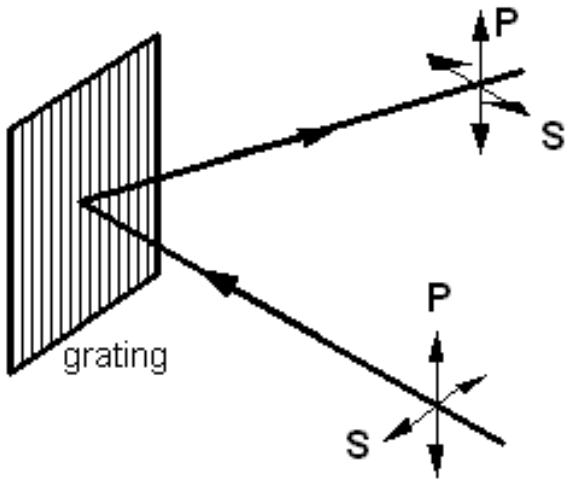

Figure 9-2. S and P polarizations The P polarization components of the incident and diffracted beams are polarized parallel to the grating grooves; the S components are polarized perpendicular to the P components. Both the S and P components are perpendicular to the propagation directions.

Anomalies are locations on an efficiency curve (efficiency plotted *vs.* wavelength) at which the efficiency changes abruptly. First observed by R. W. Wood, these sharp peaks and troughs in an efficiency curve are sometimes referred to as Wood's anomalies. Anomalies are rarely observed in P polarization efficiency curves, but they are often seen in S polarization curves (see Figure 9-3).

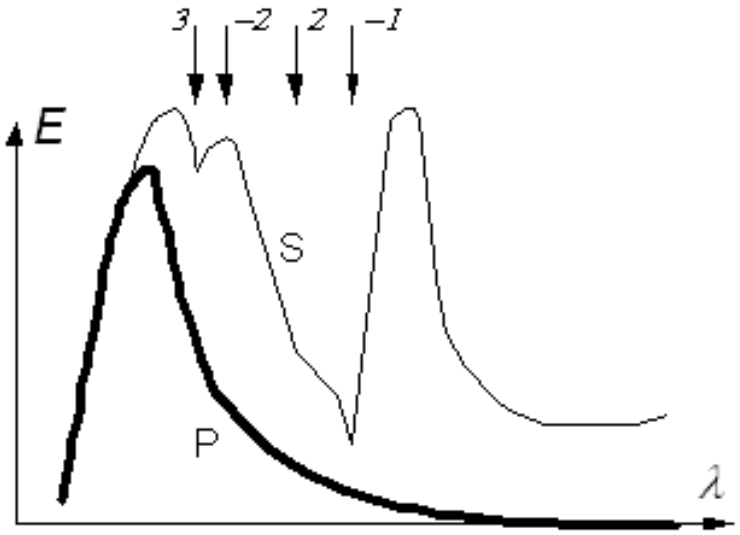

Figure 9-3. Anomalies in the first order for a typical grating with triangular grooves. The P efficiency curve (thick line) is smooth, but anomalies are evident in the S curve (thin line). The passing-off locations are identified by their spectral order at the top of the figure.

Lord Rayleigh predicted the locations (in the spectrum) where such anomalies would be found: he suggested that anomalies occur when light of a given wavelength λ' and spectral order m' is diffracted at $|\beta| = 90°$ from the grating normal (*i.e.*, it passes over the grating horizon). For wavelengths $\lambda < \lambda'$, $|\beta| < 90°$, so diffraction is possible in order m' (and all lower orders), but for $\lambda > \lambda'$ no diffraction is possible in order m' (but it is still possible in lower orders). Thus there is a discontinuity in the diffracted power *vs.* λ in order m' at wavelength λ, and the power that would diffract into this order for $\lambda > \lambda'$ is redistributed among the other spectral orders. This causes abrupt changes in the power diffracted into these other orders.

The Rayleigh explanation does not cover the extension towards longer wavelengths, where anomalies are due to resonance effects. The position of an anomaly depends to some degree on the optical constants of the reflecting material of the grating surface.

9.1. GRATING EFFICIENCY AND GROOVE SHAPE [top]

The maximum efficiency of a grating is typically obtained with a simple smooth triangular groove profile, as shown in Figure 9-4, when the groove (or

---

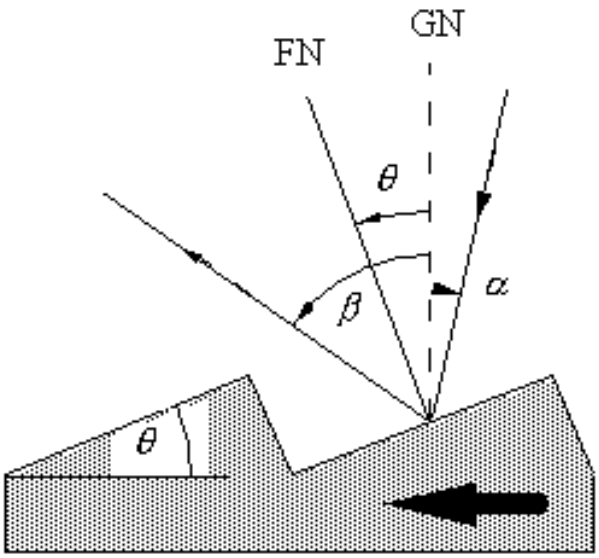

Figure 9-4. Triangular groove geometry. The angles of incidence α and diffraction β are shown in relation to the facet angle θ for the blaze condition. GN is the grating normal and FN is the facet normal. The facet normal bisects the angle between the incident and diffracted rays. The blaze arrow (shown) points from GN to FN.

---

blaze) angle θ is such that the specular reflection angle for the angle of incidence is equal (in magnitude and opposite in sign) to the angle of diffraction. Ideally, the groove facet should be flat with smooth straight edges, and be generally free from irregularities on a scale comparable to the small fraction (< 1/10) of the wavelength of light being diffracted.

Fraunhofer was well aware that the distribution of power among the various diffraction orders depended on the shape of the individual grating grooves. Wood, many decades later, was the first to achieve a degree of control over the groove shape, thereby concentrating spectral energy into one angular region. Wood's gratings were seen to light up, or 'blaze', when viewed at the correct angle.

9.2. EFFICIENCY CHARACTERISTICS FOR TRIANGULAR-GROOVE GRATINGS [top]

Gratings with triangular grooves can be generated by mechanical ruling, or by blazing sinusoidal groove profiles by ion etching. The efficiency behavior of gratings with triangular groove profiles (*i.e.*, blazed gratings) may be divided into six families, depending on the blaze angle:[9]

family	*blaze angle*
very low blaze angle	$\theta < 5°$
low blaze angle	$5° < \theta < 10°$
medium blaze angle	$10° < \theta < 18°$
special low anomaly	$18° < \theta < 22°$
high blaze angle	$22° < \theta < 38°$
very higb blaze angle	$\theta > 38°$

Very low blaze angle gratings ($\theta < 5°$) exhibit efficiency behavior that is almost perfectly scalar; that is, polarization effects are virtually nonexistent. In this region, a simple picture of blazing is applicable, in which each groove facet can be considered a simple flat mirror. The diffracted efficiency is greatest for that wavelength that is diffracted by the grating in the same direction as it would be reflected by the facets. This efficiency peak occurs at $\lambda/d = 2 \sin\theta$ (provided the angle between the incident and diffracted beams is not excessive). At $\lambda_B/2$, where λ_B is the blaze wavelength, the diffracted efficiency will be virtually zero (Figure 9-5) since for this wavelength the second-order efficiency will be at its peak. Fifty-percent absolute efficiency is obtained from roughly $0.67\lambda_B$ to $1.8\lambda_B$.

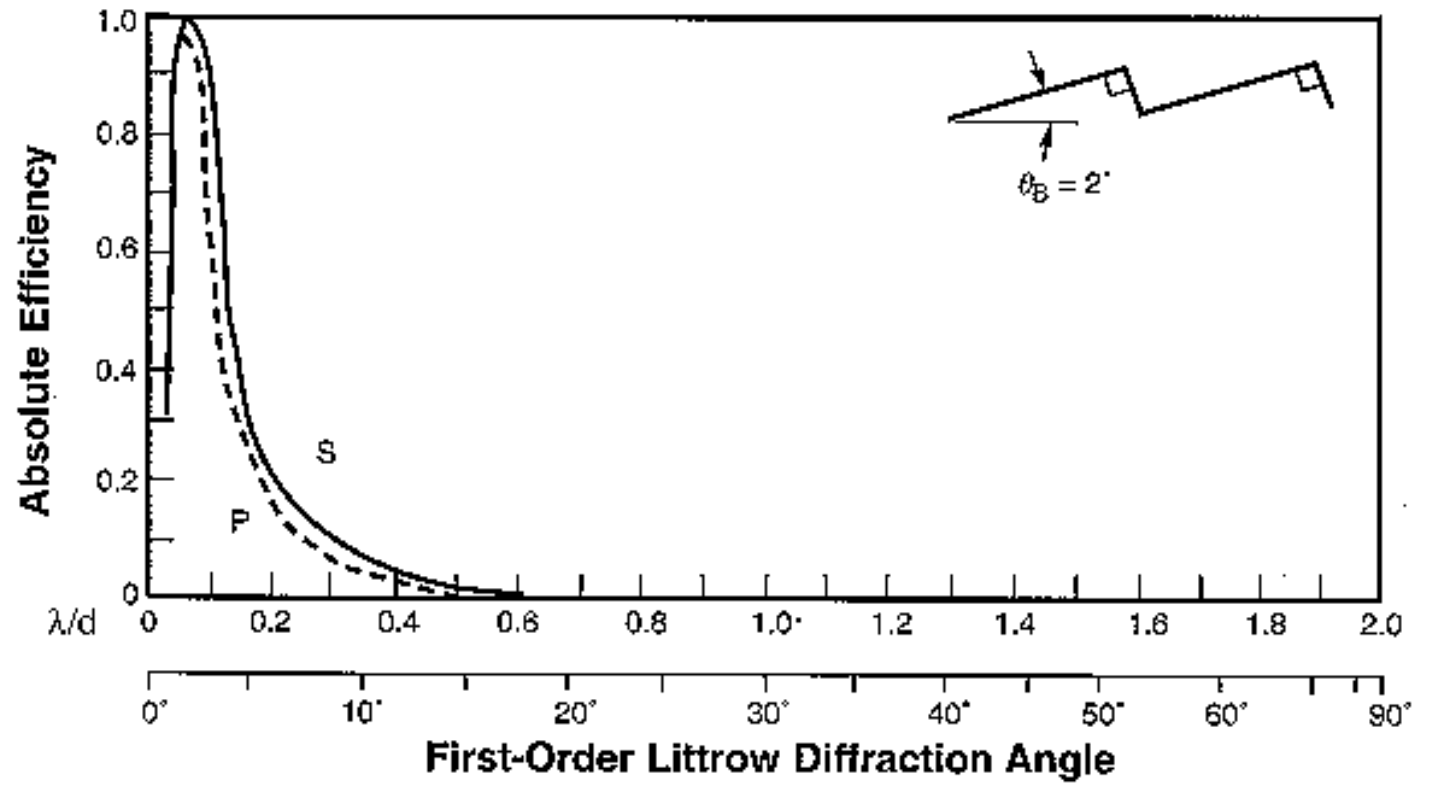

Figure 9-5. First-order theoretical efficiency curve: 2° blaze angle and Littrow mounting (2K = 0). Solid curve, S-plane; dashed curve, P-plane.

For *low blaze angle* gratings (5° < θ < 10°), polarization effects will occur within their usable range (see Figure 9-6). In particular, a strong anomaly is seen near $\lambda/d = 2/3$. Also observed is the theoretical S-plane theoretical efficiency peak of 100% exactly at the nominal blaze, combined with a P-plane peak that is lower and at a shorter wavelength. It is characteristic of all P-plane curves to decrease monotonically from their peak toward zero as $\lambda/d \rightarrow 2$, beyond which diffraction is not possible (see Eq. (2-1)). Even though the wavelength band over which 50% efficiency is attained in unpolarized light is from $0.67\lambda_B$ to $1.8\lambda_B$, gratings of this type (with 1200 groove per millimeter, for example) are widely used, because they most effectively cover the wavelength range between 200 and 800 nm (in which most ultraviolet-visible (U5-Vis) spectrophotometers operate).

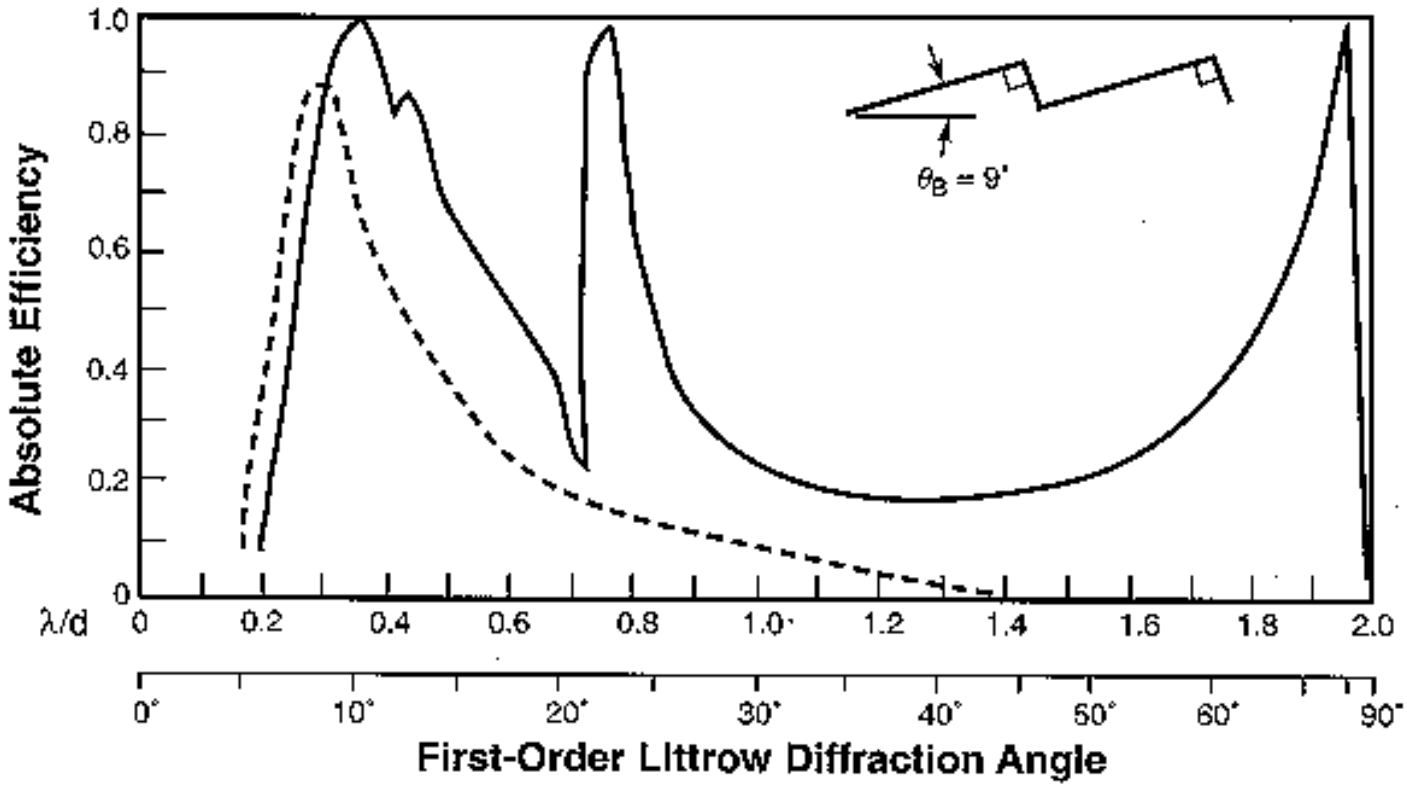

Figure 9-6. Same as Figure 9-5, except 9° blaze angle.

A typical efficiency curve for a *medium blaze angle* grating (10° < θ < 18°) is shown in Figure 9-7. As a reminder that for unpolarized light the efficiency is simply the arithmetic average of the S- and P-plane efficiencies, such a curve is shown in this figure only, to keep the other presentations simple.

The *low-anomaly blaze angle* region (18° < θ < 22°) is a special one. Due to the fact that the strong anomaly that corresponds to the -1 and +2 orders passing off ($\lambda/d = 2/3$) occurs just where

these gratings have their peak efficiency, this anomaly ends up being severely suppressed (Figure 9-8). This property is quite well maintained over a large range of angular deviations (the angle between the incident and diffracted beams), namely up to 25°, but it depends on the grooves having an apex angle near 90°. The relatively low P-plane efficiency of this family of blazed gratings holds the 50% efficiency band from $0.7\lambda_B$ to $1.9\lambda_B$.

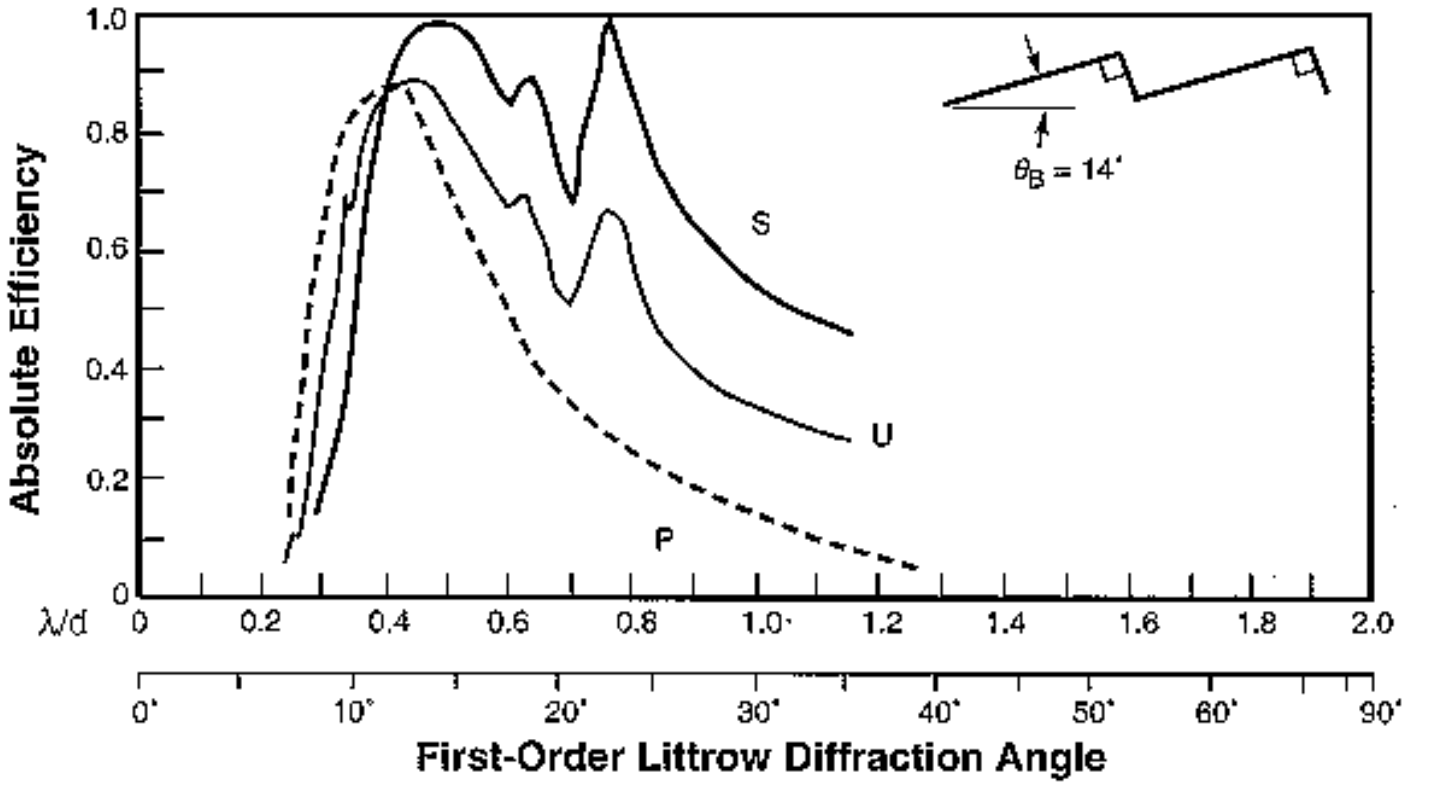

Figure 9-7. Same as Figure 9-5, except 14° blaze angle. The curve for unpolarized light (marked U) is also shown; it lies exactly halfway between the S and P curves.

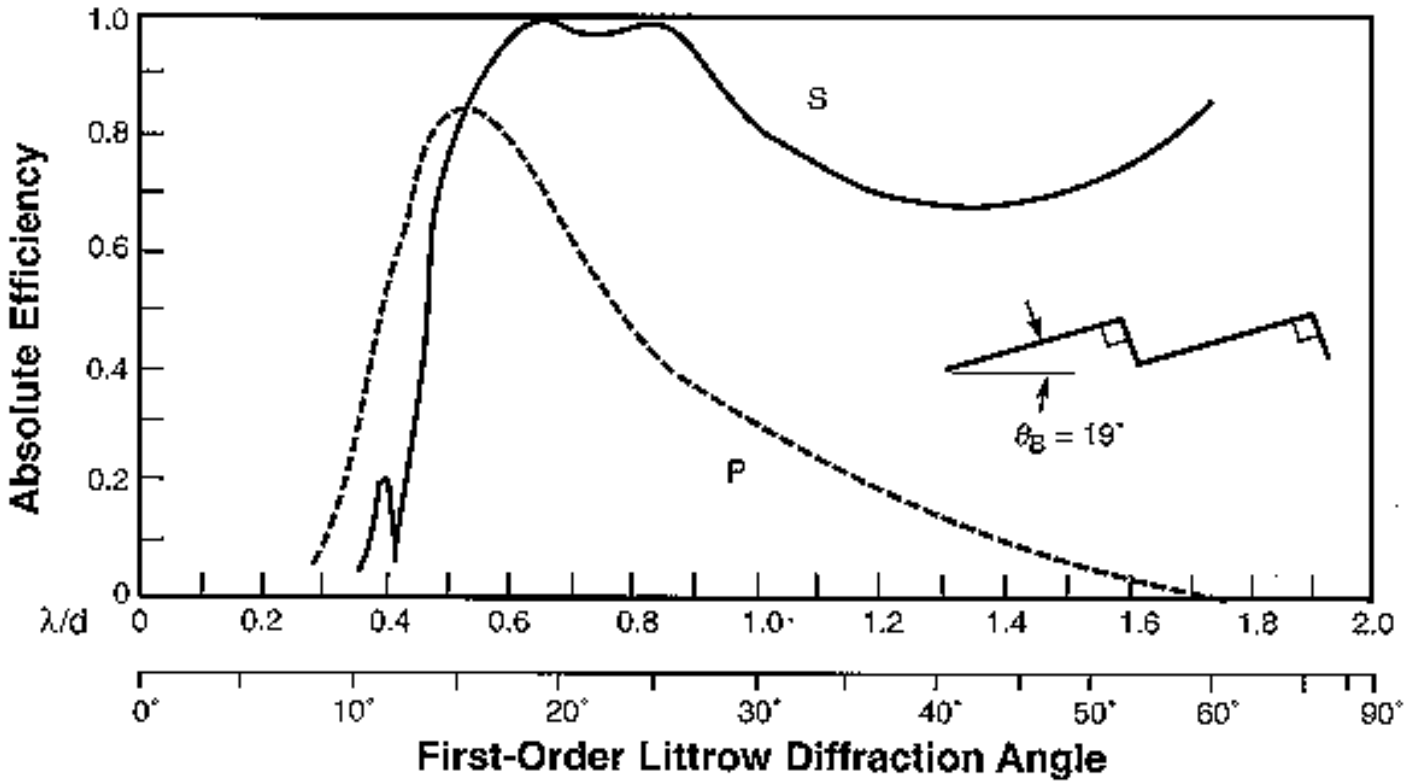

Figure 9-8. Same as Figure 9-5, except 19° blaze angle.

High blaze angle gratings ($22° < \theta < 38°$) are widely used, despite the presence of a very strong anomaly in their efficiency curves (Figure 9-9). For unpolarized light, the effect of this anomaly is greatly attenuated by its coincidence with the P-plane peak. Another method for reducing anomalies for such gratings is to use them at angular deviations above 45°, although this involves some sacrifice in efficiency and wavelength range. The 50% efficiency is theoretically attainable in the Littrow configuration from $0.6\lambda_B$ to $2\lambda_B$, but in practice the long-wavelength end corresponds to such an extreme angle of diffraction that instrumental difficulties arise.

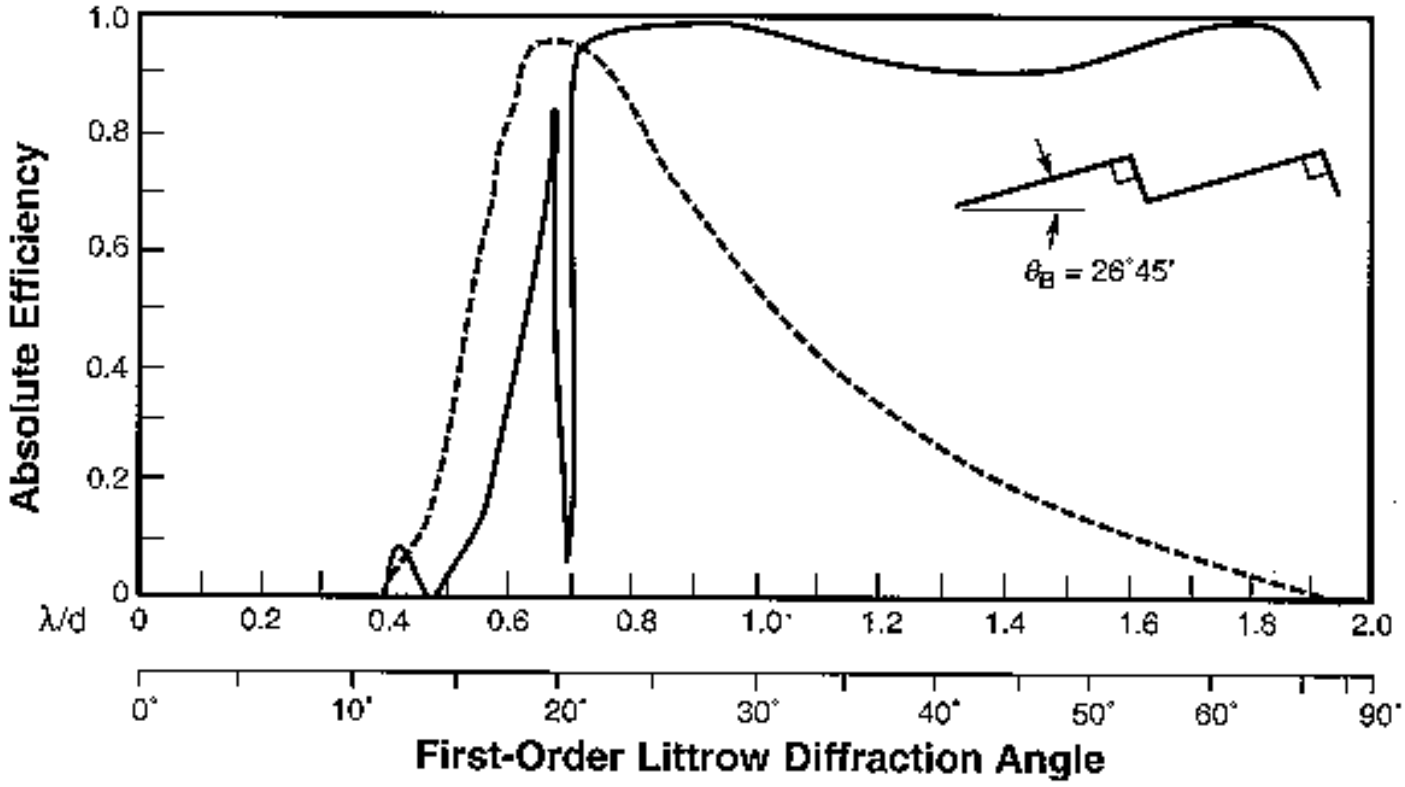

Figure 9-9. Same as Figure 9-5, except 26° 45' blaze angle.

Theoretically, all gratings have a second high-efficiency peak in the S-plane at angles corresponding to the complement of the blaze angle (90° – θ); in practice, this peak is fully developed only on steeper groove-angle gratings, and then only when the steep face of the groove is not too badly deformed by the lateral plastic flow inherent in the diamond tool burnishing process. The strong polarization observed at all high angles of diffraction limits the useable efficiency in unpolarized light, but it makes such gratings very useful for tuning lasers, especially molecular lasers. The groove spacing may be chosen so that the lasing band corresponds to either the first or second of the S-plane high-efficiency plateaus. The latter will give at least twice the dispersion (in fact the maximum possible), as it is proportional to the tangent of the angle of diffraction under the Littrow conditions typical of laser tuning.

Very-high blaze angle gratings (θ > 38°) are rarely used in the first order; their efficiency curves are interesting only because of the high P-plane values (Figure 9-10). In high orders they are often used in tuning dye lasers, where high dispersion is important and where tuning through several orders can cover a wide spectral region with good efficiency. Efficiency curves for this family of gratings are shown for two configurations. With an angular deviation of 8°, the efficiency does not differ too much from Littrow; when this angle is 45°, the deep groove results in sharp reductions in efficiency. Some of the missing energy shows up in the zeroth order, but some of it can be absorbed by the grating.

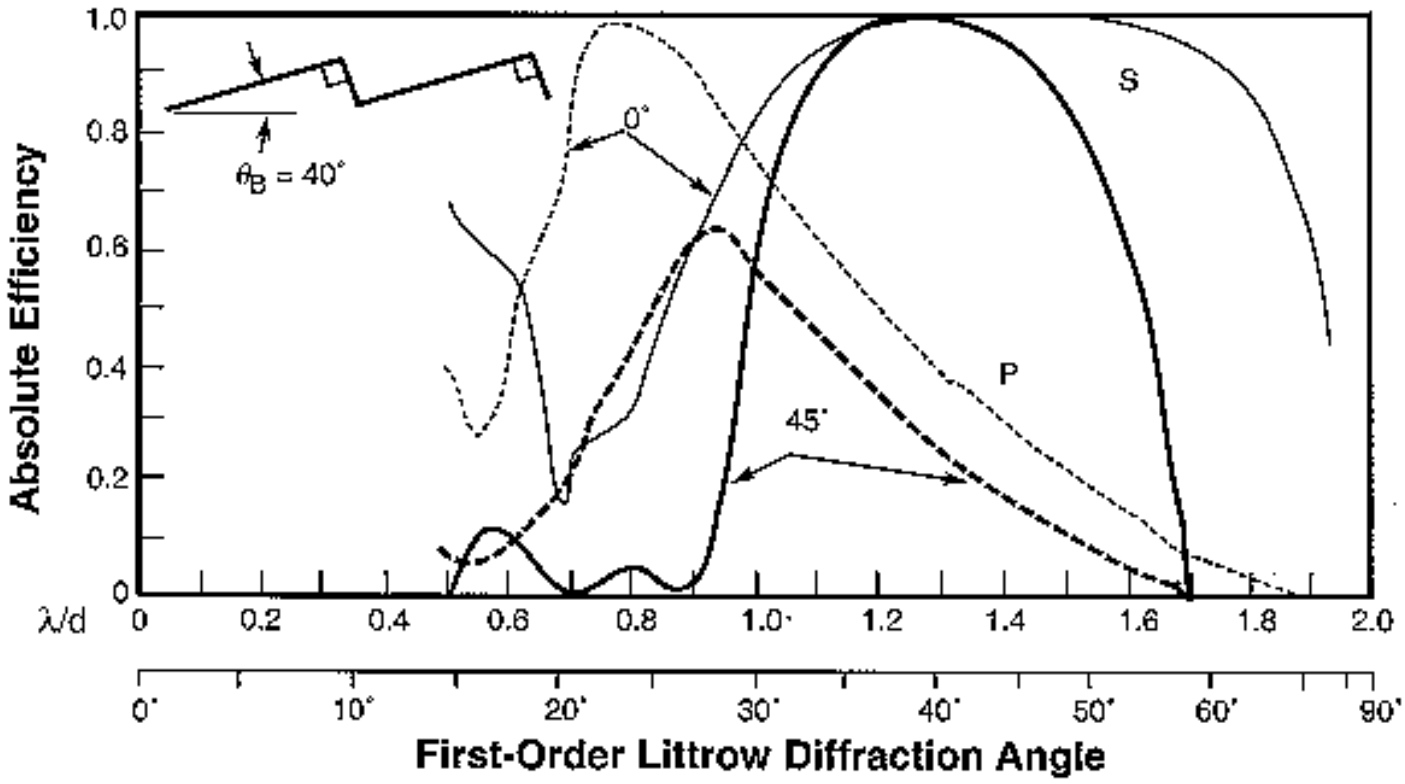

Figure 9-10. Same as Figure 9-5, except 46° blaze angle and 8° and 45° between the incident and diffracted beams (shown as light and heavy lines, respectively).

9.3. EFFICIENCY CHARACTERISTICS FOR SINUSOIDAL-GROOVE GRATINGS [top]

A sinusoidal-groove grating can be obtained by the interferometric (holographic) recording techniques described in Chapter 4. Sinusoidal gratings have a somewhat different diffracted efficiency behavior than do triangular-groove gratings, and are treated separately.

It is convenient to consider five domains of sinusoidal-groove gratings, with progressively increasing modulation μ, where

$$\mu = \frac{h}{d} \qquad (9\text{-}1)$$

h is the groove height and *d* is the groove spacing:[10]

domain	*modulation*
very low	$\mu < 0.05$
low	$0.05 < \mu < 0.15$
medium	$0.15 < \mu < 0.25$
high	$0.25 < \mu < 0.4$
very higb	$\mu > 0.4$

Very low modulation gratings ($\mu < 0.05$) operate in the scalar domain, where the theoretical efficiency peak for sinusoidal grooves is only 33.8% (Figure 9-11). This figure may be readily scaled, and specification is a simple matter as soon as it becomes clear that the peak wavelength always occurs at $\lambda_B = 3.4h = 3.4\mu d$. A blazed grating with an equivalent peak wavelength will require a groove depth 1.7 times greater.

Low modulation gratings ($0.05 < \mu < 0.15$) are quite useful in that they have a low but rather flat efficiency over a λ/d band from 0.35 to 1.4 (Figure 9-12). This figure includes not only the infinite conductivity values shown on all previous ones, but includes the effects of finite conductivity by adding the curves for an 1800 g/mm aluminum surface. The most significant effect is in the behavior of the anomaly, which is the typical result of the finite conductivity of real metals.

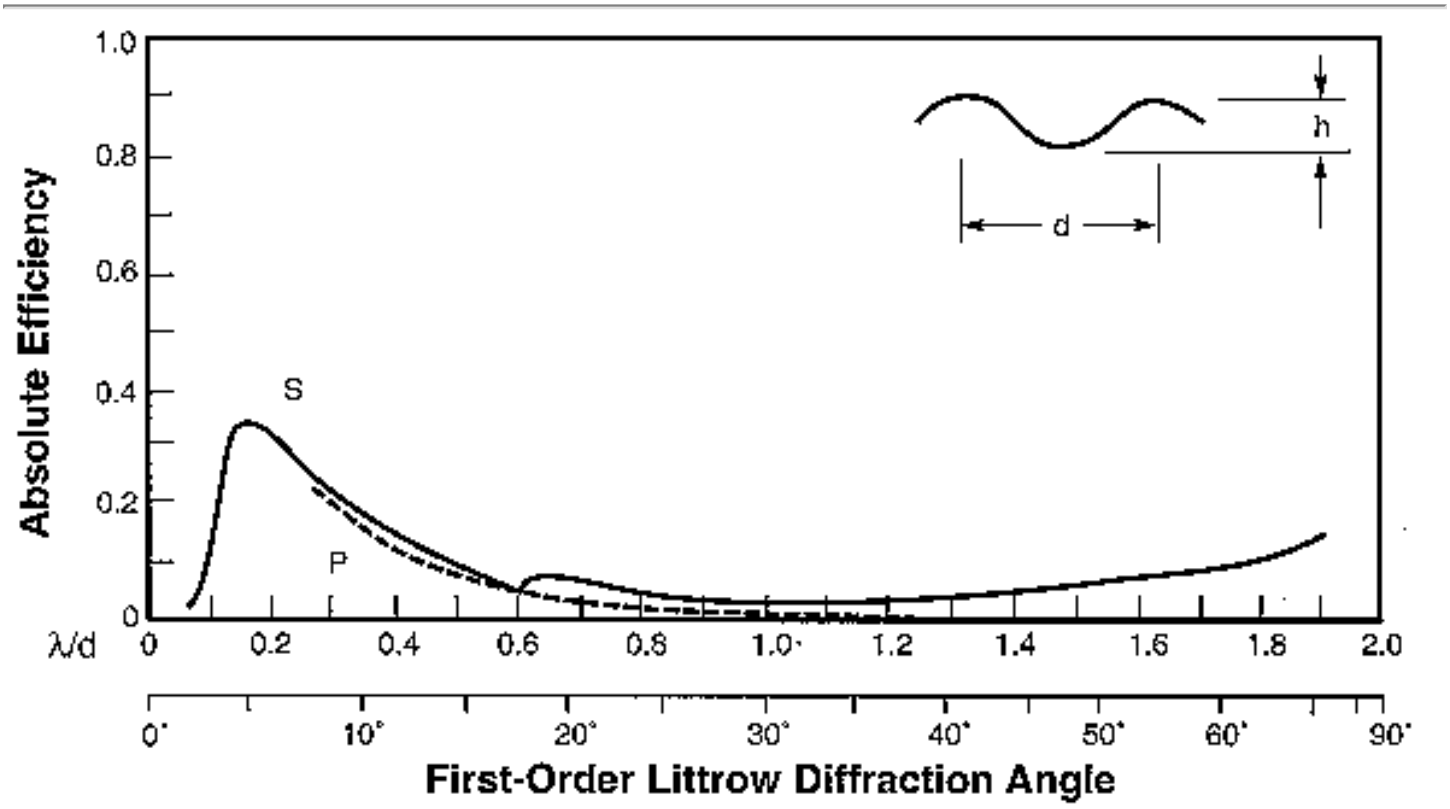

Figure 9-11. First-order theoretical efficiency curve: sinusoidal grating, μ = h/d = 0.05 and Littrow mounting (2K = 0)

Figure 9-13 is a good example of a *medium modulation* grating ($0.15 < \mu < 0.25$). It demonstrates an important aspect of such sinusoidal gratings, namely that reasonable efficiency requirements confine first-order applications to values of $\lambda/d > 0.45$, which eliminates them from systems with wide wavelength ranges. Over this restricted region, however, efficiencies are comparable to those of triangular grooves, including the high degree of polarization. This figure also demonstrates how a departure from Littrow to an angular deviation of 8° splits the anomaly into two branches, corresponding to the new locations of the –1 and +2 order passing-off conditions.

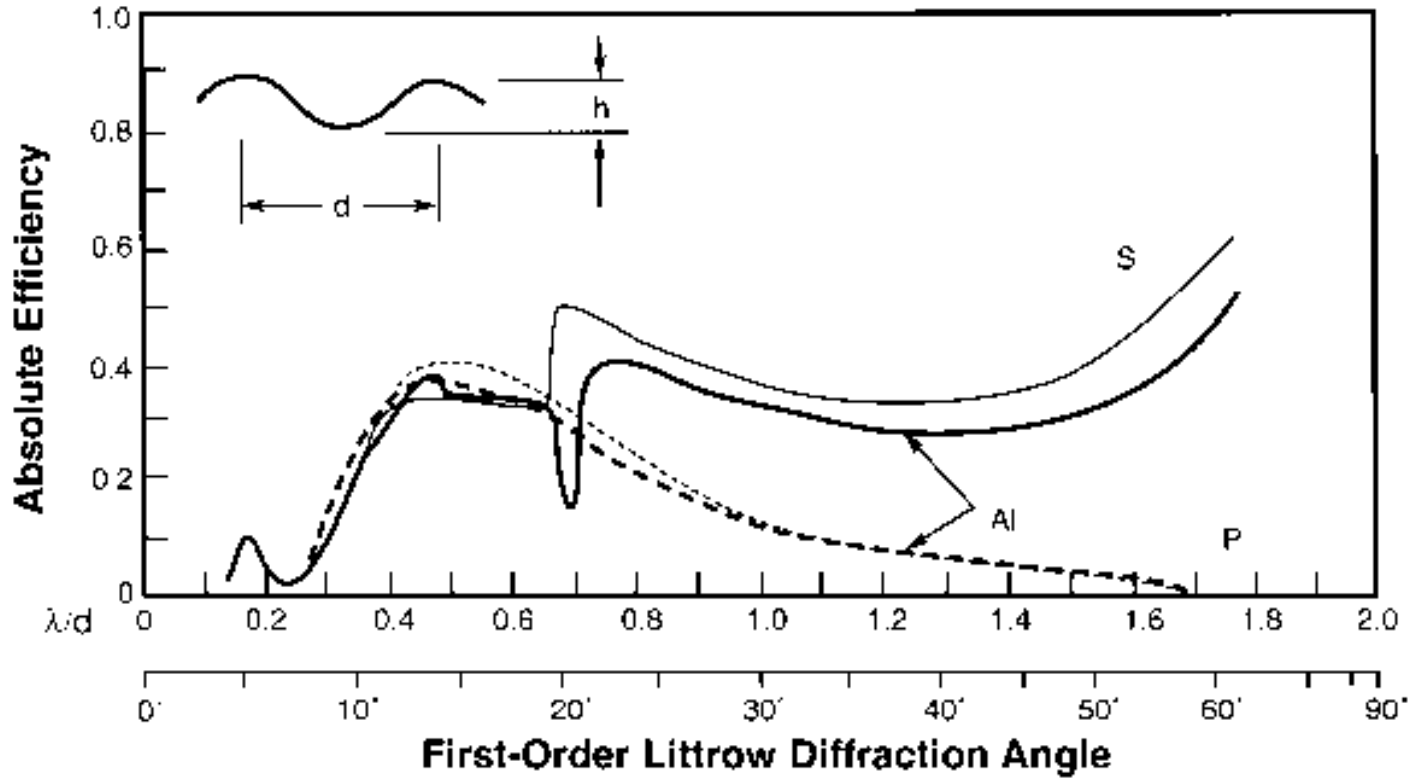

Figure 9-12. First-order theoretical efficiency curve: sinusoidal grating, aluminum coating, 1800 grooves per millimeter, μ = 0.14 and Littrow mounting. Solid curves, S-plane; dashed curves, P-plane. For reference, the curves for a perfectly conducting surface are shown as well (light curves).

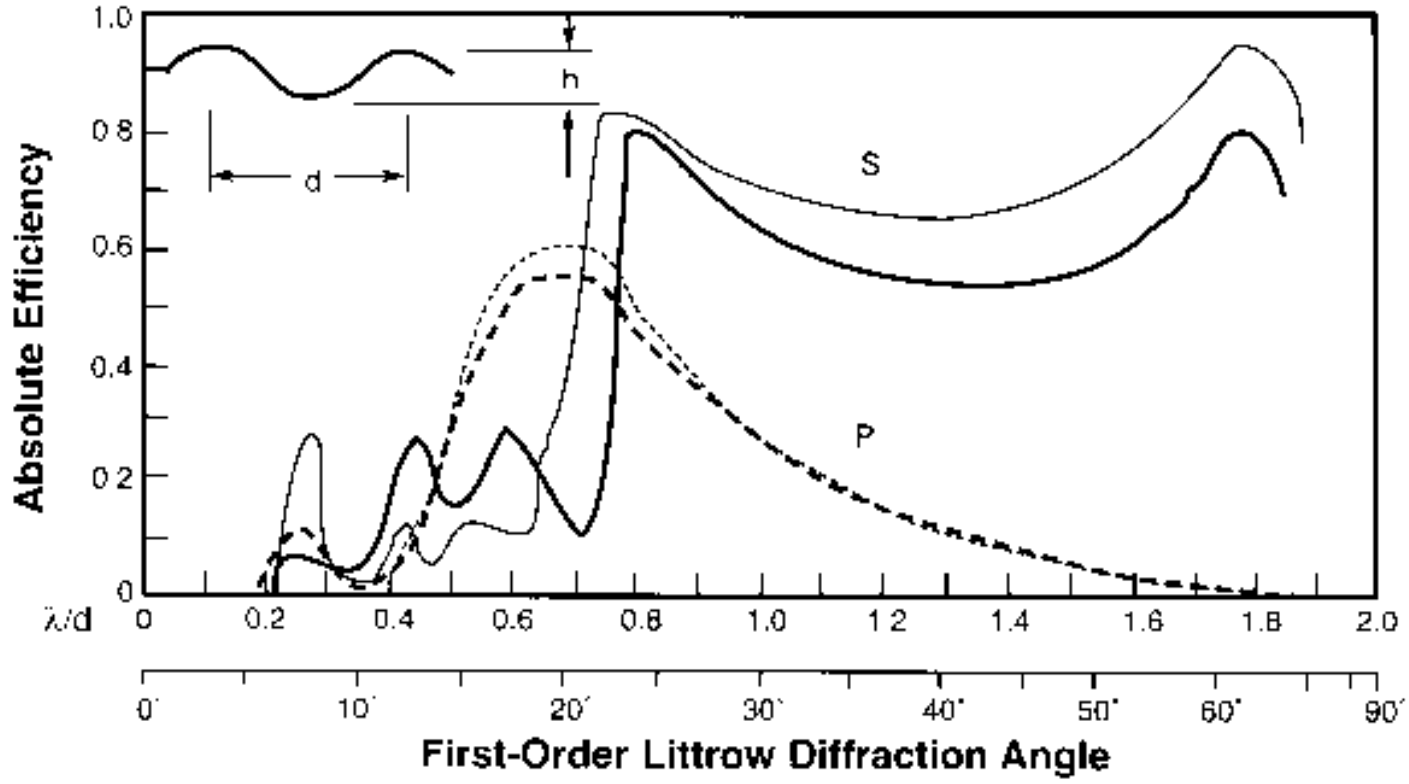

Figure 9-13. Same as Figure 9-12, except $\mu = 0.22$ *and 8° between incident and diffracted beams (2K = 8°).*

High modulation gratings ($0.25 < \mu < 0.40$), such as shown in Figure 9-14, have the maximum useful first-order efficiencies of sinusoidal-groove gratings. Provided they are restricted to the domain in which higher orders diffract (*i.e.*, $\lambda/d > 0.65$), their efficiencies are very similar to those of triangular-groove gratings having similar groove depths (*i.e.*, $26° < \theta < 35°$).

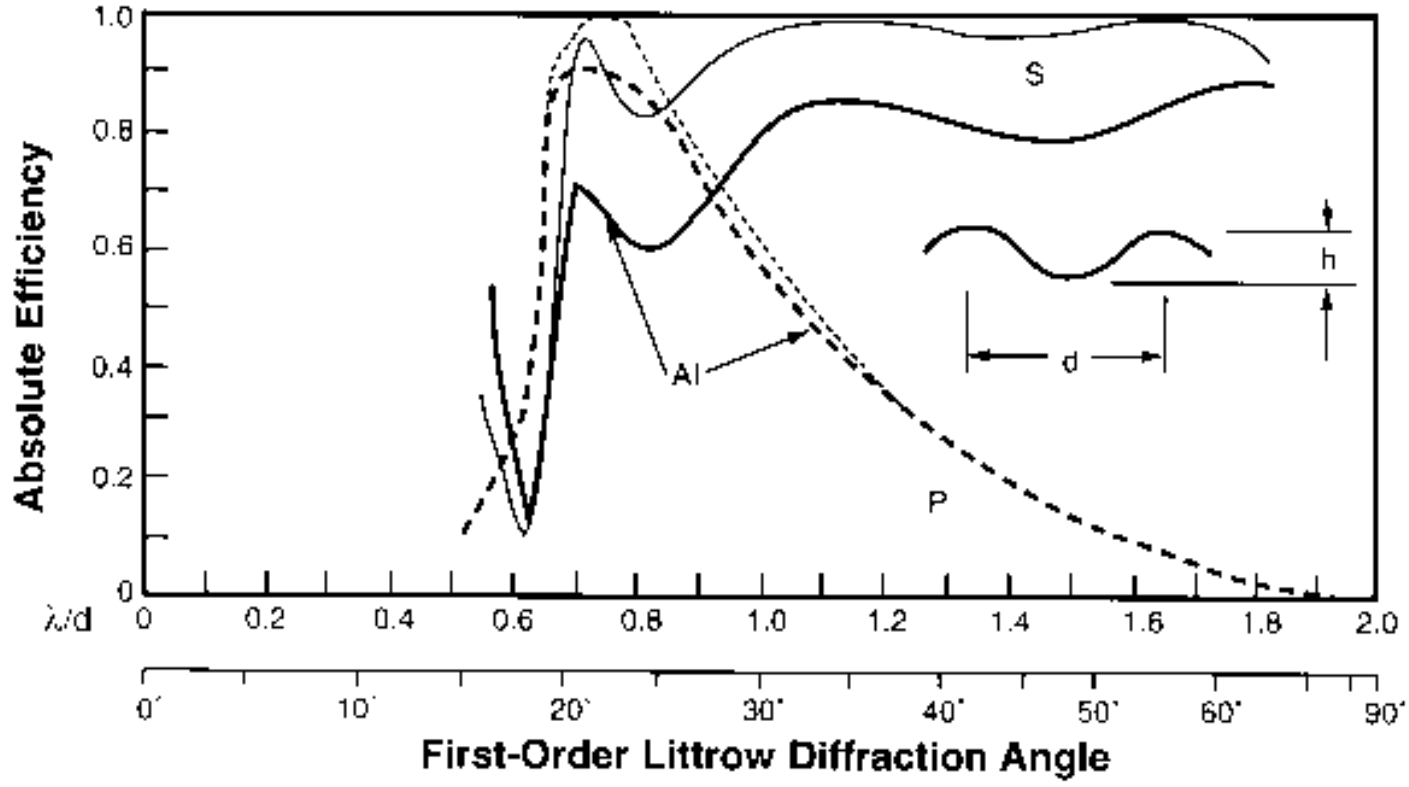

Figure 9-14. Same as Figure 9-12, except $\mu = 0.36$.

Very-high modulation gratings ($\mu > 0.40$), in common with equivalent triangular-groove gratings, have little application in the first order due to their relatively low efficiencies except perhaps over narrow wavelengths ranges and for grazing incidence applications.

9.4. THE EFFECTS OF FINITE CONDUCTIVITY [top]

For metal-coated reflection gratings, the finite conductivity of the metal is of little importance for wavelengths of diffraction above 4 μm, but the complex nature of the dielectric constant and the index of refraction begin to effect efficiency behavior noticeably for wavelengths below 1 μm, and progressively more so as the wavelength decreases. In the P-plane, their effect is a simple reduction in efficiency, in direct proportion to the reflectance. In the S-plane, the effect is more complicated, especially for deeper grooves and shorter wavelengths.

Figure 9-15 shows the first-order efficiency curve for a widely-used grating: 1200 g/mm, triangular grooves, medium blaze angle ($\theta = 10°$), coated with aluminum and used with an angular deviation of 8°. The finite conductivity of the metal cause a reduction in efficiency; also, severe modification of the anomaly is apparent. It is typical that the anomaly is broadened and shifted toward a longer wavelength with respect to the infinite conductivity curve. Even for an angular deviation as small as 8°, the single anomaly in the figure is separated into a double anomaly.

For sinusoidal gratings, the situation is shown in Figures 9-12 and 9-14. Figure 9-13 is interesting in that it clearly shows a series of new anomalies that are traceable to the role of aluminum.

With scalar domain gratings (either $\theta < 5°$ or $\mu < 0.10$), the role of finite conductivity is simply to reduce the efficiency by the ratio of surface reflectance.

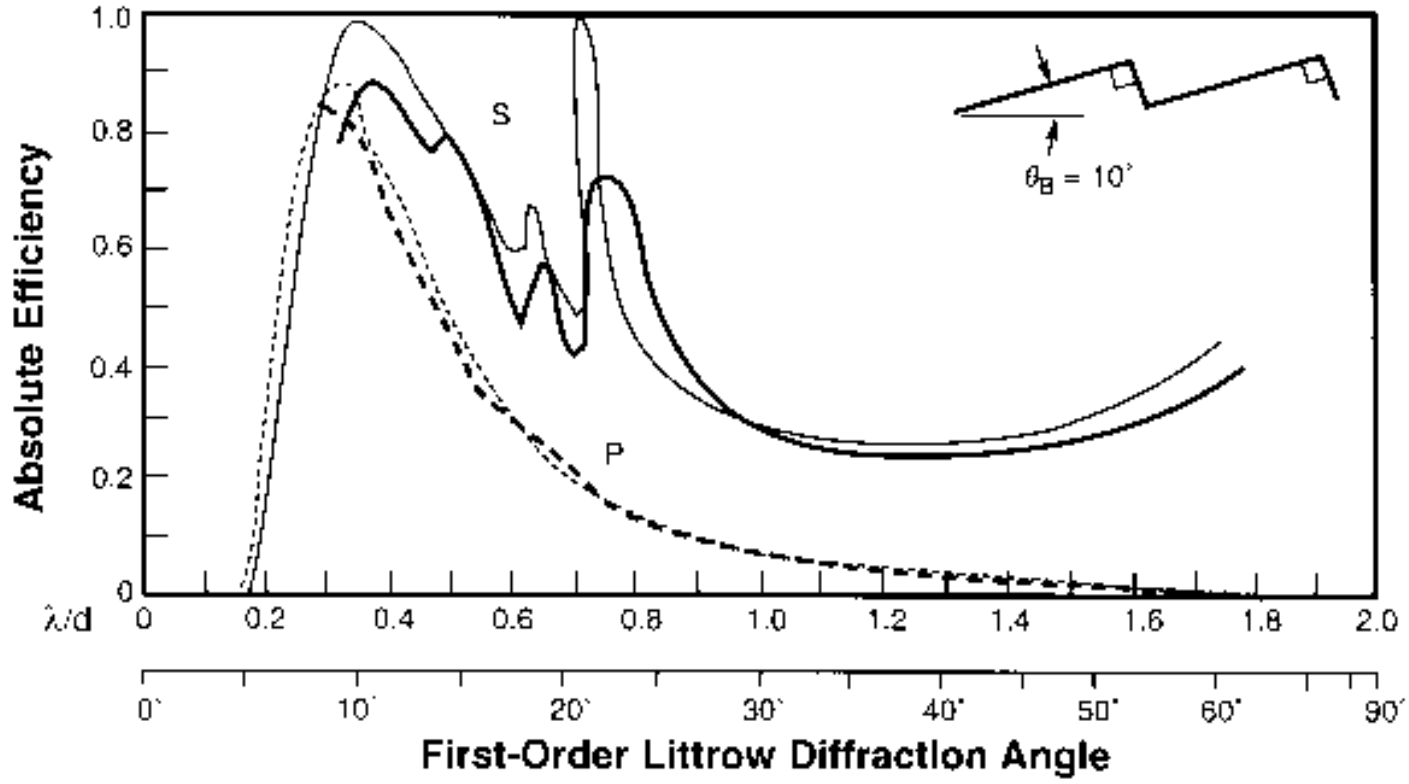

Figure 9-15. First-order theoretical efficiency curve: triangular-groove grating, aluminum coating, 1200 grooves per millimeter, 10° blaze angle and 2K = 8°. Solid curves, S-plane; dashed curves, P-plane. For reference, the curves for a perfectly conducting surface are shown as well (light curves).

9.5. DISTRIBUTION OF ENERGY BY DIFFRACTION ORDER [top]

Gratings are most often used in higher diffraction orders to extend the spectral range of a single grating to shorter wavelengths than can be covered in lower orders. For blazed gratings, the second-order peak will be at one-half the wavelength of the nominal first-order peak, the third-order peak at one-third, *etc.* Since the ratio λ/d will be progressively smaller as $|m|$ increases, polarization effects will become less significant; anomalies are usually negligible in diffraction

orders for which $|m| > 2$. Figures 9-16 and -17 show the second- and third-order theoretical Littrow efficiencies, respectively, for a blazed grating with $\theta = 26°45'$; they are plotted as a function of $m\lambda/d$ in order to demonstrate the proper angular ranges of use. These curves should be compared with Figure 9-9 for corresponding first-order behavior.

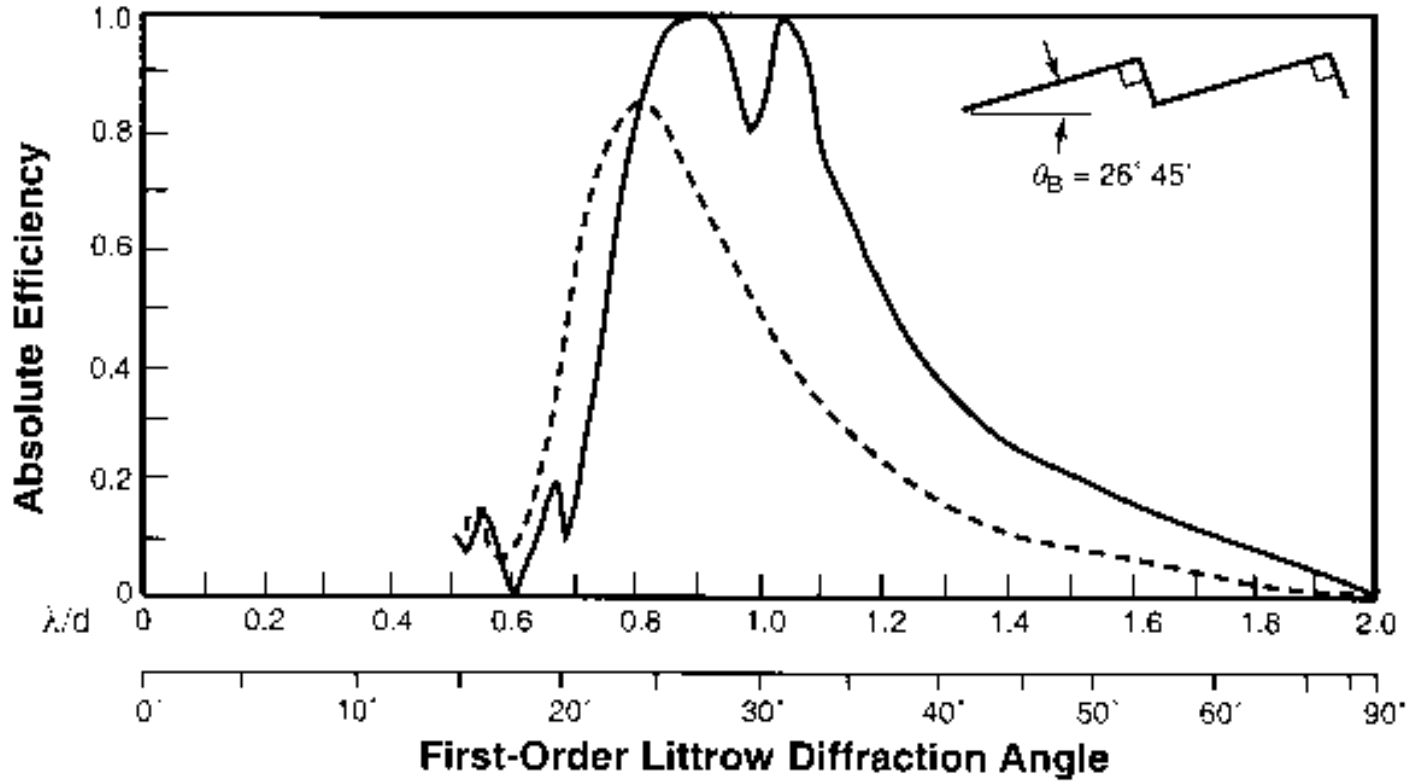

Figure 9-16. Second-order theoretical efficiency curve: 26° 45' blaze angle and Littrow mounting. Solid curve, S-plane; dashed curve, P-plane.

For gratings with sinusoidally shaped grooves, higher orders can also be used, but if efficiency is important, the choice is likely to be a finer pitch first-order grating instead. When groove modulations are very low (so that the grating is used in the scalar domain), the second-order efficiency curve looks similar to Figure 9-18, except that the theoretical peak value is about 23% (instead of 33.8%) and occurs at a wavelength 0.6 times that of the first-order peak, which corresponds to $2.05h$ (instead of $3.41h$), where h is the groove depth. Successive higher-order curves for gratings with sinusoidal grooves are not only closer together, but drop off more sharply with order than for gratings with triangular grooves. For sufficiently deeply modulated sinusoidal grooves, the second order can often be used effectively, though (as Figure 9-18 shows) polarization effects are relatively strong. The corresponding third-order theoretical curve is shown in Figure 9-19.

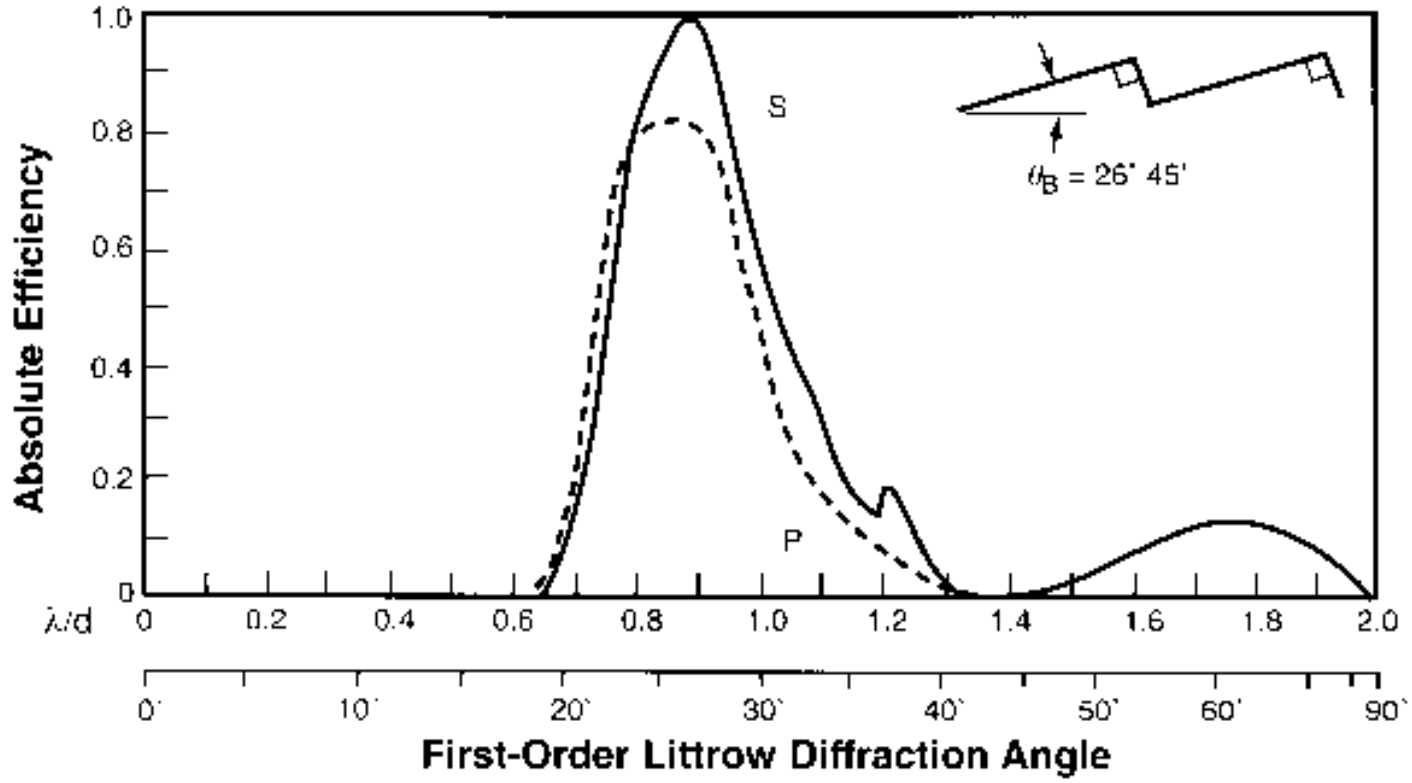

Figure 9-17. Same as Figure 9-16, except third order.

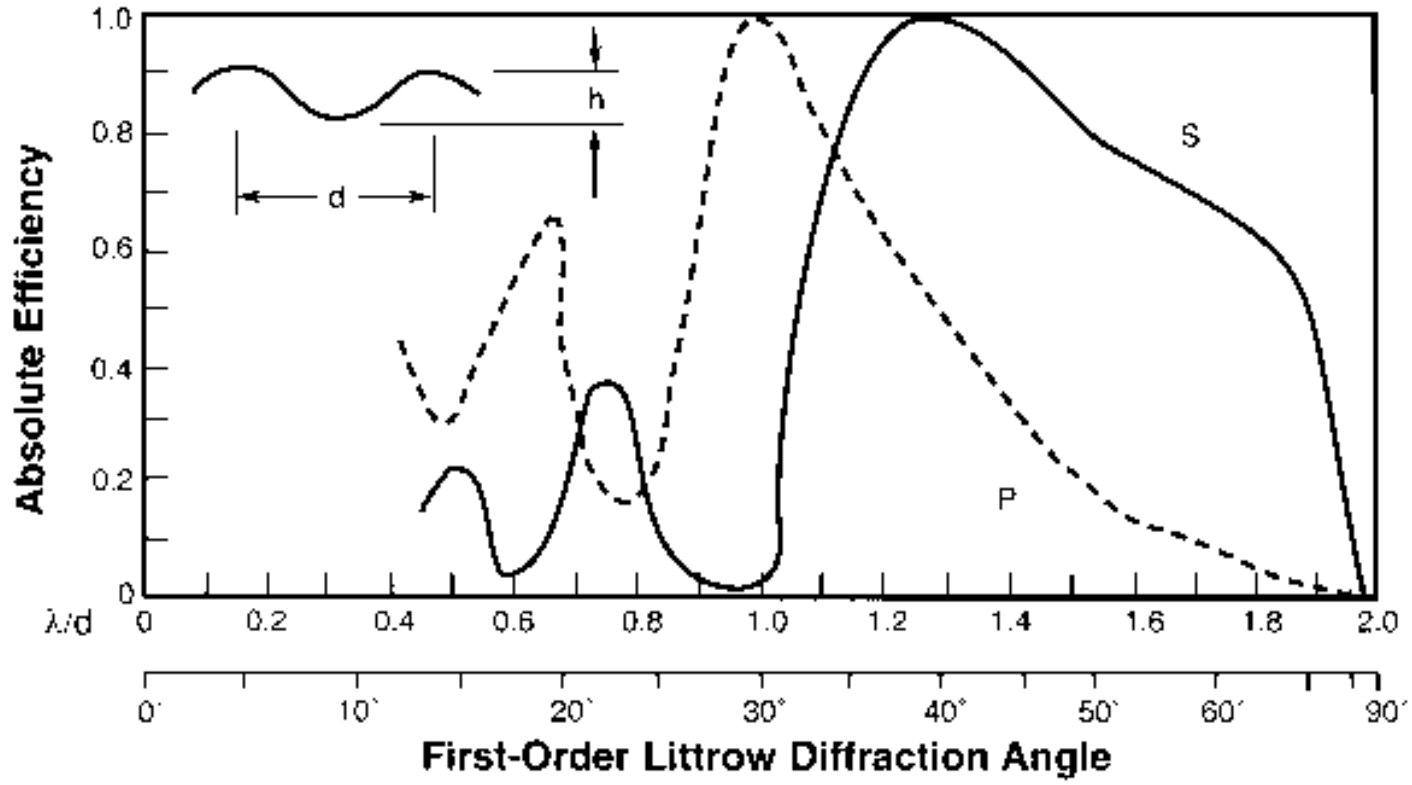

Figure 9-18. Second-order theoretical efficiency curve: sinusoidal grating, μ = 0.36 and Littrow

mounting. Solid curve, S-plane; dashed curve, P-plane.

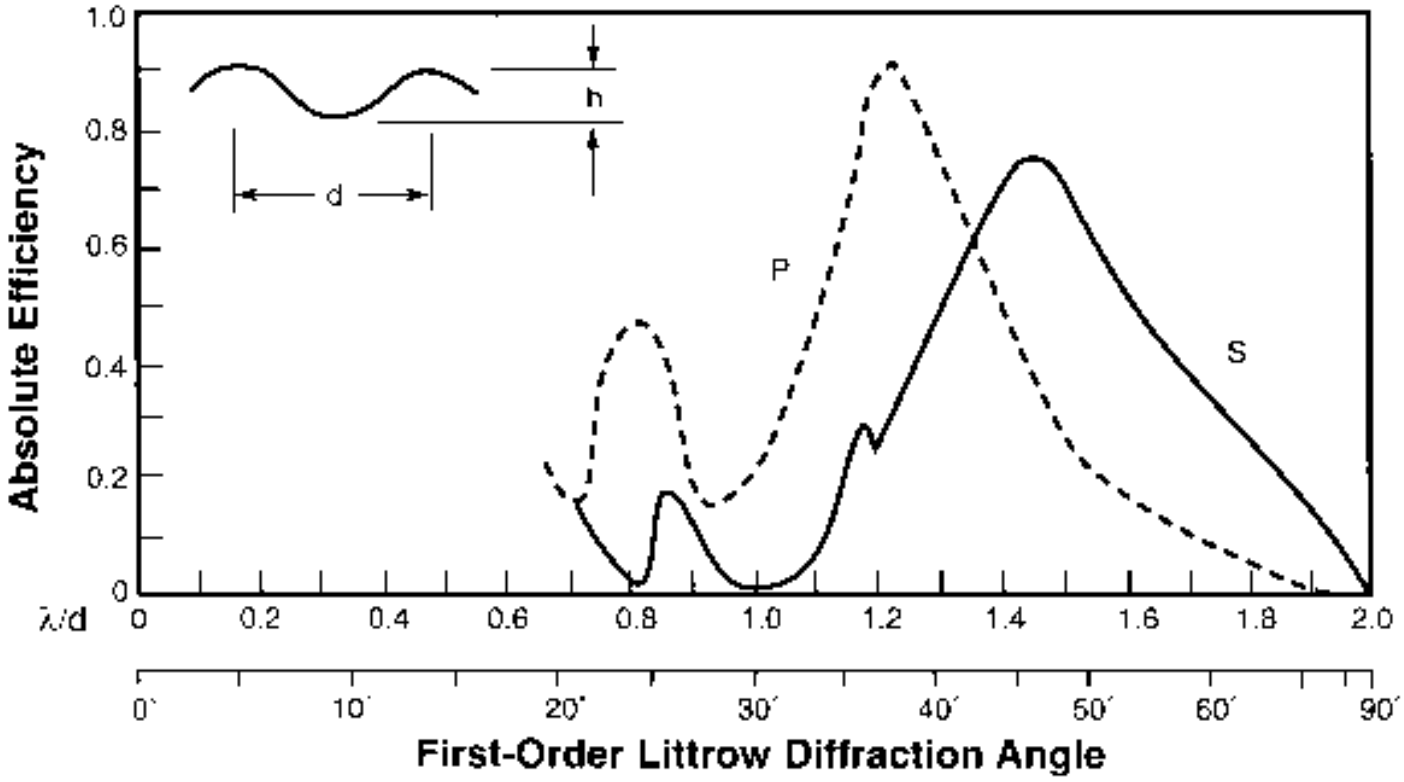

Figure 9-19. Same as Figure 9-18, except third order.

9.6. USEFUL WAVELENGTH RANGE [top]

A grating is of little use if high-grade imaging is not accompanied by sufficient diffraction efficiency. The laws governing diffracted efficiency are quite complicated, but a very rough rule of thumb can be used to estimate the useful range of wavelengths available on either side of the blaze (peak) wavelength for triangular-groove gratings.

For coarse gratings (for which $d = 2\lambda$), in the first diffraction order the efficiency is roughly half its maximum (which is at λ_B) at $2\lambda_B/3$ and $3\lambda_B/2$. Curves of similar shape are obtained in the second and third orders, but the efficiencies are typically 20% less everywhere, as compared with the first order.

Grating of fine pitch ($d \approx \lambda$) have a somewhat lower peak efficiency than do coarse gratings, though the useful wavelength range is greater.

9.7. BLAZING OF RULED TRANSMISSION GRATINGS [top]

Because they have no metallic overcoating, triangular-groove transmission gratings display far simpler efficiency characteristics than do their ruled counterparts. In particular, transmission gratings have efficiency curves almost completely free of polarization effects.

The peak wavelength generally occurs when the direction of refraction of the incident beam through a groove (thought of as a small prism) equals the direction dictated by the grating equation. [This is in direct analogy with the model of reflection grating blazing in that the grooves are thought of as small mirrors.] Due to the index of refraction of the grating, though, the groove angle exceeds the blaze angle for a transmission grating.

9.8. BLAZING OF HOLOGRAPHIC REFLECTION GRATINGS [top]

Although holographic gratings generally do not have the triangular groove profile found in ruled gratings, holographic gratings may still exhibit blazing characteristics (see, for example, Figure 9-18). For this reason it is not correct to say that all blazed gratings have triangular profiles, or that all blazed gratings are ruled gratings - blazing refers to high diffraction efficiency, regardless of the profile of the grooves or the method used to generate them.

This being said, there are some cases in which it would be preferable for a holographic grating to have a triangular groove profile rather than a sinusoidal profile. A useful technique for rendering sinusoidal groove profiles more nearly triangular is *ion etching*. By bombarding a surface with energetic ions, the material can be removed (etched) by an amount per unit time dependent on the angle between the beam and the local surface normal. The etching of a sinusoidal profile by an ion beam provides a continuously varying angle between the ion beam and the surface normal, which preferentially removes material at some parts of the profile while leaving other parts hardly etched. The surface evolves toward a triangular groove profile as the ions bombard it.

9.9. OVERCOATING OF REFLECTION GRATINGS [top]

All standard reflection gratings are furnished with an aluminum (Al) reflecting surface. While no other metal has more general application, there are a number of special situations where alternative surfaces or coatings are recommended.

The metallic coating on a reflection grating is evaporated onto the substrate. This produces a surface whose reflectivity is higher than that of the same metal electroplated onto the grating surface. The thickness of the metallic layer is chosen to enhance the diffraction efficiency

throughout the spectral region of interest.

The reflectivity of aluminum drops rather sharply for wavelengths below 170 nm. While freshly deposited, fast-fired pure aluminum in high vacuum maintains its reflectivity to wavelengths shorter than 100 nm, the thin layer of oxide normally present absorbs wavelengths below about 170 nm.

Fortunately, a method borrowed from mirror technology makes it possible to preserve the reflectivity of aluminum to shorter wavelengths. The process involves overcoating the grating with a thin layer of fast-fired aluminum, which is followed immediately by a coating of magnesium fluoride (MgF_2) approximately 25 nm thick; the grating is kept at room temperature for both coatings. The main purpose of the MgF_2 coating is to protect the aluminum from oxidation. The advantage of this coating is especially marked in the region between 120 and 170 nm. While reflectivity drops off sharply below this region, it remains higher than that of gold and comparable to that of platinum, the most commonly used alternative materials, down to 70 nm.

On an experimental basis, the use of lithium fluoride (LiF) instead of MgF_2 has proved effective in maintaining relatively high reflectivity in the 100 to 110 nm region. Unfortunately, a LiF film deteriorates unless maintained in a low humidity environment, which has curtailed its use, though it can be protected by a very thin layer of MgF_2.

Gratings coated with gold (Au) and platinum (Pt) have been used for some time. Gold gratings have the great advantage that they can be replicated directly from either gold or aluminum master gratings, and are therefore most likely to maintain their groove profiles.

Overcoating gratings so that their surfaces are coated with two layers of different metals sometimes leads to a change in diffraction efficiency over time. Hunter *et al*.[11] have found the cause of this change to be intermetallic diffusion. For example, they measured a drastic decrease (over time) in efficiency at 122 nm for gratings coated in Au and then overcoated in Al + MgF_2; this decrease was attributed to the formation of intermetallic compounds, primarily $AuAl_2$ and Au_2Al. Placing a suitable dielectric layer such as SiO between the two metallic layers prevents this diffusion.

As mentioned elsewhere, fingerprints are a danger to aluminized optics. It is possible to overcoat such optics, both gratings and mirrors, with dielectrics like MgF_2, to prevent finger acids from attacking the aluminum. These MgF_2 coatings cannot be baked, as is customary for glass optics, and therefore must not be cleaned with water. Spectrographic-grade organic solvents are the only recommended cleaning agents, and they should be used sparingly and with care.

Multilayer dielectric overcoatings, which are so useful in enhancing plane mirror surfaces, are of little value on a typical diffraction grating used in the visible and infrared spectra, as these coatings lead to complex guided wave effects that are rarely useful. For wavelengths below 30 nm,

though, in which grazing angles of incidence and diffraction are common, multilayer coatings can enhance efficiency considerably.[12]

PREVIOUS CHAPTER NEXT CHAPTER

Back to top

10. TESTING AND CHARACTERIZING DIFFRACTION GRATINGS

PREVIOUS CHAPTER
NEXT CHAPTER

TABLE OF CONTENTS

10.1. SPECTRAL DEFECTS [top]

It is fundamental to the nature of diffraction gratings that errors are relatively easy to measure, although not all attributes are equally detectable or sometimes even definable.

For example, an optically clean grating, *i.e.*, one with low background in the form of scatter or satellites, can be simply tested for Rowland ghosts on an optical bench. With a mercury lamp or a laser source, and a scanning slit connected to a detector and recorder, a ghost having intensity 0.002% of the intensity of the main line can be located readily. The periodic error in the groove spacing giving rise to such a ghost may be less than one nanometer, a

mechanical precision seldom achieved with man-made objects.

Grating ghosts are measured at Thermo RGL by making the grating part of a scanning spectrometer and illuminating it with monochromatic light, such as that from a mercury isotope lamp (isotope 198 or 202) or a helium-neon laser. On scanning both sides of the parent line, using a chart recorder and calibrated attenuators, it is easy to identify all ghost lines and to measure their intensities relative to the parent line. The importance of ghosts in grating applications varies considerably. In most spectrophotometers, and in work with low-intensity sources, ghosts play a negligible role. In Raman spectroscopy, however, even the weakest ghost may appear to be a Raman line, especially when investigating solid samples, and hence these ghosts must be suppressed to truly negligible values.

Ghosts are usually classified as Rowland ghosts and Lyman ghosts. Another grating deficiency is the presence of satellites; if excessive, satellites lying within a line contour may reduce the attainable resolution, and hence are of great concern in high resolution spectroscopy. Satellites should be at a minimum for Raman spectroscopy.

10.1.1. Rowland Ghosts

Rowland ghosts are spurious lines seen in some grating spectra that result from periodic errors in the spacing of the grooves (see Figure 10-1). These lines are usually located symmetrically with respect to each strong spectral line at a spectral distance from it, which depends on the period of the error, and with an intensity that depends on the amplitude of this error.

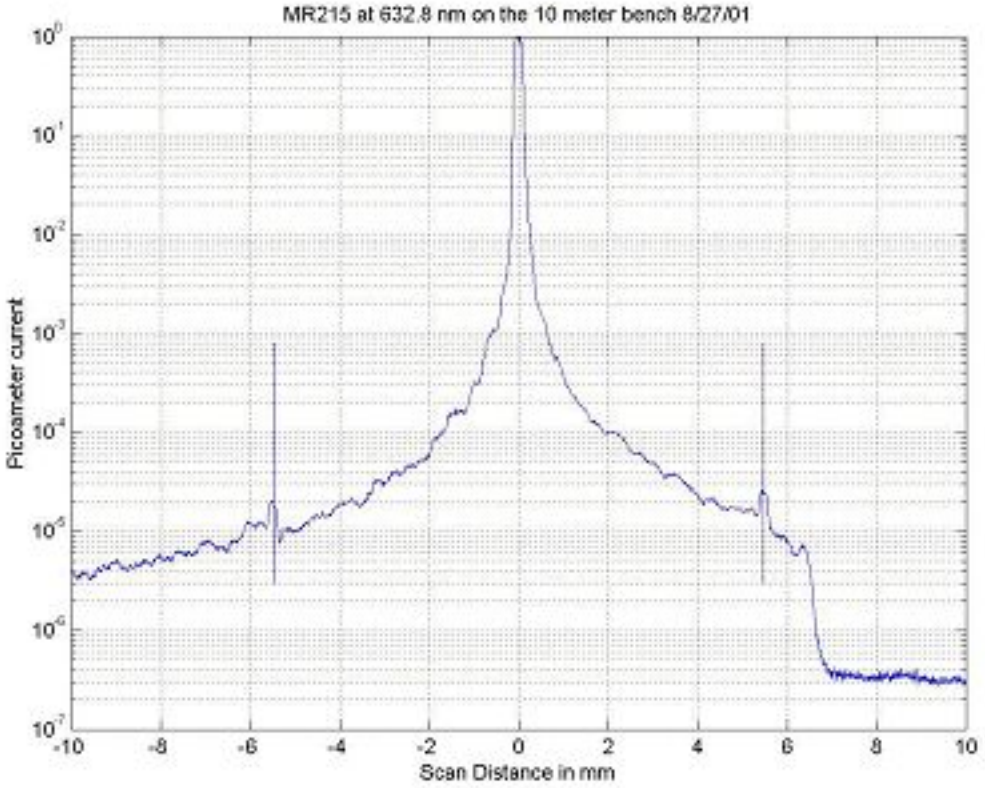

Figure 10-1. 'Ghost' trace showing Rowland ghosts caused by the periodic error of 2.54 mm in the lead screw of the Thermo RGL MIT 'B' engine. MR215 is an echelle grating, with 52.67 g/mm, in this case tested in the 54th order.

If the curve of groove spacing error *vs.* position is not simply sinusoidal, there will be a number of ghosts on each side of the parent line representing the various orders from each of the harmonics of the error curve. On engines with mechanical drives, Rowland ghosts are associated primarily with errors in the lead or pitch of the precision screw, or with the bearings of the ruling engine. As a consequence, their location depends upon the number of grooves ruled for each complete turn of the screw. For example, if the ruling engine has a pitch of 2 mm, and a ruling is made at 1200 grooves/mm, 2400 grooves will be ruled per turn of the screw, and the ghosts in the first order can be expected to lie at $\Delta\lambda = \pm \lambda/2400$ from the parent line λ, with additional ghosts located at integral multiples of $\Delta\lambda$. In gratings ruled on engines with interferometric feedback correction mechanisms, Rowland ghosts are usually much less intense, but they can arise from the mechanisms used in the correction system if care is not taken to prevent their occurrence.

If the character of the periodic errors in a ruling engine were simply harmonic, which is rarely true in practice, the ratio of the diffracted intensities of the first order Rowland ghost ($I_{RG\ (m\ =\ 1)}$) to that of the parent line (I_{PL}) is

$$\frac{I_{RG(m=1)}}{I_{PL}} = 4\left(\frac{\pi A \sin\alpha}{\lambda}\right)^2, \qquad (10\text{-}1)$$

where A is the peak simple harmonic error amplitude, α is the angle of incidence, and λ is the diffracted wavelength. The second-order Rowland ghost $I_{RG\ (m\ =\ 2)}$ will be much less intense (note the exponent):

$$\frac{I_{RG(m=2)}}{I_{PL}} = 4\left(\frac{\pi A \sin\alpha}{\lambda}\right)^4. \qquad (10\text{-}2)$$

Higher-order Rowland ghosts would be virtually invisible. The ghost intensity is independent of the diffraction order m of the parent line, and of the groove spacing d. In the Littrow configuration, Eq. (10-1) becomes

$$\frac{I_{RG(m=1)}}{I_{PL}} = \left(\frac{\pi m A}{d}\right)^2, \quad \text{in Littrow,} \qquad (10\text{-}3)$$

an expression derived in 1893 by Rowland.

These simple mathematical formulae do not always apply in practice when describing higher-order ghost intensities, since the harmonic content of actual error curves gives rise to complex amplitudes that must be added vectorially and then squared to obtain intensity functions. A fortunate result of this is that ghost intensities are generally smaller than those predicted from the peak error amplitude.

The order of magnitude of the fundamental harmonic error amplitude can be derived from Eq. (10-1) [or Eq. (10-3)]. For example, a 1200 g/mm grating used in the m = 1 order in Littrow will show a 0.14% first-order ghost intensity, compared with the parent line, for a fundamental harmonic error

amplitude of 10 nm. For some applications this intensity is unacceptably high, which illustrates the importance of making a concerted effort to minimize periodic errors of ruling. For Raman gratings and echelles, the amplitude of the periodic error must not exceed one nanometer; the fact that this has been accomplished is a remarkable achievement.

10.1.2. Lyman Ghosts

Ghost lines observed at large spectral distances from their parent lines are called Lyman ghosts. They result from compounded periodic errors in the spacing of the grating grooves. Lyman ghosts differ from Rowland ghosts in that the period of Lyman ghosts is on the order of a few times the groove spacing. Lyman ghosts can be said to be in fractional-order positions (see Figure 10-2). Thus, if every other groove is misplaced so that the period contains just two grooves, ghosts are seen in the half-order positions. The number of grooves per period determines the fractional-order position of Lyman ghosts. Usually it is possible to find the origin of the error in the ruling engine once its periodicity is determined. It is important that Lyman ghosts be kept to a minimum, because they are not nearly as easy to identify as Rowland ghosts.

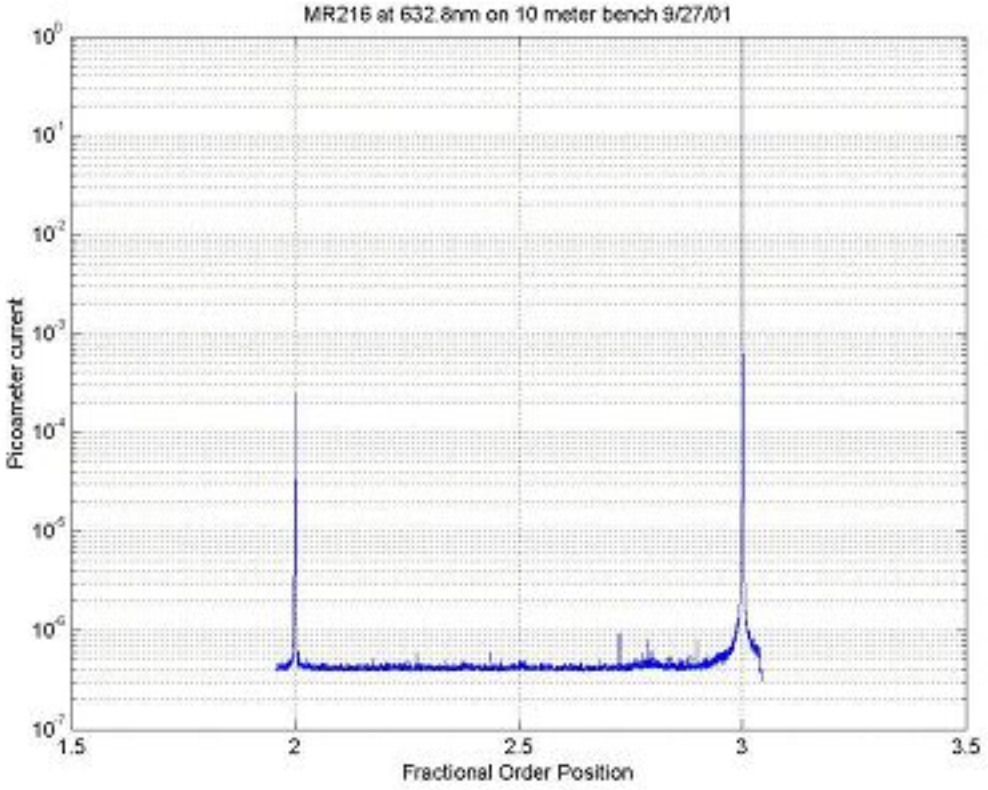

Figure 10-2. 'Ghost' trace showing Lyman ghosts (the small spikes between orders 2 and 3), which can be associated with fractional order positions, e.g. an error every five grooves corresponds to a fraction order of 1/5.

10.1.3. Satellites

Satellites are false spectral lines usually occurring very close to the parent line. Individual gratings vary greatly in the number and intensity of satellites which they produce. In a poor grating, they give rise to much scattered light, referred to as *grass* (so called since this low intensity scattered light appears like a strip of lawn when viewed with green mercury light). Satellites are absent in a "clean" grating. In contrast to Rowland ghosts, which usually arise from errors extending over large areas of the grating, each satellite usually originates from a small number of randomly misplaced grooves in a localized part of the grating. With laser illumination a relative background intensity of 10-7 is easily observable with the eye.

10.2. EFFICIENCY MEASUREMENT [top]

Grating efficiency measurements are generally performed with a double monochromator system. The first monochromator supplies monochromatic light derived from a tungsten lamp, mercury arc, or deuterium lamp, depending on the spectral region involved. The grating being tested serves as the dispersing element in the second monochromator. In the normal mode of operation, the output is compared with that from a high-grade mirror coated with the same material as the grating. The efficiency of the grating relative to that of the mirror is reported (relative efficiency), although absolute efficiency values can also be obtained (either by direct measurement or through knowledge of the variation of mirror reflectivity with wavelength). For plane reflection gratings, the wavelength region covered is usually 190 nm to 2.50 µm; gratings blazed farther into the infrared are measured in higher orders. Concave reflection gratings focus as well as disperse the light, so the entrance and exit slits of the second monochromator are placed at the positions for which the grating was designed (that is, concave grating efficiencies are measured in the geometry in which the gratings are to be used). Transmission gratings are tested on the same equipment, with values given as the ratio of diffracted light to light falling directly on the detector, (*i.e.*, absolute efficiency).

Curves of efficiency *vs.* wavelength for plane gratings are made routinely on all new master gratings, both plane and concave, with light polarized in the S and P planes to assess the presence and amplitudes (if any) of anomalies. Such curves are furnished by Thermo RGL upon request (for an example, see Figure 10-3).

10.3. FOUCAULT KNIFE-EDGE TEST [top]

One of the most critical tests an optical system can undergo is the Foucault knife-edge test. This test not only reveals a great deal about wavefront deficiencies but also locates specific areas (or zones) where they originate. The test is suited equally well to plane and concave gratings (for the former, the use of very high grade collimating optics is required). The sensitivity of the test

depends on the radius of the concave grating (or the focal length of the collimating system), and may easily exceed that of interferometric testing, although the latter is more quantitative.

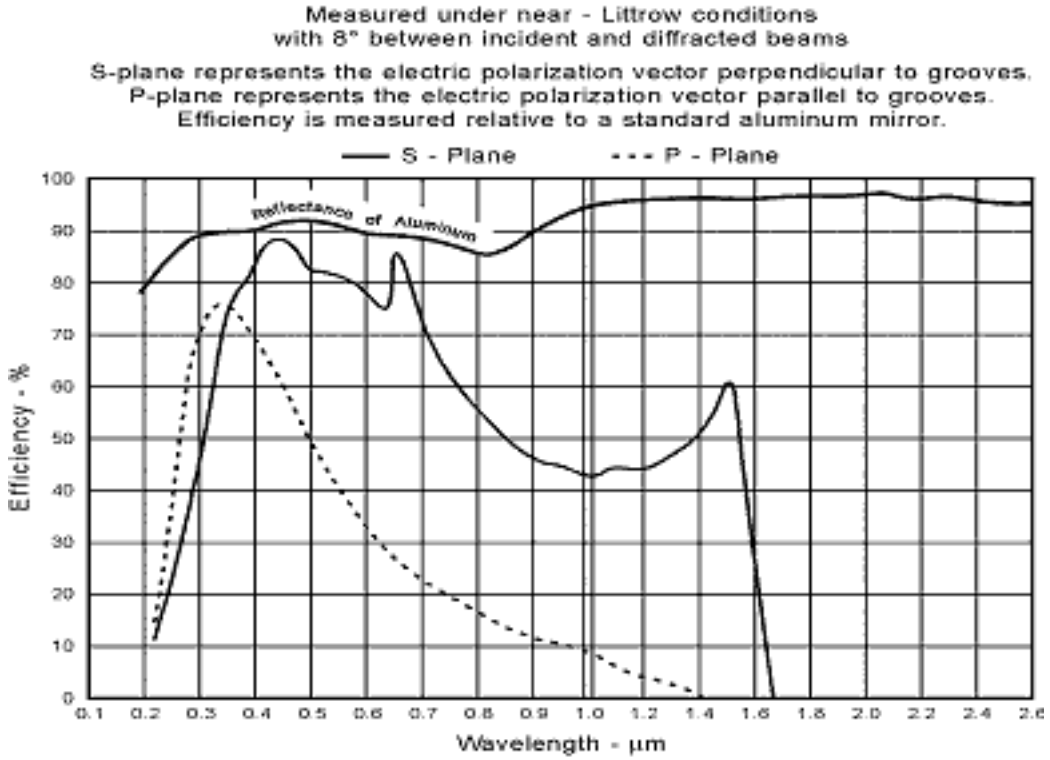

Figure 10-3. Example of an efficiency curve. This efficiency curve is specific to the particular grating under test, as well as the conditions of illumination (the incidence and diffraction angles).

By setting on ghost wavelengths, it is easy to see from which areas of the grating they originate. Errors of run, which are progressive changes in the groove spacing across the surface of the grating, are quite apparent to the practiced observer. This is also true of fanning error, which results when the groove spacing at the top of the grating differs from that at the bottom (resulting in a fan-shaped groove pattern). The sharper its knife-edge cutoff, the more likely that a grating will yield high resolution.

The Foucault test is a sensitive and powerful tool, but experience is required to interpret each effect that it makes evident. All Thermo RGL master plane gratings, large plane replicas and large-radius concave gratings are

checked by this method (see Figure 10-4).

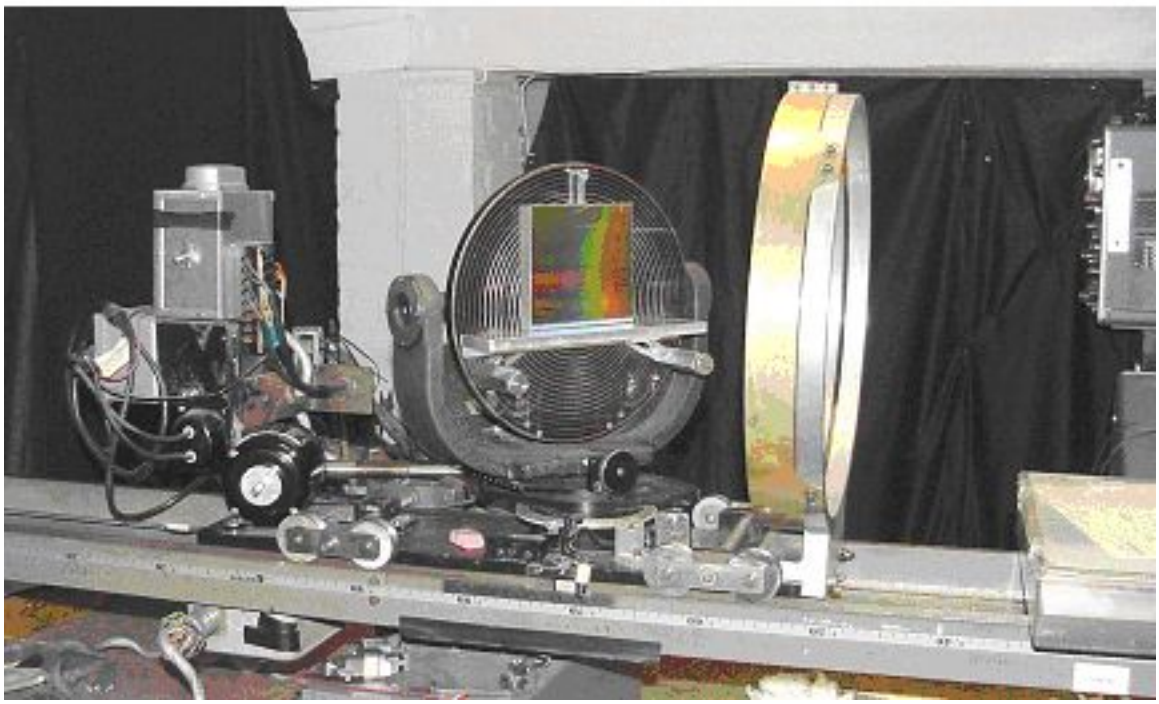

Figure 10-4. A grating under test on the Thermo RGL 5-meter test bench. Light from a mercury source (not shown, about 5 meters to the right) is collimated by the lens (shown) which illuminates the grating (shown on a rotation stage); the same lens refocuses the diffracted light to a plane very near the light source, where the diffracted wavefront can be inspected.

10.4. DIRECT WAVEFRONT TESTING [top]

Any departure from perfect flatness of the surface of a plane grating, or from a perfect sphere of the surface of a concave grating, as well as variations in the groove spacing, depth or parallelism, will result in a diffracted wavefront that is less than perfect. According to the Rayleigh criterion, resolution is lost whenever the deficiency exceeds $\lambda/4$, where λ is the wavelength of the light used in the test. To obtain an understanding of the magnitudes involved, it is necessary to consider the angle at which the grating is used. For simplicity, consider this to be the blaze angle, under Littrow conditions. Any surface figure error of height h will cause a wavefront deformation of $2h\cos\theta$, which

decreases with increasing |θ|. On the other hand, a groove position error *p* introduces a wavefront error of 2*p* sinθ, which explains why ruling parameters are more critical for gratings used in high-angle configurations.

A plane grating may produce a slightly cylindrical wavefront if the groove spacing changes linearly, or if the surface figure is similarly deformed. In this special case, resolution is maintained, but focal distance will vary with wavelength.

Wavefront testing can be done conveniently by mounting a grating at its autocollimating angle (Littrow) in a Twyman-Green interferometer or a phase measuring interferometer (PMI; see Figure 10-5). Few such instruments exist that combine sufficiently high quality with large aperture. Thermo RGL interferometers have apertures up to 150 mm (6 inches). With coherent laser light sources, however, it is possible to make the same measurements with a much simpler Fizeau interferometer, equipped with computer fringe analysis.

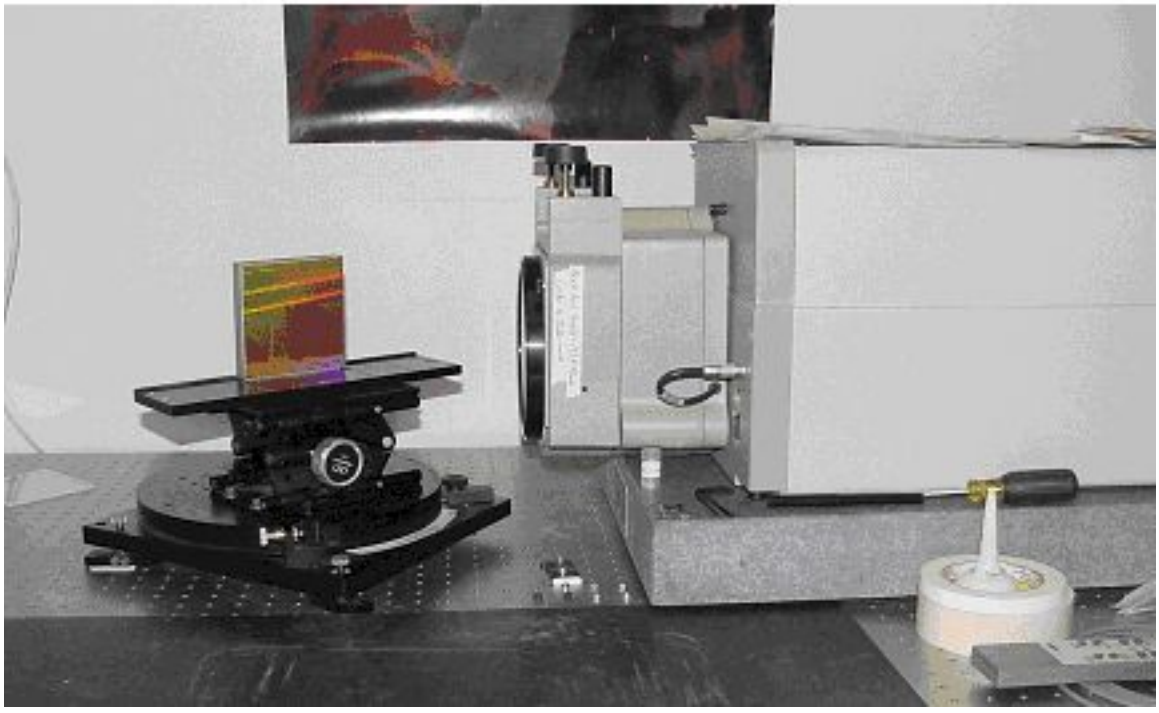

Figure 10-5. A plane grating under test on a phase measuring interferometer. The grating is tested in the Littrow configuration so that the flatness of the diffracted wavefront is evaluated.

Periodic errors show up as zig-zag fringe displacements. A sudden change in groove position gives rise to a step in the fringe pattern; in the spectrum, this is likely to appear as a satellite. Curved fringes due to progressive ruling error can be distinguished from figure problems by observing fringes obtained in zero, first and higher orders. Fanning error (non-parallel grooves) will cause spreading fringes. Figure 10-6 shows a typical interferogram, for an echelle grating measured in Littrow in the diffraction order of use (m = 33).

Experience has shown that the sensitivity of standard interferograms for grating deficiencies equals or exceeds that of other plane grating testing methods only for gratings used at high angles. This is why the interferometric test is especially appropriate for the testing of echelles and other gratings used in high diffraction orders.

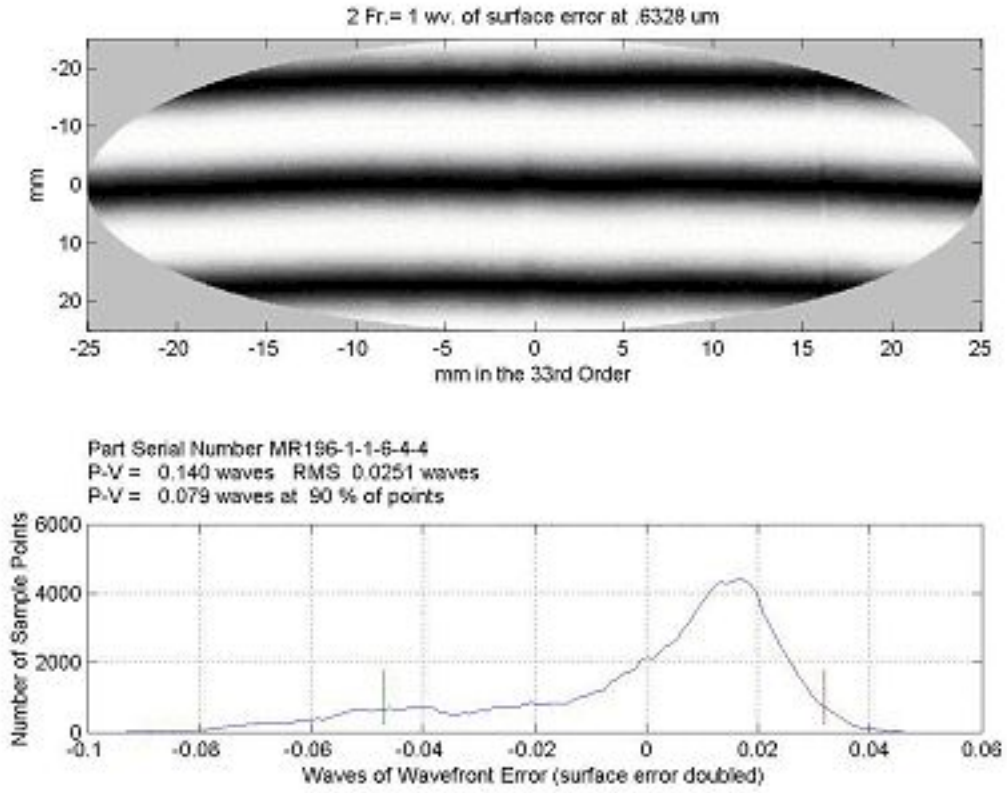

Figure 10-6. Example of an interferogram and histogram generated by a Phase Measuring Interferometer (PMI).

10.5. SCATTERED LIGHT [top]

As discussed in Chapter 2, the composite of misplaced spectral energy is called *scattered light*. *Near scatter* is usually due to large numbers of satellites and ghosts; *far scatter* is due to every kind of groove position error as well as geometrical deficiencies such as the smoothness of the grooves and the edge effects at each groove. Such deficiencies show up more at shorter wavelengths as mechanical imperfections become large relative to the wavelength.

The practical importance of scattered light depends on the specific application of the grating. In some cases, filters (or their equivalent in the form of narrow range detectors) can play an important role in suppressing the effects of scattered light. Another method is to use double monochromators or crossed dispersion.

Measurement methods using polychromatic light to determine far scatter depend on filters to mask parts of the spectrum. Ratios of radiometric readings made with and without the filters serve as a measure of scattered light. The approach, while functional, is arbitrary, with results affected by the diffraction efficiency of the grating, the spectrometric system used, the spectrum of the light source, and the spectral response of the detecting system.

Thermo RGL has a special apparatus to examine light scattered from small regions on the surface of a mirror or grating. This "scatter checker" provides several degrees of freedom so that light scattered between diffraction orders, or "inter-order scatter," can be attributed to areas on its surface.

Figure 10-7 shows a simplified schematic diagram of the scatter checker. The beam from a 632.8 nm HeNe laser is spatially filtered to remove speckle and is then directed onto a concave focusing mirror that brings the beam to focus at the detector plane. The detector is a photomultiplier that, in combination with a programmable-gain current amplifier, provides eight decades of dynamic range. A PC equipped with a data acquisition card is used to process and store the detector signal.

Scatter measurements are made by first obtaining a reference beam profile, or "instrument signature," by translating the test optic out of the way

and rotating the detector through the beam in incremental steps over a predetermined angular range. The test optic is then translated into the beam path and the detector passed through the reflected (or diffracted) beam from the test optic over the same angular range used to make the reference measurement. The sample and reference beam profiles are "mirror images" of one another, so it is necessary to invert one before a comparison is made. Any difference between the sample and reference beam profiles can be attributed to light scattered from the optic under test.

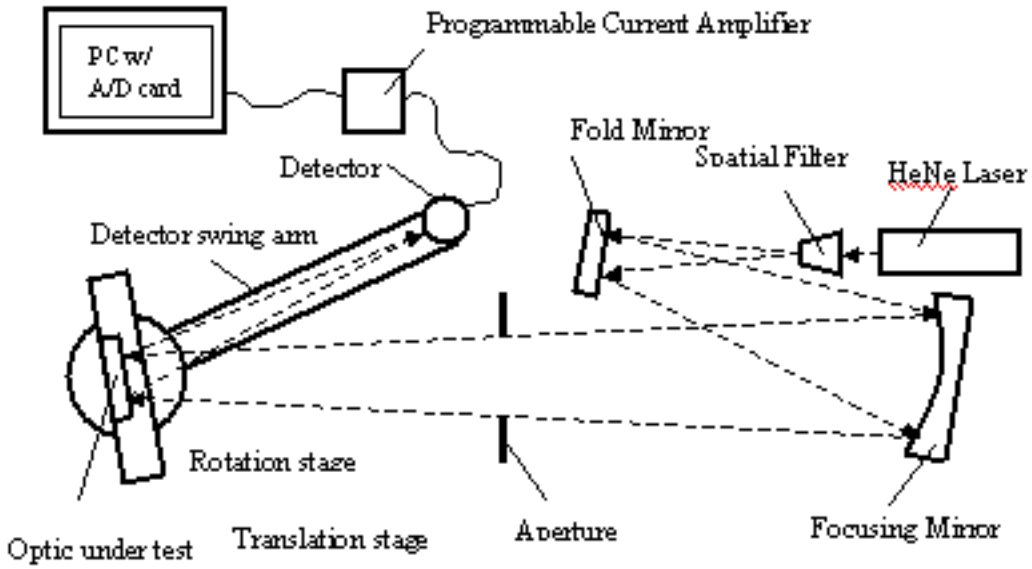

Figure 10-7. Schematic of the Thermo RGL scatter measuring apparatus.

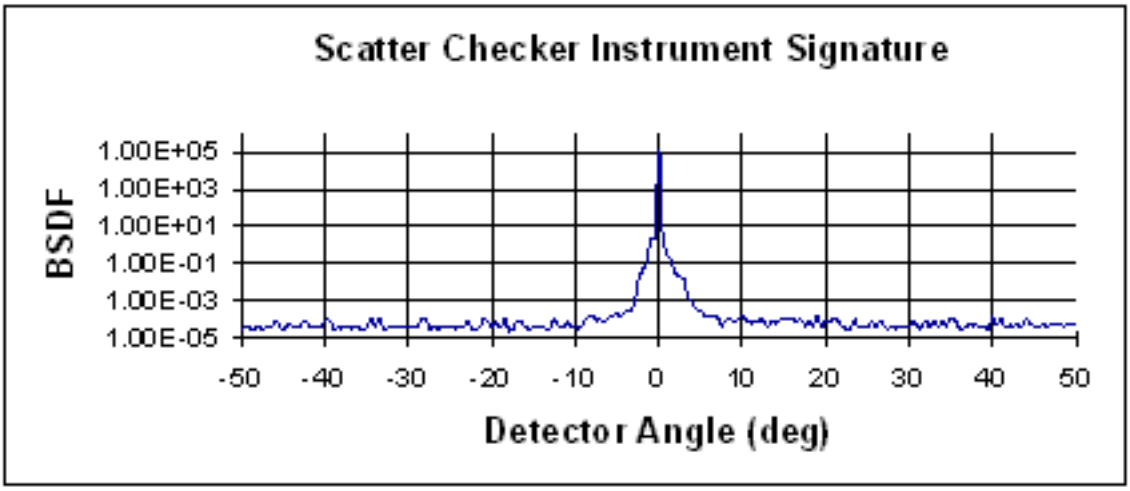

Figure 10-8. Typical plot of data obtained from the Thermo RGL scatter measuring instrument. This plot of the bi-directional scatter distribution function (BSDF) vs. angle of rotation of the detector (from a diffracted order) shows the reference beam profile (the "instrument signature").

PREVIOUS CHAPTER NEXT CHAPTER

Back to top

11. SELECTION OF DISPERSING SYSTEMS

PREVIOUS CHAPTER
NEXT CHAPTER

TABLE OF CONTENTS

11.1. REFLECTION GRATING SYSTEMS [top]

Reflection grating systems are much more common than transmission grating systems. Optical systems can be 'folded' with reflection gratings, which reflect as well as disperse, whereas transmission grating systems are 'in-line' and therefore usually of greater length. Moreover, reflection gratings are not limited by the transmission properties of the grating substrate (or resin), and can operate at much higher angles of diffraction.

11.1.1. Plane reflection grating systems.

The choice of existing plane reflection gratings is extensive and continually increasing. Sizes as large as 12 x 16 inches (about 300 x 400 mm)

have been ruled. For infrared spectra, plane reflection gratings are most suitable because of the availability of large gratings. While plane gratings have been used for visible and ultraviolet spectra for some time, they are also used increasingly for wavelengths as short as 110 nm, an extension made possible by special overcoatings that give satisfactory reflectivity even at such short wavelengths (see Chapter 9).

The most popular arrangement for plane reflection gratings is the Czerny-Turner mount, which uses two spherical concave mirrors between the grating and the entrance and exit slits. A single mirror arrangement (the Ebert-Fastie mount) can also be used. Both achieve spectral scanning through rotation of the grating. Collimating lenses are rarely used, since mirrors are inherently achromatic.

For special purposes, plane reflection gratings can be made on unusual materials, such as ceramics or metals, given special shapes, or supplied with holes for Cassegrain and Coudé-type telescopic systems.

11.1.2. Concave reflection grating systems.

The great advantage in using concave gratings lies in the fact that separate collimating optics are unnecessary. This is particularly important in the far vacuum ultraviolet region of the spectrum, for which there are no good reflectors. Two mirrors, each reflecting 20%, will reduce throughput by a factor of twenty-five. Hence, concave systems dominate the entire ultraviolet region, and at wavelengths less than 110 nm are used exclusively. Their chief deficiency lies in astigmatism, which limits the exit slit size (and, consequently, the energy throughput). The situation can be improved by using toroidal grating substrates; however, their use is restricted because of high costs.

Though most ruled gratings are flat, curved substrates can be ruled as well if their curvatures are not extreme (c. $f/9$ or greater). Concave gratings are not only more difficult to rule than plane gratings, since the tool must swing through an arc as it crosses the substrate, but they require extremely tight control over the sphericity to the substrate as well. Since each radius of curvature is a new parameter, there cannot be the large selection of rulings (in size and blaze angle) for any one given radius that there is with plane gratings.

Another limitation of ruled concave gratings appears when they are ruled at shallow groove angles. The ruled width is unfortunately limited by the radius of the substrate, since the diamond cannot rule useful grooves when the slope angle of the substrate exceeds the blaze angle. The automatic energy limitation that is thereby imposed can be overcome by ruling multipartite gratings, a Thermo RGL development. Here the ruling is interrupted once or twice, so the tool can be reset at a different angle. The resulting bipartite or tripartite gratings are very useful, as available energy is otherwise low in the short wavelength regions. One must not expect such gratings to have a resolving power in excess of that of any single section, for such an achievement would require phase matching to a degree that is beyond the present state of the art.

The advent of the holographic method of generating gratings has made the manufacture of concave gratings commonplace. Since the fringe pattern formed during the recording process is three-dimensional, a curved substrate placed in this pattern will record fringes. Unlike ruled gratings, concave interference gratings can be generated on substrates whose radii are smaller than 100 mm.

11.2. TRANSMISSION GRATING SYSTEMS [top]

In certain types of instrumentation, transmission gratings (see Figure 11-1) are much more convenient to use than reflection gratings. The most common configuration involves converting cameras into simple spectrographs by inserting a grating in front of the lens. This configuration is often used for studying the composition of falling meteors or the re-entry of space vehicles, where the distant luminous streak becomes the entrance slit. Another application where high-speed lenses and transmission gratings can be combined advantageously is in the determination of spectral sensitivity of photographic emulsions.

Transmission gratings can be made by stripping the aluminum film from the surface of a reflection grating. However, since the substrate is now part of the imaging optics, special substrates are used, made to tighter specifications for parallelism, and those used in the visible region are given a magnesium fluoride (MgF_2) antireflection coating on the back to reduce light loss and

internal reflections. The material used to form the substrate must also be chosen for its transmission properties and for the absence of bubbles, inclusions, striae and other imperfections in the glass, neither of which is a concern for reflection gratings.

In most cases, relatively coarse groove frequencies are preferred for transmission gratings, although gratings up to 600 g/mm are furnished routinely. Experimentally, transmission gratings of 1200 g/mm have been used. Energy distribution on either side of the blaze peak is very similar to that of reflection gratings in the scalar domain. For wavelengths between 220 and 300 nm, transmission gratings are made on fused silica substrates with a special resin capable of high transmission for these wavelengths.

Since transmission gratings do not have a delicate metal film they are much more readily cleaned. However, they are limited to spectral regions where substrates and resins transmit, but their main drawback is that they do not fold the optical path conveniently as a reflection grating does. Moreover, to avoid total internal reflection, their diffraction angles cannot be extreme. Even though the surface of the substrate is antireflection coated, internal reflections from the grating-air interface leads to some back reflection in several orders; this limits the maximum efficiency to 85% or less.

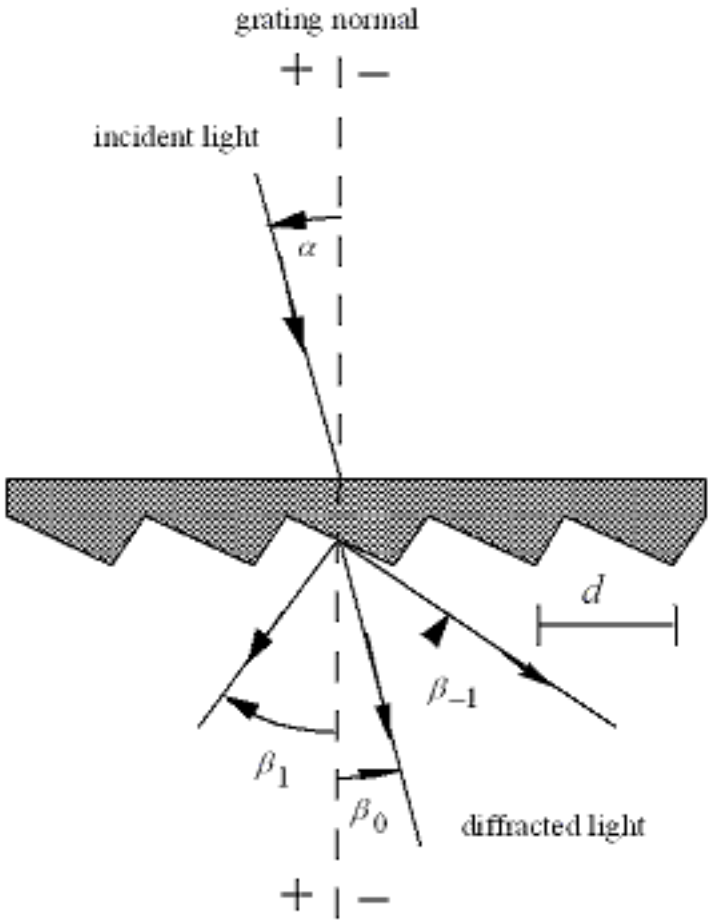

Figure 11-1. Diffraction by a plane transmission grating. A beam of monochromatic light of wavelength λ is incident on a grating and diffracted along several discrete paths; the incident and diffracted rays lies on opposite sides of the grating. The configuration shown, in which the transmission grating is illuminated from the back, is most common.

The efficiency behavior of transmission gratings can be modeled adequately over a wide spectral range and for a wide range of groove spacing by using scalar efficiency theory.[13] Unlike reflection gratings, whose efficiencies as predicted by scalar theory can reach almost 100%, transmission gratings are theoretically limited to about 80% (an effect confirmed by experiment). This results from the reflection of some light energy at the interface between the resin and air. [Antireflection (AR) coatings are generally applied to the back (glass) face of the grating to reduce reflections there.]

For a reflection grating of a given groove angle θ with first-order blaze

wavelength λ_B, the transmission grating with the same groove angle will be blazed between $\lambda_B/4$ and $\lambda_B/3$, depending on the index of refraction of the resin. This estimate is often very good, though it becomes less accurate for $\theta > 25°$.

11.3. GRATING PRISMS (GRISMS) [top]

For certain applications, such as a direct vision spectroscope, it is very useful to have a dispersing element that will provide in-line viewing for one wavelength. This can be done by replicating a transmission grating onto the hypotenuse face of a right-angle prism. The light diffracted by the grating is bent back in-line by the refracting effect of the prism. The device is commonly called a *Carpenter prism* or *grism*.

The derivation of the formula for computing the required prism angle follows (refer to Figure 11-2). On introducing Snell's law, the grating equation becomes

$$m\lambda = d\,(n \sin\alpha + n' \sin\beta), \qquad (11\text{-}1)$$

where n and n' are the refractive indices of glass and air, respectively, and $\beta < 0$ since the diffracted ray lies on the opposite side of the normal from the incident rays ($\alpha > 0$).

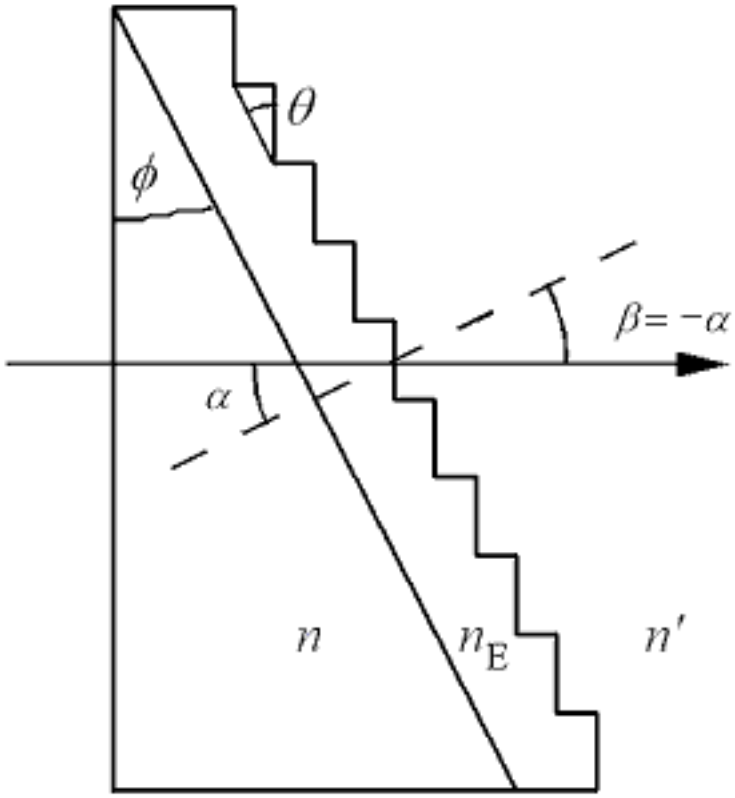

Figure 11-2. Grating prism (grism). Ray path for straight-through operation at one wavelength.

Taking $n' = 1$ for air, and setting $\alpha = -\beta = \phi$, the prism angle, Eq. (10-1) becomes

$$m\lambda = d\,(n - 1)\sin\phi\,. \qquad (11\text{-}2)$$

In this derivation it is assumed that the refractive index n of the glass is the same (or very nearly the same) as the index n_E of the resin resin at the straight-through wavelength λ. While this is not likely to be true, the resulting error is often quite small.

The dispersion of a grating prism cannot be linear, owing to the fact that the dispersive effects of the prism are superimposed on those of the grating. The following steps are useful in designing a grism:

1. Select the prism material desired (*e.g.*, BK-7 glass for visible light or fused silica for ultraviolet light).

2. Obtain the index of refraction of the prism material for the straight-through wavelength.
3. Select the grating constant *d* for the appropriate dispersion desired.
4. Determine the prism angle ϕ from Eq. (11-2).
5. For maximum efficiency in the straight-through direction, select the grating from the catalogue with groove angle θ closest to ϕ.

11.4. GRAZING INCIDENCE SYSTEMS [top]

For work in the 10-ray region (roughly the wavelength range from 1 to 25 nm), the need for high dispersion and the normally low reflectivity of materials both demand that concave gratings be used at grazing incidence (*i.e.*, $|\alpha| > 80°$, measured from the grating normal). Groove spacings of 600 to 1200 per millimeter are very effective, but exceptional groove smoothness is required on these rulings to achieve good results.

11.5. ECHELLES [top]

A need has long existed for spectroscopic devices that give higher resolution and dispersion than ordinary gratings, but with a greater free spectral range than a Fabry-Perot étalon or a reflection echelon. This gap is admirably filled by the echelle grating, first suggested by Harrison. Physically, an echelle can be thought of as lying halfway between a grating and a reflection echelon. The echelon is so difficult to make, and has such a low free spectral range, that it is now little more than a textbook curiosity. Echelles, on the other hand, are becoming ever more popular tools as large high quality rulings become available. In particular, they lead to compact instruments with high reciprocal dispersion and high throughput.

Echelles are a special class of high-angle gratings, rarely used in orders below $|m| = 5$, and sometimes used in orders beyond 100. Because of order overlap, some type of filtering is normally required with higher-order grating systems. This can take several forms, such as cutoff filters, detectors insensitive to longer wavelengths, or cross-dispersion in the form of prisms or low-dispersion gratings. The latter approach leads to a square display format

suitable for corresponding types of array detectors. In the case of dye laser tuning, the filtering is performed effectively by the choice of dyes.

As seen in Fig 11-3, an echelle looks like a coarse grating used at such a high angle (typically 63° from the normal) that the steep side of the groove becomes the optically active facet. Typical echelle groove spacings are 31.6, 79 and 316 g/mm, all blazed at 63°26' (although 76° is available for greater dispersion). With these grating, resolving powers greater than 1,000,000 for near-UV wavelengths can be obtained, using an echelle 10 inches wide. Correspondingly high values can be obtained throughout the visible spectrum and to 20 μm in the infrared.

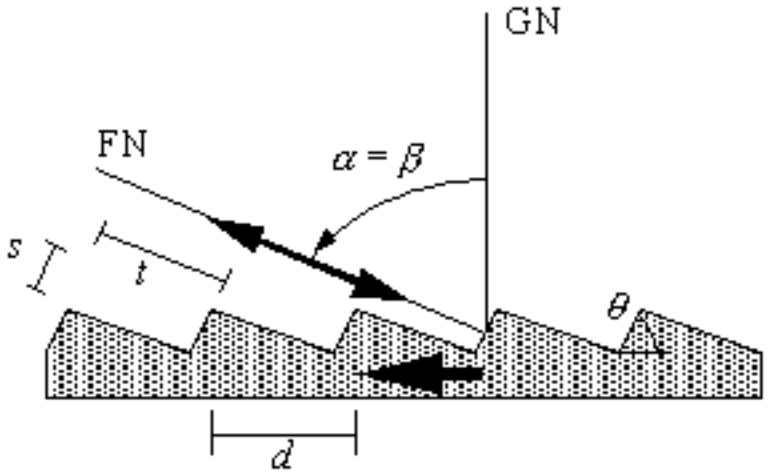

Figure 11-3. Echelle geometry. The groove spacing *d*, step width t and step height *s* are shown. GN is the grating normal and FN is the facet normal. The blaze arrow (shown) points from GN to FN.

Since echelles generally operate close to the Littrow mode, the grating equation becomes

$$m\lambda = 2d \sin\beta = 2d \sin\theta = 2t, \qquad (11\text{-}3)$$

where β is the angle of diffraction, θ the groove (blaze) angle, and *t* is the width of one echelle step (see Fig 11-3).

The free spectral range is

$$F_\lambda = \frac{\lambda}{m}. \qquad (2\text{-}24)$$

From Figure 11-3, $m = 2t/\lambda$, so

$$F_\lambda = \frac{\lambda^2}{2t}; \qquad (11\text{-}4)$$

for an echelle used in Littrow. In terms of wavenumbers, the free spectral range is

$$F_\sigma = \frac{\Delta\lambda}{\lambda^2} = \frac{1}{2t}. \qquad (11\text{-}5)$$

The linear dispersion of the spectrum is, from Eq. (2-12),

$$r' \frac{d\beta}{d\lambda} = \frac{mr'}{d\cos\beta} = \frac{mr'}{s} = \frac{r'}{s}\left(\frac{2t}{\lambda}\right), \qquad (11\text{-}6)$$

where $s = d\cos\beta$ is the step height of the echelle groove (see Fig. 11-3). The useful length l of spectrum between two consecutive diffraction orders is equal to the product of the linear dispersion and the free spectral range:

$$l = \frac{r'\lambda}{s} \qquad (11\text{-}7)$$

For example, consider a 300 g/mm echelle with a step height s = 6.5 µm, combined with an r' = 1.0 meter focal length mirror, working at a wavelength of λ = 500 nm. The useful length of one free spectral range of the spectrum is l = 77 mm.

Typically, the spectral efficiency reaches a peak in the center of each free spectral range, and drops to about half of this value at the ends of the range. An echelle remains blazed for all wavelengths in the free spectral range

(for a given diffraction order). Echelle efficiency has been addressed in detail by Loewen *et al.*[14]

The steep angles and the correspondingly high orders at which echelles are used makes their ruling much more difficult than ordinary gratings. Periodic errors of ruling must especially be limited to a few nanometers or even less, which is attainable only by using interferometric control of the ruling engine. The task is made even more difficult by the fact that the coarse, deep grooves require heavy loads on the diamond tool. Only ruling engines of exceptional rigidity can hope to rule echelles. This also explains why the problems escalate as the groove spacing increases.

Echelles are often referred to by their "R numbers". This number is the tangent of the blaze angle θ:

$$\text{R number} = \tan\theta = \frac{t}{s} \qquad (11\text{-}8)$$

(see Figure 11-2). An R2 echelle, for example, has a blaze angle of $\tan^{-1}(2) = 63.1°$; an R5 echelle has a blaze angle of $\tan^{-1}(5) = 78.7°$.

R1	45.0°
R2	63.4°
R3	71.6°
R3.5	74.1°
R4	76.0°
R5	78.7°

Table of common R numbers

Instruments using echelles can be reduced in size if the echelles are "immersed" in a liquid of high refractive index *n* (see Figure 11-4). This has the effect of reducing the effective wavelength by *n*, which has the effect of increasing the diffraction order, resolving power and dispersion of the echelle. A prism is usually used to couple the light to the grating surface, since at high angles most of the light incident from air to the high-index liquid would be reflected. Often an antireflection (AR) coating is applied to the normal face of the prism to minimize the amount of energy reflected from the prism.

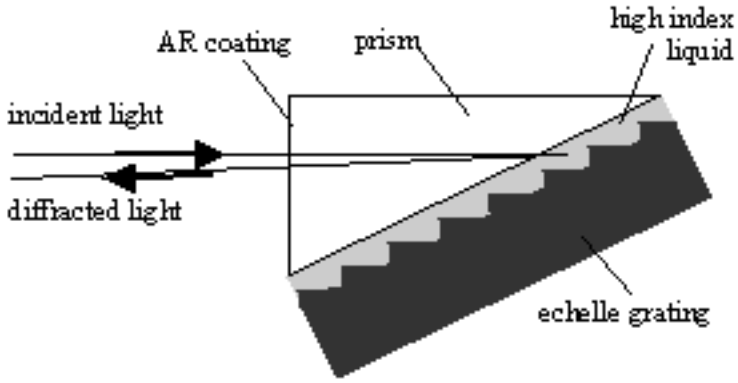

Figure 11-4. An immersed echelle grating.

PREVIOUS CHAPTER NEXT CHAPTER

Back to top

12. GRATINGS FOR SPECIAL PURPOSES

PREVIOUS CHAPTER
NEXT CHAPTER

TABLE OF CONTENTS

12.1. ASTRONOMICAL GRATINGS
12.2. GRATINGS AS FILTERS
12.3. GRATINGS FOR ELECTRON MICROSCOPE CALIBRATION
12.4. GRATINGS FOR LASER TUNING
12.5. GRATINGS AS BEAM DIVIDERS
12.6. MOSAIC GRATINGS
12.7. SPACE-BORNE SPECTROMETRY
12.8. SPECIAL GRATINGS

12.1. ASTRONOMICAL GRATINGS [top]

Large gratings for astronomical purposes were formerly available only by ruling two adjacent sections. In 1972, the MIT 'B' engine was modified to rule larger areas with a single diamond, and since then it has produced echelles and large gratings up to 308 mm x 408 mm in size. Even larger gratings can be achieved by high accuracy multiple replication onto a single substrate (see Section 12.6 below).

12.2. GRATINGS AS FILTERS [top]

It is frequently desirable to use diffraction gratings as reflectance filters

when working in the far infrared, in order to remove the unwanted second- and higher- diffraction orders from the light. For this purpose, small plane gratings are used that are blazed for the wavelength of the unwanted shorter-wavelength radiation. The grating acts as a mirror, reflecting the desired light into the instrument while diffracting shorter wavelengths out of the beam.

12.3. GRATINGS FOR ELECTRON MICROSCOPE CALIBRATION [top]

It is possible to make shadow-cast replicas from replica gratings that can be very useful for calibrating the magnification of electron microscopes. These are replica gratings made from lightly ruled master gratings so that a space is left between the grooves. Besides offering this type of grating with a variety of spacings, Thermo RGL can also rule gratings with two sets of grooves at right angles (*cross-rulings*), which forms a grid that will show distortion of the field in the electron microscope. Groove frequencies as high as 10,000 grooves per millimeter have been produced experimentally.

12.4. GRATINGS FOR LASER TUNING [top]

External-cavity semiconductor diode lasers are often used for their single-mode operation and spectral tunability. Plane reflection gratings can be used in the Littrow configuration to tune the lasing wavelength, as shown in Fig. 12-1, or in the grazing-incidence mount. In some systems a telescope is used to expand the laser beam to fill the grating, which is necessary for high resolution. A set of prisms, though, can do the same job more simply. Grazing-incidence tuning with one grating associated with a mirror or a second grating can also be used to tune dye lasers.

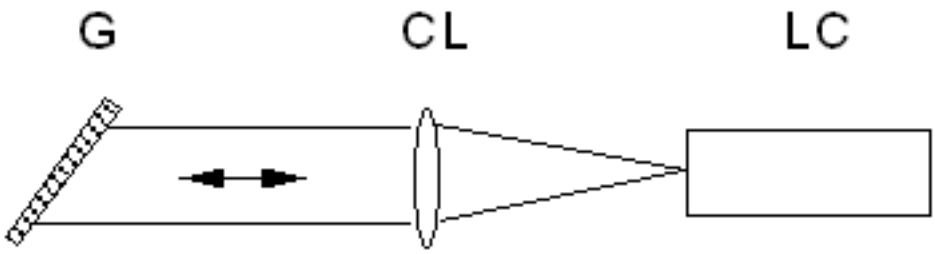

Figure 12-1. Littrow tuning of a dye laser. Light from the laser cavity [LC] diverges toward the collimating lens [CL], which directs it toward the grating [G], which is oriented so that light of the power wavelength is redirected back toward the lens, which focuses it into the laser cavity.

Molecular lasers, operating in either a pulsed or continuous-wave (cw) mode, have their output wavelength tuned by Littrow-mounted gratings. High efficiency is obtained by using the first diffraction order at diffraction angles $|\beta| > 20°$. The output is polarized in the S-plane, since the efficiency in the P plane is quite low.

Some molecular lasers operate at powers high enough to destroy gratings. For pulsed laser tuning, extra-thick replica films may help, but at maximum power only master gratings survive. Due to their far greater thermal conductivity, replica gratings on metal substrates are superior to glass for cw laser applications; in some cases, the grating substrates must be water-cooled to prevent failure.

12.5. GRATINGS AS BEAM DIVIDERS [top]

Gratings ruled with symmetrically-shaped grooves, as well as laminar transmission gratings, are capable of being used as beam dividers in conjunction with Moiré fringe applications or interferometers. A diffraction grating used as a beam divider provides higher efficiencies when its groove profile is rectangular, whereas a grating used for spectroscopic purposes should have a sinusoidal or triangular groove profile.

12.6. MOSAIC GRATINGS [top]

In the mid 1990's, Thermo RGL developed the capability to replicate two large submaster gratings onto one monolithic substrate. Except for a "dead space" between the two replicated areas, the entire face of the larger product substrate contains the groove pattern. This *mosaic grating* must have its two grating areas aligned to very high accuracy if the mosaic is to perform as one high-quality grating. Typical specifications for two 308 x 408 mm ruled areas on a 320 x 840 mm substrate are one arc second alignment of the groove directions, one arc second tilt between the two faces, and one micron displacement between the two grating planes.

A large mosaic echelle grating produced by Thermo RGL for the European Southern Observatory is shown in Figure 12-2. Two submasters from Thermo RGL master MR160 (a 31.6 g/mm echelle blazed at 75.1°) were independently replicated onto a large monolithic substrate to form this mosaic grating; the two halves of its surface are clearly seen in the photograph.

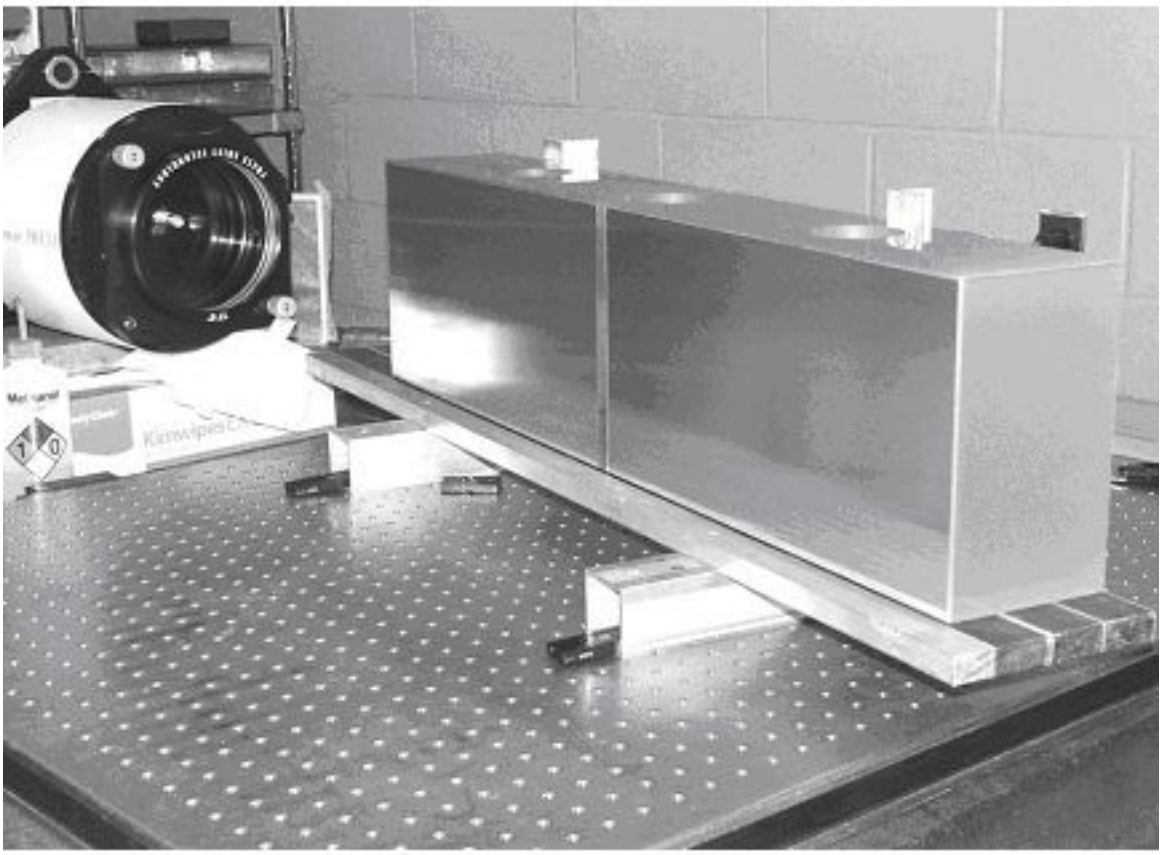

Figure 12-2. A large mosaic grating. A monolithic 214 x 840 mm replica

mosaic grating was produced from two 214 x 415 mm submasters.

Figure 12-3 shows a six-inch aperture Fizeau interferogram of an echelle mosaic (31.6 g/mm) in the $m = 99^{th}$ order, tested at $\lambda = 632.8$ nm. The grooves are vertical in the photos and the blaze arrow is facing left. One fringe over this aperture is 0.43 arc seconds. These measurements indicate that the two sides of the mosaic are aligned to 0.3 arc seconds.

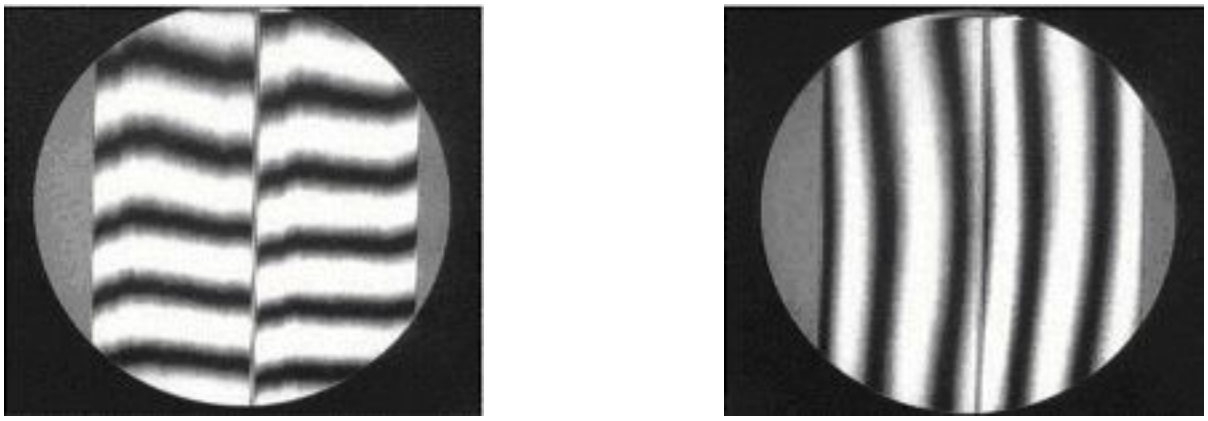

Figure 12-3. Six-inch-aperture Fizeau interferograms of an echelle mosaic produced from two 214 x 415 mm submasters. The photograph on the left shows alignment perpendicular to the grooves; that on the right shows alignment in the direction of the grooves. These interferograms were taken in the 99^{th} diffraction order.

Figure 12-4 shows a focal plane scan on a ten-meter optical test bench using a mode-stabilized HeNe laser ($\lambda = 632.8$ nm) as the light source. The entrance slit width is 25 microns, and the exit slit is opened just enough to get signal through. The grating is operating in the $m = 97^{th}$ order with full aperture illumination. The image seems to be dominated by the wavefront characteristics of the individual segments, but still indicates a system resolving power better than $R = 900{,}000$.

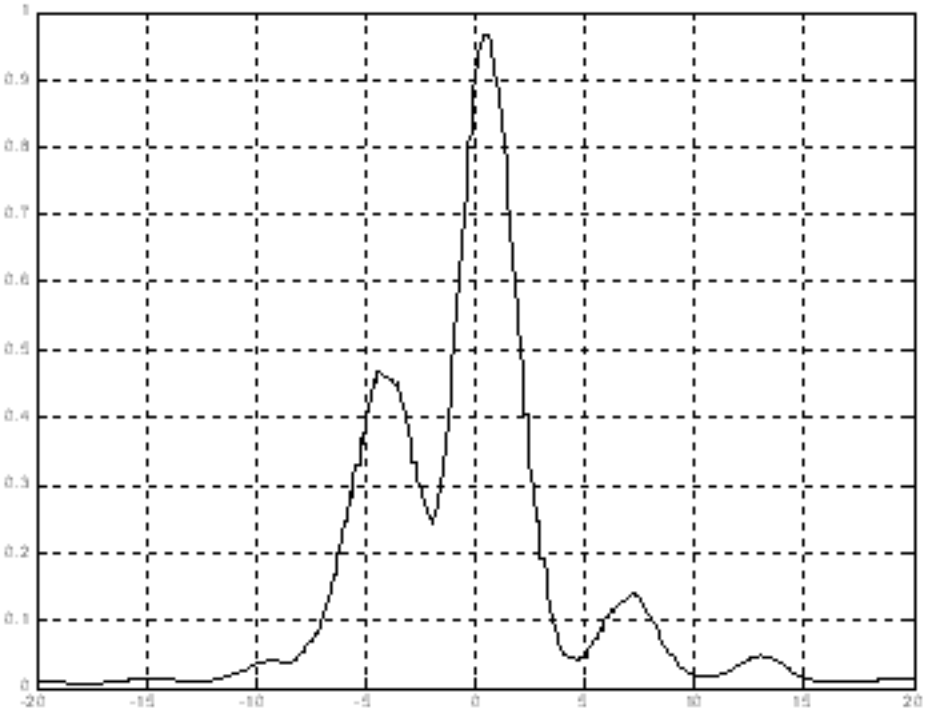

Figure 12-4. Signal trace of the HARPS echelle mosaic at 632.8nm in the 97th order.

12.7. SPACE-BORNE SPECTROMETRY [top]

Neither master nor replica substrates suffer in any measurable way over extended periods of time in a space environment. The advantage of replicas lies not only in their greater availability and lower cost, but in making possible the provision of exact duplicates whenever needed.

Since most space work involves the study of ultraviolet (UV) and extreme ultraviolet (EUV) wavelengths, special problems exist in setting and aligning the optics. For this purpose Thermo RGL can rule gratings matching the EUV grating but with a groove spacing modified so that the mercury 546.1-nm line lies in the spectrum just where the main wavelength under study will lie. Another possibility is to rule a small section on the main grating with similar coarse spacings and then mask off this area when the alignment is

complete. Sometimes special tolerances on substrate radii are required for complete interchangeability.

12.8. SPECIAL GRATINGS [top]

Usually some of the standard gratings offered in the latest *Grating Catalog* will satisfy a customer's requirements for groove spacing and blaze angle.

Substrate size. Grating size is usually dictated by the light throughput desired (and, in the case of concave gratings, imaging and instrument size limitations as well). Should none of the standard substrate sizes listed in the *Catalog* be suitable to match an instrument design, these same gratings can be supplied on special size substrates. Special elongated substrate shapes are available for echelles and laser tuning gratings.

Substrate material. The standard material for small and medium-sized grating substrates is specially annealed boro-silicate crown glass (BK-7). Low-expansion material, such as ZeroDur® or fused silica, can be supplied upon request. For large gratings (approximately 135 x 265 mm or larger), low-expansion material is standard; BK-7 can be requested as well. For certain applications, it is possible to furnish metal substrates (*e.g.*, copper or aluminum) that are good heat sinks.

Grating coatings. While evaporated aluminum is the standard coating for reflection gratings, fast-fired aluminum with overcoatings of magnesium fluoride (MgF_2) can be used to enhance efficiency in the spectrum between 120 and 160 nm. For the extreme ultraviolet (below 50 nm), gold replica gratings are recommended, while platinum is recommended for 80-110 nm. Gold replicas also have higher reflectivity in most regions of the infrared spectrum, and are particularly useful for fiber-optic telecommunications applications in the S, C and L (infrared) transmission bands.

PREVIOUS CHAPTER NEXT CHAPTER

Back to top

13. ADVICE TO GRATING USERS

PREVIOUS CHAPTER
NEXT CHAPTER

TABLE OF CONTENTS

13.1. CHOOSING A SPECIFIC GRATING [top]

If a diffraction grating is to be used only to disperse light (rather than provide focusing as well), then choosing the proper grating is often a simple matter involving the specification of the blaze angle and groove spacing. In other instances, the problem is one of deciding on the spectrometric system itself. The main parameters that must be specified are

Spectral region (wavelength range)

Speed (focal ratio) or throughput

Resolution or resolving power

Dispersion

Free spectral range

Output optics

Size limitations

The spectral region will usually dictate the choice of plane vs. concave design, as well as the coating (if the grating is reflecting). Imaging (or spectral resolution) requirements and dispersion are also of primary importance. The size and weight of the system, the method of receiving output data, the intensity, polarization and spectral distribution of the energy available, etc., must also be considered. The nature of the detection system, especially for array detectors, plays a major role in system design: its size, resolution, and image field flatness are critical issues in the specification of the optical system.

Resolving power depends on many aspects of the optical system and the quality of its components. In some cases, the grating may be the limiting component. The decision here involves the size of the grating and the angle at which it is to be used, but not on the number of grooves on the grating or the groove spacing (see Chapter 2).

Speed (or throughput) determines the focal length as well as the sizes of the optical elements and of the system itself. Special overcoatings become important in certain regions of the spectrum, especially the vacuum ultraviolet. For example, Al + MgF_2 is advisable in the 100-170 nm region, and Au and Pt in the 30-110 nm region

When thermal stability is important, gratings should be made on a low expansion material, such as ZeroDur™ or ULE® fused silica.

Guidelines for specifying gratings are found in Chapter 15.

13.2. CLEANING AND RECOATING GRATINGS [top]

Gratings last a long time in the proper environment, but sometimes hostile conditions cannot be avoided. For example, oil vapor in a vacuum system can be baked onto optical surfaces by ultraviolet light. Experience has shown that damaged gratings can sometimes be restored to almost original

efficiency by careful cleaning, which may or may not be followed by recoating. Visual appearance is not always a good indicator of whether such an operation will be successful. [For more information, please see section 14.4.]

13.3. APPEARANCE [top]

In the early days of diffraction grating manufacture, R.W. Wood remarked that the best gratings were nearly always the worst ones in their cosmetic or visual appearance. While no one would go so far today, it is important to realize that a grating with certain types of blemishes may well perform better than one that appears perfect to the eye.

13.3.1. Ruled gratings

Cosmetic defects on ruled gratings may be caused by small droplets of metal or oxide that have raised the ruling diamond, or streaks may be caused by temporary adhesion of aluminum to the sides of the diamond tool. On ruled concave gratings, one can usually detect by eye a series of concentric rings called a *target pattern*. It is caused by minor changes in tool shape as the diamond swings through the arc required to rule on a curved surface. Every effort is made to reduce the visibility of target patterns to negligible proportions.

Some ruled master gratings have visible surface defects. The most common sort of defect is a region of grooves that are burnished too lightly (in relation to the rest of the grating surface). While readily seen with the eye, such a region has little effect on spectroscopic performance.

13.3.2. Holographic gratings

Holographic gratings are susceptible to a different set of cosmetic defects. *Comets* are caused by specks on the substrate; when the substrate is rotated (spun) as the photoresist is applied, these specks cause the photoresist to flow around them, leaving comet-like trails. Artifacts created during the

recording process are also defects; these are holograms of the optical components used in the recording of the grating.

13.4. GRATING MOUNTING [top]

The basic rule of mounting a grating is that for any precise optical element: its shape should not be changed accidentally through excessive clamping pressure. This problem can be circumvented by kinematic (three-point) cementing, using a nonrigid cement, or by supporting the surface opposite the point where clamping pressure is applied.

If a grating is to be mounted from the rear, the relative orientations of the front and rear surfaces is more important than if the grating if to be mounted from the front. Generally front-mounting (by contacting the surface of the grating, near its edge and outside the free aperture), allows the cost of the substrate to be lower, since the relative parallelism of the front and back surfaces (for a plane grating, for example) need not be so tightly controlled.

PREVIOUS CHAPTER NEXT CHAPTER

Back to top

14. HANDLING GRATINGS

PREVIOUS CHAPTER
NEXT CHAPTER

TABLE OF CONTENTS

A diffraction grating is a *first surface optic*, so its surface cannot be touched or otherwise come in contact with another object without damaging it and perhaps affecting its performance. Damage can take the form of contamination (as in the adherence of finger oils) or distortion of the microscopic groove profile in the region of contact. This chapter describes the reasons why a grating must be handled carefully and provides guidelines for doing so.

14.1. THE GRATING SURFACE [top]

Commercially available diffraction gratings are replicated optics comprised of three layers: a substrate, a resin layer, and (usually) a reflective coating. Each layer meets a different purpose: (1) the metallic layer provides high reflectivity, (2) the resin layer holds the groove pattern and groove profile and (3) the substrate (usually glass) keeps the optical surface rigid.

14.2. PROTECTIVE COATINGS [top]

Since the groove profile is maintained by the resin layer, rather than the reflective (metallic) coating on top of it, protective coatings such as those that meet the military specification MIL-M-13508 (regarding first-surface aluminum mirrors) do not serve their intended purpose. Even if the aluminum coating itself were to be well-protected against contact damage, it is too thin to protect the softer resin layer underneath it. "Fully cured" resin is not very hard, resembling modeling clay in its resistance to contact damage. Consequently gratings are not provided with contact-protecting coatings.

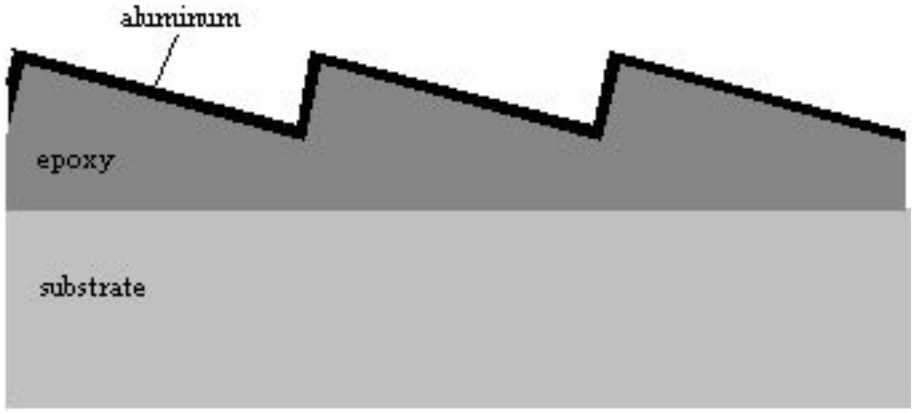

Figure 14-1. Composition of a replica diffraction grating. A section of a standard blazed grating with an aluminum coating is shown. Layer thicknesses are not shown to scale: generally the aluminum film thickness is about 1 micron, and the resin layer is between 30 and 50 microns; the substrate thickness is usually between 3 and 100 millimeters.

14.3. GRATING COSMETICS AND PERFORMANCE [top]

Warnings against touching the grating surface notwithstanding, damage to the surface occasionally occurs. Contact from handling, mounting or packaging can leave permanent visible marks on the grating surface. Moreover, some gratings have cosmetic defects that do not adversely impair the optical

performance, or perhaps represent the best available quality for a grating with a particular set of specifications. For example, some gratings have 'worm tracks' due to mechanical ruling of the master grating from which the replicated grating was taken, others have coating defects like spit or spatter, and others have 'pinholes' (tiny voids in the reflective coating), *etc*. The many possible classifications of surface defects and the many opportunities to render the surface permanently damaged conspire to make the surfaces of many gratings look less than cosmetically perfect.

While this damage may be apparent upon looking that the grating, it is not straightforward to determine the effect this damage has on the performance of the grating. Often the area affected by damage or contamination is a small fraction of the total area of the grating. Therefore, only a small portion of the total number of grooves under illumination may be damaged, displaced or contaminated. A damaged or contaminated region on the surface of a grating may have little, if any, noticeable effect on the performance of the optical system because, a diffraction grating is usually used as an integrating optic (meaning that all light of a given wavelength diffracted from the grating surface is brought to focus in the spectral order of interest). In contrast, a lens or mirror that does not focus (say, an eyeglass lens or a bathroom mirror) will show a distortion in its image corresponding to the damaged region of the optic. This familiar experience - the annoying effect of a chip on an eyeglass lens or a smudge on a bathroom mirror - has led many to assume that a similar defect on the surface of a grating will lead to a similar deficiency in performance. The most appropriate performance test of a grating with surface damage or cosmetic defects is not visual inspection but instead to use the grating in its optical system and determine whether the entire system meets its specifications.

Damage to a region of grooves, or their displacement, will theoretically have some effect on the efficiency of the light diffracted from that region, as well as the total resolving power of the grating, but in practice such effects are generally not noticeable. Of more concern, since it may be measurable, is the effect surface damage may have on light scattered from the grating, which may decrease the signal-to-noise (SNR) of the optical system. Most forms of surface damage can be thought of as creating scattering centers where light that should be diffracted (according to the grating equation) is scattered into other directions instead.

14.4. UNDOING DAMAGE TO THE GRATING SURFACE

[top]

Damage to the microscopic groove profile is, unfortunately, irreversible; the resin layer, like modeling clay, will retain a permanent imprint. Contamination of the grating surface with finger oils, moisture, vacuum pump oil, *etc*. is also often permanent, particularly if the contaminated grating surface has been irradiated. If you have a damaged or contaminated grating, call the manufacturer to ask for advice, or to have us clean and inspect your grating.

Sometimes surface contamination can be removed partially, and once in a while completely, using a mild unscented dishwashing liquid. Care should be taken not to apply any pressure (even gentle scrubbing) to the grating surface. If contaminants remain, try using spectroscopic-grade solvents; the purity of such solvents should be ascertained before use, and only the purest form available used. The use of carbon dioxide (CO2) snow, which reaches the grating surface in a sublimed state and evaporates, carrying with it the contaminants, has also been used with some success. The key to cleaning a grating surface is to provide no friction (*e.g.*, scrubbing) that might damage the delicate groove structure.

14.5. GUIDELINES FOR HANDLING GRATINGS [top]

- *Never touch the grooved surface of a diffraction grating.* Handle a grating by holding it by its edges. If possible, use powder free gloves while handling gratings.
- *Never allow any mount or cover to come in contact with the grooved surface of a diffraction grating.* A grating that will be shipped should have its surface protected with a specially-designed cover that does not touch the surface itself. Gratings that are not in use, either in the laboratory or on the manufacturing floor, should be kept in a closed box when not covered. Keep any oils that may be used to lubricate grating mount adjustments away from the front surface of the grating.
- *Do not talk or breathe over the grooved surface of a diffraction grating.* Wear a nose and face mask when it is required that you talk over the surface of a grating. Breath spray is particularly bad for reflection gratings, so one should not speak directly over the surface; instead,

either turn away or cover the mouth (with the hand or a surgical mask).

PREVIOUS CHAPTER NEXT CHAPTER

Back to top

15. GUIDELINES FOR SPECIFYING GRATINGS

PREVIOUS CHAPTER
APPENDIX A

TABLE OF CONTENTS

Proper technical specifications are needed to ensure that the part supplied by the manufacturer meets the requirements of the customer. This is especially true for diffraction gratings, whose complete performance features may not be fully recognized. Documents that provide guidance in the specification of optical components, such as the ISO 10110 series ("Optics and optical instruments: Preparation of drawings for optical elements and systems"), do not lend themselves to the specification of diffraction gratings. This chapter provide guidelines for generating clear and complete technical specifications for gratings.

Specifications should meet the following criteria.

- They should refer to *measurable* properties of the grating.
- They should be as *objective* as possible (avoiding judgment or interpretation).
- They should be *quantitative* where possible.
- They should employ common *units* where applicable (metric is preferred).
- They should contain *tolerances*.

A properly written engineering print for a diffraction grating will be clear and understandable to both the customer and the manufacturer.

15.1. REQUIRED SPECIFICATIONS [top]

All grating prints should contain, at a minimum, the following specifications.

1. *Free Aperture.* The free aperture, also called the *clear aperture*, of a grating is the maximum area of the surface that will be illuminated. The free aperture is assumed to be centered within the *ruled area* (see below) unless otherwise indicated. For configurations in which the grating will rotate, such as in a monochromator, it is important to specify the free aperture as the maximum dimensions of the beam on the grating surface (*i.e.*, when the grating is rotated most obliquely to the incident beam). Also, it is important to ensure that the free aperture specifies an area that is completely circumscribed by the ruled area, so that the illuminated area never includes part of the grating surface that does not have grooves.

   The free aperture of the grating is that portion of the grating surface for which the optical specifications apply (*e.g., Diffraction Efficiency*, *Wavefront Flatness or Curvature*, *Scattered Light* - see below).

2. *Ruled Area.* The ruled area of a grating is the maximum area of the surface that will be covered by the groove pattern. The ruled area is assumed to be centered on the substrate face unless otherwise indicated. By convention, the ruled area of a rectangular grating is specified as "groove length by ruled width" - that is, the grooves are parallel to the first dimension; for example, a ruled area of 30 mm x 50 mm indicates that the grooves are 30 mm long.

   Most rectangular gratings have their grooves parallel to the shorter substrate dimension. For gratings whose grooves are parallel to the longer dimension, it is helpful to specify "long lines" to ensure that the grooves are made parallel to the longer dimension.

3. *Substrate Dimensions.* The substrate dimensions (width, length, and thickness) should be called out, as should their tolerances. If the grating

is designed to be front-mounted, the substrate specifications can be somewhat looser than if the grating surface will be positioned or oriented by the precise placement of the substrate. Front-mounting a grating generally reduces its cost and production time (see *Alignment* below).

A grating substrate should have bevels on its active face, so that it is easier to produce and to reduce chipping the edges while in use. Bevel dimensions should be specified explicitly and should be considered in matching the *Ruled Area* (above) with the substrate dimensions. For custom (special-size) substrates, certain minimum bevel dimensions may be required to ensure that the grating is manufacturable - please contact us for advice.

4. *Substrate Material.* The particular substrate material should be specified. If the material choice is of little consequence, this can be left to the manufacturer, but especially for applications requiring substrates with low thermal expansion coefficients, or requiring gratings that can withstand high heat loads, the substrate material and its grade should be identified. For transmission gratings, the proper specification of the substrate material should include reference to the fact that the substrate will be used in transmission, and may additionally refer to specifications for inclusions, bubbles, striae, *etc*.

5. *Nominal Surface Figure.* Plane (flat) gratings should be specified as being planar; concave gratings should have a radius specified, and the tolerance in the radius should be indicated in either millimeters or fringes of red HeNe light (λ = 632.8 nm) (a "wave" being a single wavelength, equaling 632.8 nm, and a "fringe" being a single half-wavelength, equaling 316.4 nm). Deviations from the nominal surface figure are specified separately as "wavefront flatness" or "wavefront curvature" (see below).

6. *Wavefront Flatness or Curvature.* This specification refers to the allowable deviation of the optical surface from its *Nominal Surface Figure* (see above). Plane gratings should ideally diffract plane wavefronts when illuminated by collimated incident light. Concave gratings should ideally diffract spherical wavefronts that converge toward wavelength-specific foci. In both cases, the ideal radius of the diffracted wavefront should be specified (it is infinite for a plane grating)

and maximum deviations from the ideal radius should also be called out (*e.g.*, the tolerance in the radius, higher-power irregularity in the wavefront). It is important to specify that grating wavefront testing be done in the diffraction order of use if possible, not in zero order, since the latter technique does not measure the effect of the groove pattern on the diffracted wavefronts. Deviations from a perfect wavefront are most often specified in terms of waves or fringes of red HeNe light (λ = 632.8 nm). Generally, wavefront is specified as an allowable deviation from focus ("power") and allowable higher-order curvature ("irregularity").

7. *Groove Spacing or Frequency.* The number of grooves per millimeter, or the spacing between adjacent grooves, should be specified, but not both (unless one is subjugated to the other by labeling it as "reference"). For a grating whose groove spacing varies across the surface (*e.g.*, an aberration-corrected concave holographic grating), the groove spacing (or frequency) is specified at the center of the grating surface.

8. *Groove Alignment.* Alignment refers to the angle between the groove direction and an edge of the grating substrate. Sometimes this angular tolerance is specified as a linear tolerance by stating the maximum displacement of one end of a groove (to an edge) relative to the other end of the groove. Generally a tight alignment specification increases manufacturing cost; it is often recommended that alignment be allowed to be somewhat loose and that the grating substrate dimensions not be considered for precise alignment but that the grating surface be oriented and positioned optically instead of mechanically (see comments in *Substrate Dimensions* above).

9. *Diffraction Efficiency.* Grating efficiency is generally specified as a minimum at a particular wavelength; often this is the *peak wavelength* (*i.e.*, the wavelength of maximum efficiency). Occasionally efficiency specifications at more than one wavelength are called out.

   Either relative or absolute diffraction efficiency should be specified. Relative efficiency is specified as the percentage of the power (or, more loosely, energy) at a given wavelength that would be reflected by a mirror (of the same coating as the grating) that is diffracted into a particular order by the grating (that is, efficiency relative to a mirror). Absolute efficiency is specified as the percentage of the power incident

on the grating that is diffracted into a particular order by the grating.

In addition to the wavelength and the diffraction order, grating efficiency depends on the incidence and diffraction angles α and β (the "configuration" or "conditions of use"); if these angles are not explicitly stated, the standard configuration (namely the Littrow configuration, in which the incident and diffracted beams are coincident) will be assumed. Unless otherwise noted on the curves themselves, all Thermo RGL efficiency curves are generated for the standard (Littrow) conditions of use: $\alpha = \beta$.

Generally diffraction gratings are polarizing elements, so that the efficiency in both polarizations should be considered:

P-plane	TE	light polarized parallel to grooves
S-plane	TM	light polarized perpendicular to grooves

For each wavelength that has an efficiency specification, the following should be indicated: the wavelength, the efficiency (in percent), whether the efficiency specification is relative or absolute, the diffraction order, the polarization of the light, and the conditions of use. In some cases, the bandwidth of the exit slit in the spectrometer used to measure the grating efficiency may need to be called out as well.

15.2. SUPPLEMENTAL SPECIFICATIONS [top]

Additional specifications are sometimes required based on the particular application in which the grating is to be used.

10. *Blaze Angle.* Although it is better to specify diffraction efficiency, which is a performance characteristic of the grating, sometimes the blaze angle is specified instead (or additionally). A blaze angle should be specified only if it is to be measured and verified (often done by measuring efficiency anyway), and a tolerance should be noted. In cases where both the diffraction efficiency and the blaze angle are specified, the efficiency specification should be controlling and the blaze angle specification should be for reference only.

11. *Coating Material.* Generally the *Diffraction Efficiency* specifications will dictate the coating material, but sometimes a choice exists and a particular coating should be specified. Additionally, dielectric overcoatings may be called out that are not implied by the efficiency specifications.

12. *Scattered Light.* Grating scattered light is usually specified by requiring that the fraction of monochromatic light power incident on the grating and measured a particular angle away from the diffracted order falls below a certain upper limit. Increasingly, this specification is provided in decibels. The proper specification of scattered light would call out the test configuration, the polarization and wavelength of the incident light, the incidence angle, the solid angle subtended by the detector aperture, and the dimensions of the exit slit. Grating scatter is measured at Thermo RGL using red HeNe light.

13. *Cosmetics.* The cosmetic appearance of a diffraction grating does not correlate strongly with the performance of the grating, and for this reason specifications limiting the type, number and size of cosmetic defects are not recommended. Nevertheless, all Thermo RGL gratings undergo a rigorous cosmetic inspection before shipment.

14. *Imaging Characteristics.* Concave holographic gratings may be aberration-corrected, in which case they can provide focusing without the use of auxiliary optics. In these cases, imaging characteristics should be specified, generally by calling out the *full width at half maximum intensity* (FWHM) of the images.

15. *Damage Threshold.* In some instances, such as pulsed laser applications, diffracted gratings are subjected to beams of high power density that may cause damage to the delicate grating surface, in which case the maximum power per unit area that the grating surface must withstand should be specified.

16. *Other specifications.* Other specifications that relate to the functional performance of the grating should be called out in the print. For example, if the grating must perform in extreme environments (*e.g.*, a satellite or space-borne rocket, high heat and/or humidity environments),

this should be noted in the specifications.

PREVIOUS CHAPTER APPENDIX A

Back to top

APPENDIX A. Sources Of Error In Monochromator-Mode Efficiency Measurements Of Plane Diffraction Gratings

Jeffrey L. Olson

Thermo RGL

PREVIOUS CHAPTER
BIBLIOGRAPHY

TABLE OF CONTENTS

While simple in principle, measuring the efficiency of diffraction gratings is a complex process requiring precise methods to achieve acceptable results. Every optical, mechanical, and electronic component comprising an efficiency measuring system is a potential source of error. Environmental factors may also contribute to the overall measurement uncertainty. Each source of error is identified and its effect on efficiency measurement is discussed in detail.

A.0. INTRODUCTION [top]

In his 1982 book *Diffraction Gratings*, M.C. Hutley makes the following statement regarding the measurement of diffraction grating efficiency:

> "One seldom requires a very high degree of photometric accuracy in these measurements as one is usually content to know that a grating is 60% efficient rather than 50% and the distinction between, say, 61% and 60% is of little practical significance."[15]

While this statement may have been true at the time it was written, it is no longer the case today. Certain industries, such as laser tuning and telecommunications, demand gratings with efficiencies approaching theoretical

limits. The efficiency specifications for these gratings are well defined, and measurement errors as small as one percent may mean the difference between the acceptance and rejection of a particular grating.

In principle, measuring the efficiency of diffraction gratings is simple. A ratiometric approach is used in which the energy of a diffracted beam is compared to the energy of the incident beam. The incident beam may be either measured directly (absolute measurement) or indirectly (relative measurement, by reflection from a reference mirror). Conversion from relative to absolute efficiency can be made easily by multiplying the known reflectance of the reference mirror by the relative efficiency of the grating. (Exceptions to this rule have been noted, namely 1800 to 2400 g/mm gold or copper gratings measured at wavelengths below 600 nm).[16]

As mentioned in Section 10.2, a monochromator mode efficiency-measuring instrument, in essence, is a double grating monochromator, with the grating under test serving as the dispersing element in the second monochromator. The first monochromator scans through the spectral range while the test grating rotates in order to keep the diffracted beam incident upon a detector that remains in a fixed position throughout the measurement.

A typical efficiency measuring apparatus (see Figure A-1) consists of a monochromator, collimator, polarizer, grating rotation stage, grating mount, detector positioning stage, detector and associated optics, amplifier, and signal processing hardware. Once the beam exits the monochromator it is collimated, polarized, and, if necessary, stopped-down to a diameter appropriate for the grating being tested. The beam is then directed toward the grating to be tested where it is diffracted toward the detector. The electronic signal generated by the detector is amplified, filtered, and presented to the user via any number of devices ranging from a simple analog meter to a computer. In any case, a comparison is made between a reference signal, obtained by direct or indirect measurement of the incident beam, and the signal from the grating being tested.

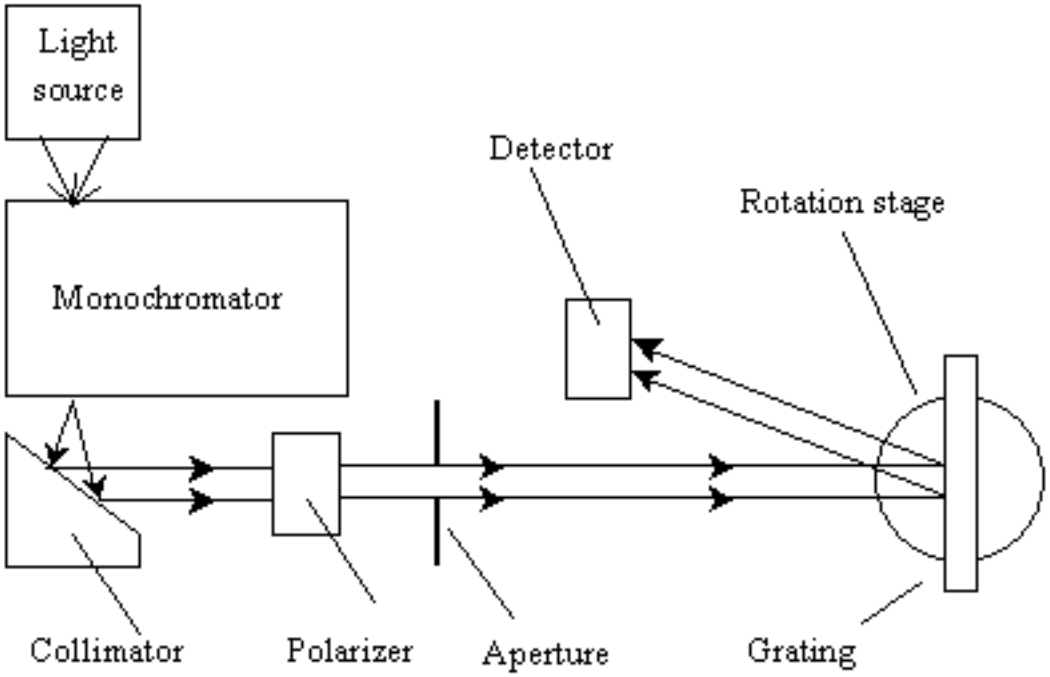

Figure A-1. Typical monochromator-mode efficiency measuring apparatus.

Efficiency measurement results are normally reported on a graph (see Figure A-2) with wavelength on the X-axis and percent efficiency (absolute or relative) on the Y-axis. It is very unusual to see a published efficiency curve with error bars or some other indication of the measurement uncertainty. It must be understood that these measurements are not exact, and may be in error by several percent. A complete understanding of the measurement process as well as the sources of error and how to minimize them would be of great value to the technician or engineer making the measurements as well as those involved in making decisions to accept or reject gratings based on efficiency.

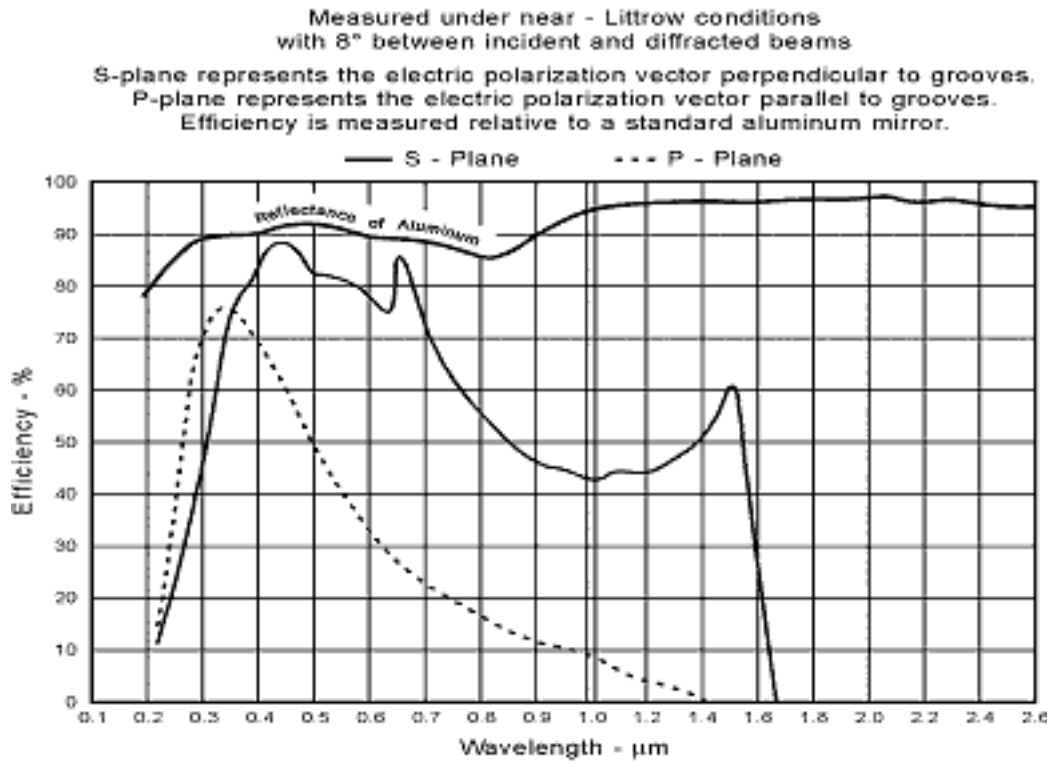

Figure A-2. Typical efficiency curve.

A.1. OPTICAL SOURCES OF ERROR [top]

A.1.1. Wavelength error

Perhaps the most obvious error of an optical nature is an error in wavelength. If the monochromator does not accurately select the desired wavelength, efficiency peaks, anomalies, etc., will appear at the wrong spectral position on the efficiency curve. If the grating being measured is rotated to the appropriate incident angle for a given wavelength, the diffracted beam may partially or totally miss the detector if the wavelength is not correct. This is less of a problem in manually controlled instruments, since the operator can adjust the wavelength or grating rotation angle to obtain a maximum reading. On an automated instrument, however, a significant error may result unless the instrument has the ability to "hunt" for the efficiency peak.

Wavelength errors are usually caused by a failure of the monochromator

indexing mechanism to move the grating to the correct rotation angle. Most computer based monochromator systems employ correction factors or calibration tables in firmware to correct systematic wavelength errors. Even so, many monochromators use open-loop stepper motor drives to position the grating. Since there is no explicit feedback from the rotation mechanism, the controller must assume that the grating is in the correct position. If the motor fails to move the proper number of steps due to binding in the mechanical system or for some other reason, the wavelength will be in error.

To ensure wavelength accuracy, periodic wavelength calibration should be done using a calibration lamp or other spectral line source. The author has used the Schumann-Runge O_2 absorption lines effectively for monochromator wavelength calibration in the far ultraviolet region near 193 nm. The well-defined Schumann-Runge transitions occurring at 192.6 nm are especially useful spectral features.[17]

A.1.2. Fluctuation of the light source intensity

One of the drawbacks of using a single detector system is that the light source intensity can change between the times the reference and sample measurements are made. With filament lamps, the intensity is proportional to the power dissipated in the filament. According to Ohm's law, power *P* is the product of current *I* and voltage *E*, and voltage is the product of current and resistance *R*, therefore:

$$P = IE = I\,(IR) = I^2R. \qquad (A\text{-}1)$$

Typically electrical power is applied to the lamp socket, rather than to the lamp directly. The contact resistance between the lamp and socket can be significant and is prone to change over time. If a constant voltage is applied to the socket and the contact resistance was to increase, the current, power, and lamp intensity will decrease as a result. If a constant current is applied instead, no change in power will occur as the result of a change in contact resistance (provided the filament resistance remains constant). For this reason current-regulated, rather than voltage-regulated, power supplies are preferred whenever filament-type lamps are used. A photo-feedback system, in which a detector monitors and controls the lamp intensity, is also a good choice. Regardless of

the type of light source used, it is always best that the sample and reference measurements be made in quick succession.

A.1.3. Bandpass

As a rule, the bandpass of the light source should always be narrower than that of the grating under test. The bandpass *B* of the grating under test is defined by the angular dispersion *D* of the grating, the distance *r* from the grating to the detector aperture, and the width *w* of the detector aperture according to the equation:

$$B = w/rD. \qquad (A\text{-}2)$$

Whenever a grating is measured using a source with a bandpass that is too broad, some of the outlying wavelengths will be diffracted away from the detector. In contrast, when the reference measurement is made using a mirror or by direct measurement of the incident beam, no dispersion occurs. Consequently, the detector captures all wavelengths contained within the incident beam during the reference measurement, but not during the grating measurement (resulting in an artificial decrease in grating efficiency). Another consequence of measuring gratings using a light source with a broad bandpass is that sharp efficiency peaks will appear flattened and broadened, and may be several percent lower than if measured using a spectrally-narrow light source. Efficiency curves should, but often do not, state the bandpass of the source used to make the measurement. When using a monochromator, it is generally best to adjust the slits to obtain the narrowest bandpass that will provide an acceptable signal-to-noise ratio (SNR). Alternatively, a narrow band spectral source, such as a laser or calibration lamp, may be used in conjunction with a monochromator or interference filter to eliminate unwanted wavelengths.

A.1.4. Superposition of diffracted orders

According to the grating equation (see Eq. (2-1)), the first order at wavelength λ and the second order at wavelength $\lambda/2$ will diffract at exactly the same angle (see section 2.2.2). Therefore the light emerging from a

monochromator exit slit will contain wavelengths other than those desired. The unwanted orders must be removed in order to accurately determine the efficiency at the desired wavelength. "Order-sorting" filters are most commonly used for this purpose. These are essentially high-pass optical filters that transmit longer wavelengths while blocking the shorter wavelengths.

Another problematic situation arises when the adjacent diffracted orders are very closely spaced. In this case, adjacent orders must be prevented from overlapping at the detector aperture, which would result in a significant error. This situation can be avoided by ensuring that the bandpass of the source is less than the free spectral range of the grating being tested. As shown in section 2.7, the free spectral range F_λ is defined as the range of wavelengths $\Delta\lambda$ in a given spectral order m that are not overlapped by an adjacent order, expressed by Eq. (2-24):

$$F_\lambda = \Delta\lambda = \frac{\lambda_1}{m} . \qquad (2\text{-}24)$$

For an echelle being measured in the $m = 100^{th}$ order at $\lambda = 250$ nm, the free spectral range is 2.5 nm. The detector aperture must also be sufficiently narrow to prevent adjacent orders from being detected, but not so narrow as to violate the "rule" regarding the bandpass of the light source and grating under test.

A.1.5. Degradation of the reference mirror

When a mirror is used to determine the incident light energy, its reflectance as a function of wavelength needs to be well characterized. Mirrors tend to degrade over time due to atmospheric exposure, and if not re-characterized periodically, optimistic measurements of grating efficiency will result. At the National Physical Laboratory (NPL) in England, an aluminum-coated silica flat was used as a reference mirror. This is nothing new, but in this case the "buried" surface of the mirror was used as the mirror surface instead of the metal surface itself. Since the aluminum is never exposed to the atmosphere, its reflectance is stable, and since the mirror was characterized through the silica substrate, its influence is automatically accounted for.[18] The restriction in using the "buried surface" method is that the incident beam must be normal to the mirror surface to avoid beam separation caused by multiple

reflections from the front and buried surfaces. When an unprotected mirror surface is used as a reference, absolute measurements of its reflectance should be made on a regular basis.

A.1.6. Collimation

If the incident beam is not reasonably well collimated, the rays will fall upon the grating at a variety of angles and will be diffracted at different angles. In the case of a diverging diffracted beam, the beam will spread, possibly overfilling the detector. Since the reference beam does not encounter a dispersing element in its path (but the sample beam does), it is possible that all of the energy will be collected during the reference measurement but not during the sample measurement, causing the measured efficiency to be low.

Whenever a monochromator-based light source is used it is difficult, if not impossible, to perfectly collimate the beam emerging from the exit slit in both planes. It is important to collimate the beam in the direction perpendicular to the grooves, but it is not as critical for the beam to be well collimated in the direction parallel to the grooves, since no diffraction occurs in that direction. A limiting aperture may be used to restrict the beam size and prevent overfilling the grating under test.

It should be emphasized that beam collimation is not nearly as important in an efficiency measuring system as it is in an imaging system, such as a spectrograph. It is only necessary to ensure that the detector collects all of the diffracted light. The degree of collimation required largely depends on the dispersion of the grating under test, but in most cases a beam collimated to within 0.1o is adequate. For example, an angular spread of 0.1o in a beam incident upon a 1200 g/mm grating measured in the 1st order at 632.8 nm (Littrow configuration) will produce a corresponding spread in the diffracted beam of less than 1 mm over a distance of 500 mm.

A.1.7. Stray light or "optical noise"

The influence of stray radiation must always be taken into consideration when making efficiency measurements. If the level of background radiation is

very high, the detector may be biased enough to result in a significant error. This is especially true when simple DC detection methods are used. Any bias introduced by background radiation must be subtracted from both the reference and sample measurements before the ratio is computed. For example, if the background radiation equals 2% of the reference beam, and the grating being tested measures 50% relative efficiency, the actual efficiency is 48/98 or 49%. This represents an error of 1% of the full-scale measured efficiency. In many cases simply operating the instrument in a dark lab or enclosure is sufficient to reduce background light to insignificant levels. Averaging is often used to "smooth out" noisy signals, but unlike other more random noise sources that tend to be bipolar, stray light-induced noise is always positive. Averaging several measurements containing a significant level of optical noise may bias the final measurement. In most cases, it is best to use phase-sensitive detection to remove the effects of unwanted radiation.

A.1.8. Polarization

Most efficiency curves display the S and P as well as the 45-degree polarization efficiency *vs.* wavelength. When making polarized efficiency measurements using an unpolarized source, it is necessary to use some form of optical element to separate the two polarization vectors. It is critical that the polarizer be aligned as closely as possible to be parallel (P plane) or perpendicular (S plane) to the grooves or a polarization mixing error will result. To determine the 45-degree polarization efficiency of a grating, it seems easy enough to set the polarizer to 45 degrees and make the measurement, but unless the output from the light source is exactly balanced in both S and P planes, an error will result.

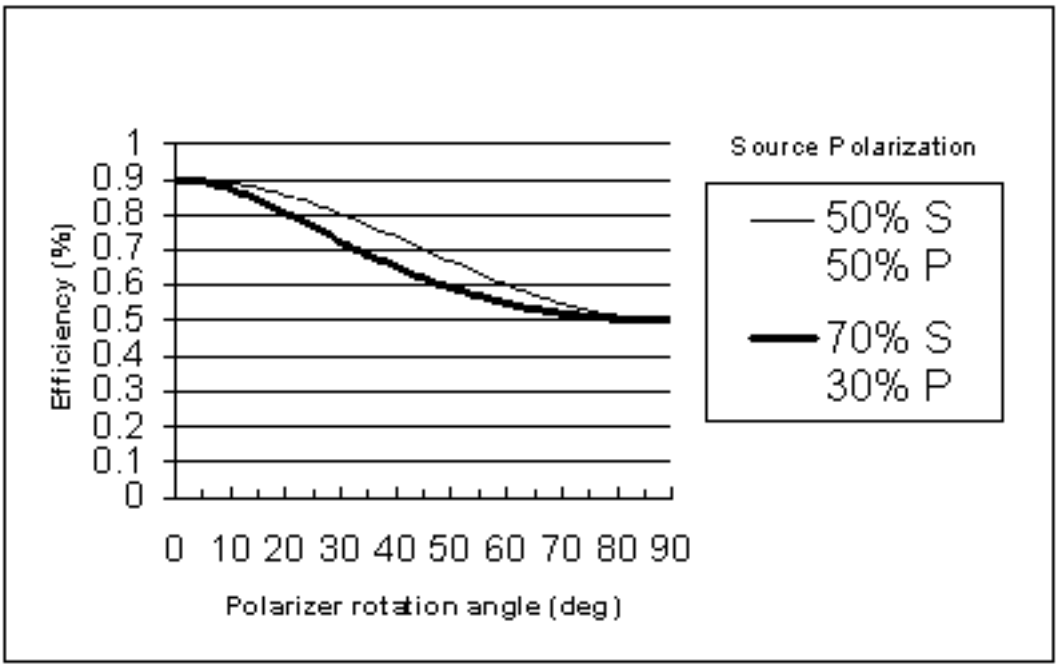

Figure A-3. Efficiency comparison with balanced and unbalanced source polarization (0º = P, 90º = S).

Figure A-3 shows the effect of source polarization on the measured efficiency of a hypothetical grating having efficiencies of 90% in the P plane and 50% in the S plane at some arbitrary wavelength. In one case the light source contains equal S and P intensities while the other has a 70:30 S to P ratio. In the case of the balanced light source, as the polarizer is rotated to 45o, the efficiency is 70%, exactly the average of the S and P measurements. On the other hand, the unbalanced source results in a measured efficiency of 60%. This represents an error of 10% of the full-scale measured value. For that reason it is always recommended to make separate S and P measurements and then average them to determine the grating's 45-degree polarization efficiency.

A.1.9. Unequal path length

An error can result in a single detector system purely as the result of the optical path being different between the reference and sample measurements. This is especially true at UV wavelengths where the atmospheric absorption is significant. Different optical path lengths are not as much of a problem in dual

detector systems since the relative calibration of the two detectors can compensate for atmospheric effects.

A.2. MECHANICAL SOURCES OF ERROR [top]

A.2.1. Alignment of incident beam to grating rotation axis

It is critical to align the incident beam to the rotation axis of the grating stage and mount. If not, the beam will "walk" across the grating surface at relatively low incident angles, and partially miss the grating surface at very high incident angles. Since the incident and diffracted beams are displaced from their correct location, it is entirely possible that all or part of the diffracted beam will miss the detector aperture.

A.2.2. Alignment of grating surface to grating rotation axis

The effect of not having the grating surface located exactly over the rotation axis will be similar to that of not having the beam aligned to the grating rotation axis. Optimally, a grating mount that references the grating's front surface, rather than the sides or back of the grating substrate, may be used to ensure alignment. This is often not practical since the contact points on the mount may leave an impression on the grating surface. To avoid this problem, an inclined lip or rail is sometimes used that makes contact with the grating on the extreme outer edge only. On beveled grating substrates this can be a source of error since the dimensional variation of the bevels can be significant. If the grating mount does not reference the front surface, an adjustment must be provided in order to accommodate gratings of various thicknesses.

A.2.3. Orientation of the grating grooves (tilt adjustment)

On grating mounts that use the substrate to locate the grating to be tested, the plane in which the diffracted orders lie will be tilted if the grooves are not properly aligned with the sides of the grating substrate. This may cause

the diffracted beam to pass above or below the detector aperture. Most gratings do not have perfect alignment of the grooves to the substrate, so it is necessary to incorporate a method for rotating the grating a small amount in order to compensate for groove misalignment.

A.2.4. Orientation of the grating surface (tip adjustment)

Due to some wedge in the grating substrate, for example, the grating surface may not be parallel to the grating rotation axis. This will cause the diffracted beam to fall above or below the detector aperture. On most grating mounts an adjustment is provided to correct this situation. Ideally the grating tip, tilt, and rotation axes all intersect at a common point on the grating surface, but in fact it is extremely rare to find a grating mount in which the tip axis does so. In most cases the tip axis is located behind or below the grating substrate, so when adjusted, the grating surface will no longer lie on the rotation axis. The ideal situation is one in which the grating is front-surface referenced on the mount so that no adjustment is needed.

A.2.5. Grating movement

It is essential that the grating being tested be held securely in the mount during the testing process. Vibration from motors and stages as well as the inertia generated by the grating as it is rotated may cause it to slip. Any motion of the grating relative to the mount will result in alignment errors and invalidate any measurements taken after the movement occurred.

A.3. ELECTRICAL SOURCES OF ERROR [top]

A.3.1. Detector linearity

In principle, all that is required to make satisfactory ratiometric measurements is a linear response from the sensing element and associated electronics. Nearly all detectors have response curves that exhibit non-linearity

near saturation and cut off. It is extremely important to ensure that the detector is biased such that it is operating within the linear region of its response curve. In addition, the detector preamplifier and signal processing electronics must also have a linear response, or at least have the non-linearity well characterized in order for a correction to be applied. Neutral density filters may be inserted into the optical path to verify or characterize the detection system linearity. The following set of five calibrated neutral density filters is sufficient, in most cases, for verifying the detector response to within ± 1%:

Optical Density	Transmission*
0.1	79%
0.3	50%
0.6	25%
1.0	10%
2.0	1%

*rounded to nearest whole percent.

Detector non-linearity becomes a major source of error when the reference and grating signals differ significantly in intensity. Unless the linearity of the detector and associated electronics has been well established, using a mirror with a reflectance of 90% or higher as a reference may introduce an error if the grating being measured has an efficiency of 20%. This is analogous to sighting in a rifle at 100 yards and using it to shoot at targets 25 yards away. In some situations it is best to use a well-characterized grating as nearly identical to the grating to be tested as possible. This method is especially useful for making "go/no-go" efficiency measurements. If the reference grating is carefully chosen to be one that is marginally acceptable, then the efficiency measuring instrument will have its greatest accuracy at the most critical point. All gratings measuring greater than or equal to 100% relative to the reference grating are assumed to be good and those below 100% are rejected. Of course this method requires periodic recharacterization of the reference grating in order to maintain measurement integrity.

A.3.2. Changes in detector sensitivity

Some efficiency measuring instruments use separate detectors for making the reference and grating measurements (these are not to be confused with systems that use secondary detectors to monitor light source fluctuations). Most, however, use a single detector for both the reference and grating measurements instead. There are very good reasons for doing this. First of all, detectors and the associated electronics are expensive, so using a single detector is far more cost effective. Detector response characteristics change over time, so frequent calibration is necessary in a dual-detector system to ensure that the photometric accuracy of each detector has not changed relative to the other. By using the same detector for sample and reference measurements, photometric accuracy is not an issue, since an error in the reference measurement will also be present in the grating measurement and consequently nullified.

A.3.3. Sensitivity variation across detector surface

A significant error can result if the reference or diffracted beam is focused down to form a spot that is much smaller than the detector's active area. Some detectors, especially photomultipliers, may exhibit a sensitivity variation amounting to several percent as the spot moves across the detector surface. It is often sufficient to place the detector aperture far enough away from the detector such that the spot is defocused and just under-fills the active area. Alternately a diffuser or integrating sphere is sometimes used to distribute the light more uniformly across the detector surface.

A.3.4. Sensitivity variation across detector surface

Any form of optical or electronic noise can influence efficiency measurements. It is desirable to maintain the highest signal-to-noise ratio (SNR) possible, but often a trade-off must be made between signal strength and spectral resolution. Decreasing the monochromator slit width in order to narrow the bandpass of the source results in a reduced detector output signal. Care

must be taken not to limit the intensity to a point where electronic (and optical) noise becomes a significant factor. In most cases, an SNR value of 200:1 is adequate.

A.4. ENVIRONMENTAL FACTORS [top]

A.4.1. Temperature

Normally it is not necessary to perform efficiency measurements in an extremely well regulated environment, but there are a few cases in which temperature control is needed. Whenever very high spectral resolution measurements are made, (1 nm or less), temperature variation within the monochromator may cause a significant wavelength drift. Temperature fluctuations may cause optical mounts to expand or contract resulting in a displacement of the beam. It is always a good idea to keep heat sources well away from all optical and mechanical components that may affect the grating being tested or the beam. It is also wise to allow gratings that are to be tested to acclimate in the same environment as the test instrument.

A.4.2. Humidity

Humidity is not usually a significant error source, but since it can affect the system optics and electronics, it merits mentioning. A high humidity level may influence measurements at wavelengths where atmospheric absorption varies with relative humidity. Low humidity promotes the generation of static electricity that may threaten sensitive electronic components. In general, the humidity level should be maintained in a range suitable for optical testing.

A.4.3. Vibration

Vibration becomes an error source when its amplitude is sufficient to cause the grating under test or any of the optical components to become displaced. If the vibration is from a source other than the instrument itself, then

mounting the instrument on a vibration isolated optical bench will solve the problem. If the instrument itself is the vibration source, then the problem becomes a little more difficult. Stepper-motors are most often used to rotate and translate the grating being tested, as well as tune the monochromator, select filters, etc. As the motors ramp up to predetermined velocity, a resonant frequency is often encountered that will set up an oscillation with one or more mechanical components in the system. While it is sometimes necessary to pass through these resonant frequencies, it is never advisable to operate continuously at those frequencies. Most motion controllers have provisions for tuning the motion profile to minimize resonance. Some motion controllers allow micro-stepped operation of the motors, producing a much smoother motion. Although generally more expensive, servo controllers, amplifiers, and motors provide exceptional accuracy and very smooth motion.

A.5. SUMMARY [top]

Many of the error sources identified can be eliminated entirely, but only at the expense of decreased functionality. Greater accuracy can be obtained using an instrument that operates at a fixed wavelength in a fixed geometry and is only used to test gratings that have identical physical properties. When a large variety of gratings are to be tested, each with a different size, shape, groove frequency, wavelength range, test geometry, *etc.*, it is not practical to construct a dedicated instrument for each. In this case a more complex instrument is called for. In specifying such an instrument, each source of error should be identified, and if possible, quantified. An error budget can then be generated that will determine if the instrument is able to perform at the desired level. Most likely it will not, and then a decision needs to be made regarding which features can be compromised, eliminated, or implemented on another instrument.

Disagreements often arise between measurements made of the same grating on different efficiency measuring instruments. Slight differences in test geometry, bandpass, and beam size can have a surprisingly large effect on efficiency measurements. What is sometimes difficult to understand is that it is possible for two instruments to measure the same grating and get different results that are valid!

Grating efficiency is largely determined by the groove properties of the

master from which the grating was replicated, and to some degree the coating. It is very rare for a master, regardless of the process used to create it, to have perfectly uniform efficiency at every spot along its surface. In some cases the efficiency may vary by several percent. If a grating is measured using a small diameter beam, then these efficiency variations are very noticeable compared to measurements made using a larger beam. If two different instruments are used to measure the same grating, it is possible that the beams are not exactly the same size or, in the case of a small beam diameter, are not sampling exactly the same spot on the grating surface. Both instruments are correct in their measurements, but still do not agree. For this reason, whenever comparisons between instruments are made, the differences in their configuration must be taken into consideration.

The goal of efficiency measurement is to characterize the grating under test, not the apparatus making the measurements. For this reason, efficiency curves should report not only the relative or absolute efficiency vs. wavelength, but the properties of the instrument making the measurement as well. Only then is it possible to reproduce the results obtained with any degree of accuracy.

PREVIOUS CHAPTER APPENDIX A BIBLIOGRAPHY

Back to top

BIBLIOGRAPHY

APPENDIX
TECHNICAL PUBLICATIONS OF THERMO RGL

TABLE OF CONTENTS

Born, M., and E. Wolf, 1980. *Principles of Optics*, Pergamon Press (Oxford, England).

Clark, B. J., T. Frost and M. A. Russell, 1993. *UV Spectroscopy: Techniques, instrumentation, data handling*, Chapman and Hall (London, England).

Harris, D. A. and C. L. Bashford, editors, 1987. *Spectrophotometry and Spectrofluorimetry*, IRL Press (Oxford, England).

Hunter, W. R., 1985. "Diffraction Gratings and Mountings for the Vacuum Ultraviolet Spectral Region," *Spectrometric Techniques, vol. IV.*, 63-180 (1985). This article provides a very thorough and detailed review of the use and manufacture of diffraction gratings.

Hutley, M. C., 1976. "Interference (holographic) diffraction gratings," *J. Phys. E.* **9**, 513-520 (1976). This article offers more detail on interference gratings, and compares them with ruled gratings.

Hutley, M. C., 1982. *Diffraction Gratings*, Academic Press (New York, New York). This book provides a complete and thorough tour of diffraction gratings, their manufacture and their application.

Loewen *et al.* 1977. E. G. Loewen *et al.*, "Grating Efficiency

Theory as it Applies to Blazed and Holographic Gratings," *Appl. Optics* **16**, 2711-2721 (1977).

Loewen, E. G., 1983. "Diffraction Gratings, Ruled and Holographic," in *Applied Optics and Optical Engineering*, vol. IX (chapter 2), R. Shannon, ed., Academic Press (New York, New York). This chapter describes developments in grating efficiency theory as well as those in concave grating aberration reduction.

Loewen, E.G. and E. Popov, 1997. *Diffraction Gratings and Applications*, Marcel Dekker (New York, New York).

Meltzer, R. J., 1969. "Spectrographs and Monochromators," in *Applied Optics and Optical Engineering*, vol. V (chapter 3), R. Shannon, ed., Academic Press (New York, New York).

Petit, R., editor, 1980. *Electromagnetic Theory of Gratings*, Springer-Verlag (New York, New York); volume 22 in "Topics in Current Physics" series.

Richardson, D., 1969. "Diffraction Gratings", in *Applied Optics and Optical Engineering*, vol. V (chapter 2), R. Shannon, ed., Academic Press (New York, New York).

Schroeder, D. J., 1987. *Astronomical Optics*, Academic Press (San Diego, California). Chapters 12 through 15 serve as an excellent introduction to gratings and their instruments, with application toward stellar spectrometry. Chapters 2 through 5 form a clear and quite complete introduction to the ideas of geometrical optics used to design lens, mirror, and grating systems.

Samson, J. A. R., 1967. *Techniques of Vacuum Ultraviolet Spectroscopy*, John Wiley & Sons (New York, New York).

Skoog, D. A., 1988. *Principles of Instrumental Analysis*, third edition, Saunders (Philadelphia, Pennsylvania). The chapters on spectroscopy serve as a good introduction to the subject.

Stover, J. C., 1990. *Optical Scattering*, McGraw-Hill, Inc. (New York, New York).

Williard, H. H., et al., 1988. *Instrumental Methods of Analysis*, seventh edition, Wadsworth. (Belmont, California). The chapters on absorption and emission spectroscopy, and ultraviolet and visible spectroscopic instrumentation, are of particular interest.

Back to top

ACKNOWLEDGMENTS

FIRST CHAPTER

TABLE OF CONTENTS

I gratefully acknowledge the following people for their thorough and critical review of the second edition of this *Handbook*: **Peter Gray** (Anglo-Australian Observatory, Epping, New South Wales, Australia), **W. R. Hunter** (SFA Inc., Landover, Maryland), **Robert P. Madden** (National Institute of Standards and Technology, Gaithersburg, Maryland), and **Daniel J. Schroeder** (Beloit College, Beloit, Wisconsin).

A number of people at Thermo RGL deserve thanks for their review of certain sections of the fifth edition, as well as their insightful comments and suggestions for improvement, notably **Thomas Blasiak** and **Semyon Zheleznyak**.

I especially wish to thank my long-time colleague **Jeffrey Olson** of Thermo RGL for his critical review of and contributions to many sections of the *Handbook*, as well as for permitting me to include his recent manuscript, "Sources of Error in Monochromator-Mode Efficiency Measurements of Plane Diffraction Gratings", in this edition of the *Handbook* as Appendix A.

TECHNICAL PUBLICATIONS OF THERMO RGL

BIBLIOGRAPHY

TABLE OF CONTENTS

Below is a partial list of publications by Thermo RGL scientists and engineers pertaining to diffraction gratings and their uses.

Reference Books

E.G. Loewen and E. Popov, *Diffraction Gratings and Applications*, 1997 Marcel Dekker, Inc. (ISBN 0-8247-9923-2).

Gratings in General

A-1 D. Richardson, "Diffraction Gratings," chapter 2, volume II of *Applied Optics and Optical Engineering* , R. Kingslake, ed. (Academic Press, New York: 1969)

A-2 E.G. Loewen, Diffraction Gratings for Spectroscopy, *J. Physics* **E 3**, 953-961 (1970).

A-3 E.G. Loewen, "Diffraction Gratings, Ruled and Holographic," chapter 2, volume IX of *Applied Optics and Optical Engineering* , R. Shannon, ed. (Academic Press, New York: 1983), pp. 33-71.

A-4 E.G. Loewen, "The Ruling and Replication of Diffraction Gratings," *Optics and Photonics News* , May 1991.

A-5 C. Palmer, ed., *Diffraction Grating Handbook*, fifth edition, Thermo RGL (2002).

A-6 C. Palmer, "Diffraction Gratings: The Crucial Dispersive Component," *Spectroscopy* **10,,** 14-15 (1995).

Grating Efficiency

B-1 E.G. Loewen, M. Nevière and D. Maystre, "Grating Efficiency Theory as it applies to Blazed and Holographic Gratings," *Applied Optics* **16**, 2711-2721 (1977).

B-2 E.G. Loewen and M. Nevière, "Simple Selection Rules for VUV and XUV Diffraction Gratings," *Applied Optics* **17**, 1087-1092 (1978).

B-3 L.B. Mashev, E.K. Popov and E.G. Loewen, "Optimization of Grating Efficiency in Grazing Incidence," *Applied Optics* **26**, 4738-4741 (1987).

Grating Imaging

C-1 W.R. McKinney and C. Palmer, "Numerical design method for aberration-reduced concave grating spectrometers," *Applied Optics* **26**, 3108-3118 (1987).

C-2 C. Palmer, "Theory of second generation holographic gratings," *J. Opt. Soc. Am.* **A 6**, 1175-1188 (1989).

C-3 C. Palmer and W.R. McKinney, "Equivalence of focusing conditions for holographic and varied line-space gratings," *Applied Optics* **29**, 47-51 (1990).

C-4 C. Palmer, "Deviation of second-order focal curves in common spectrometer mounts," *J. Opt. Soc. Am.* **A 7**, 1770-1778 (1990).

C-5 C. Palmer and W. McKinney, "Imaging Theory of Plane-symmetric Varied Line-space Grating Systems," *Optical Engineering* **33**, 820-829 (1994).

C-6 C. Palmer, W. McKinney and B. Wheeler, "Imaging equations for spectroscopic systems using Lie transformations. Part I - Theoretical foundations," *Proc. SPIE* **3450**, 55-66 (1998).

C-7 C. Palmer, B. Wheeler and W. McKinney, "Imaging equations for spectroscopic systems using Lie transformations. Part II - Multi-element systems," *Proc. SPIE* **3450**, 67-77 (1998).

C-8 C. Palmer and W. McKinney, "Imaging properties of varied line-space (VLS) gratings with adjustable curvature," *Proc. SPIE* **3450**, 87-102 (1998).

Echelle Gratings

D-1 G.R. Harrison, E.G. Loewen and R.S. Wiley, "Echelle gratings: their testing and improvement," *Applied Optics* **15**, 971-976 (1976).

D-2 E.G. Loewen *et al.*, "Echelles: scalar, electromagnetic and real-groove properties," *Applied Optics* **34**, 1707-1727 (1995).

D-3 E. Loewen *et al.*, "Diffraction efficiency of echelles working in extremely high orders," *Applied Optics* **35**, 1700-1704 (1996).

D-4 J. Hoose *et al.*, "Grand Gratings: Bigger is Better, Thanks to Mosaic Technology," *Photonics Spectra* (December 1995).

D-5 E. Popov *et al.*, "Integral method for echelles covered with lossless or absorbing thin dielectric layers," *Applied Optics* **38, 47-55 (1999).**

Transmission Gratings

E-1 E.K. Popov, E.G. Loewen and M. Nevière, "Transmission gratings for beam sampling and beam splitting," *Applied Optics* **35**, 3072-3075 (1996).

Mosaic Gratings

D-4 J. Hoose *et al.*, "Grand Gratings: Bigger is Better, Thanks to Mosaic Technology," *Photonics Spectra* (December 1995).

F-1 T. Blasiak and S. Zheleznyak, "History and construction of large mosaic diffraction gratings," *Proc. SPIE* **4485** (2001).

Back to top